Document généré le 28 avr. 2024 18:37

Atlantic Geoscience
Journal of the Atlantic Geoscience Society

Re-evaluation of the Mesozoic–Cenozoic biostratigraphy of the Laurentian Subbasin of the Scotian Basin, offshore eastern Canada

Réévaluation de la biostratigraphie mésozoïque-cénozoïque du sous-bassin Laurentien du bassin Scotian, au large des côtes de l'est du Canada

Janice F. Weston, R. Andrew MacRae, Piero Ascoli, M. Kevin E. Cooper, Robert A. Fensome, David Shaw et Graham L. Williams

Volume 59, 2023

URI : https://id.erudit.org/iderudit/1108391ar
DOI : https://doi.org/10.4138/atlgeo.2023.009

Aller au sommaire du numéro

Éditeur(s)

Atlantic Geoscience Society

ISSN

2564-2987 (numérique)

Découvrir la revue

Citer cet article

Weston, J., MacRae, R., Ascoli, P., Cooper, M., Fensome, R., Shaw, D. & Williams, G. (2023). Re-evaluation of the Mesozoic–Cenozoic biostratigraphy of the Laurentian Subbasin of the Scotian Basin, offshore eastern Canada. *Atlantic Geoscience*, *59*, 183–239. https://doi.org/10.4138/atlgeo.2023.009

Résumé de l'article

Nous utilisons des données biostratigraphiques sur les microfossiles, des données palynologiques et des données sur les nanofossiles, nouvelles et existantes, conjointement avec des diagraphies lithologiques et géophysiques de quatre puits pour définir une série de phénomènes stratigraphiques séquentiels de la tranche du Mésozoïque-Cénozoïque du sous-bassin Laurentien au large des côtes de Terre-Neuve, dans l'est du Canada. Les phénomènes biostratigraphiques des puits sont intégrés à la sismique réflexion dans le secteur aux fins d'une corrélation des surfaces stratigraphiques sismiques régionales. Les quatre puits en question sont les puits Bandol-1, Emerillon C-56, East Wolverine G-37 et Heron H-73. Nous élargissons le plan stratigraphique des phénomènes précédemment créé pour la marge de Scotian, au large des côtes de la Nouvelle-Écosse, aux nouveaux secteurs à l'est le long de la zone méridionale des Grands bancs, où nous reconnaissons quatre nouveaux phénomènes stratigraphiques séquentiels dans les diagraphies des puits et nous modifions la définition d'une surface régionale antérieurement reconnue. Les nouvelles surfaces régionales modifiées sont la discordance de l'Albien précoce, la surface d'inondation maximale (SIM) du Bathonien tardif, la SIM du Bajocien tardif (SIM du Bathonien/Bajocien rebaptisée), la discordance bajocienne?/toarcienne et la SIM du Pliensbachien tardif. Nous reconnaissons la « discordance d'Avalon » et la « discordance de base-tertiaire » d'études antérieures en tant que regroupements de plusieurs discordances d'échelle plus modeste et nous déterminons leur âge de façon plus précise dans les puits étudiés. Une amélioration notable par rapport à nos plans antérieurs des phénomènes survenus dans la marge de Scotian est l'élargissement de la stratigraphie des phénomènes au cours du Jurassique précoce au moyen de repères stratigraphiques marins. Nous comparons le plan des phénomènes du Jurassique précoce au site 547B du projet de forage en eau profonde sur la marge marocaine conjuguée pour mieux limiter les intervalles éventuels de roche mère et les débuts de l'océan Atlantique central.

All Rights Reserved © Atlantic Geoscience, 2023

Ce document est protégé par la loi sur le droit d'auteur. L'utilisation des services d'Érudit (y compris la reproduction) est assujettie à sa politique d'utilisation que vous pouvez consulter en ligne.

https://apropos.erudit.org/fr/usagers/politique-dutilisation/

Cet article est diffusé et préservé par Érudit.

Érudit est un consortium interuniversitaire sans but lucratif composé de l'Université de Montréal, l'Université Laval et l'Université du Québec à Montréal. Il a pour mission la promotion et la valorisation de la recherche.

https://www.erudit.org/fr/

Re-evaluation of the Mesozoic–Cenozoic biostratigraphy of the Laurentian Subbasin of the Scotian Basin, offshore eastern Canada

Janice F. Weston[1], R. Andrew MacRae[2], Piero Ascoli[3], M. Kevin E. Cooper[4], Robert A. Fensome[3*], David Shaw[5], and Graham L. Williams[3]

1. Weston Stratigraphic Ltd., Guildford GU1 1XS, UK
2. Department of Geology, Saint Mary's University, Halifax, Nova Scotia B3H 3C3, Canada
3. Natural Resources Canada, Geological Survey of Canada (Atlantic), Bedford Institute of Oceanography, Dartmouth, Nova Scotia B2Y 4A2, Canada
4. KC Stratigraphic Ltd., Woking, Surrey GU22 8HD, UK
5. Biostratigraphic Associates (UK) Ltd., Norton Green, Stoke-on-Trent, Staffs ST6 8NE, UK
*Corresponding author: <rfensome@nrcan-rncan.gc.ca>

Date received: 8 February 2023 ¶ Date accepted: 8 August 2023

ABSTRACT

We use new and existing nannofossil, palynological, and microfossil biostratigraphic data in conjunction with lithologic and geophysical logs from four wells to establish a series of sequence-stratigraphic events in the Mesozoic–Cenozoic of the Laurentian Subbasin of offshore Newfoundland, eastern Canada. Well biostratigraphic events are integrated with reflection seismic in the area to correlate regional seismic stratigraphic surfaces. The four wells are: Bandol-1, Emerillon C-56, East Wolverine G-37, and Heron H-73. We extend the event stratigraphic scheme previously developed for the Scotian Margin, offshore Nova Scotia, into new areas to the east along the southern Grand Banks, where we recognize four new well-log sequence stratigraphic events, and we modify the definition of a previously recognized regional surface. The new and modified regional surfaces are the Early Albian Unconformity, the Late Bathonian Maximum Flooding Surface (MFS), the Late Bajocian MFS (renamed from Bathonian/Bajocian MFS), the ?Bajocian/Toarcian Unconformity, and the Late Pliensbachian MFS. We recognize the "Avalon Unconformity" and "Base-Tertiary Unconformity" of previous studies as amalgamations of multiple smaller-scale unconformities and refine their age in the studied wells. A major improvement over our earlier Scotian Margin event schemes is the extension of the event stratigraphy into the Early Jurassic using a suite of marine biostratigraphic markers. We compare the Early Jurassic event scheme to Deep Sea Drilling Project Site 547B on the conjugate Moroccan Margin to better constrain potential source rock intervals and the early history of the central Atlantic Ocean.

RÉSUMÉ

Nous utilisons des données biostratigraphiques sur les microfossiles, des données palynologiques et des données sur les nanofossiles, nouvelles et existantes, conjointement avec des diagraphies lithologiques et géophysiques de quatre puits pour définir une série de phénomènes stratigraphiques séquentiels de la tranche du Mésozoïque-Cénozoïque du sous-bassin Laurentien au large des côtes de Terre-Neuve, dans l'est du Canada. Les phénomènes biostratigraphiques des puits sont intégrés à la sismique réflexion dans le secteur aux fins d'une corrélation des surfaces stratigraphiques sismiques régionales. Les quatre puits en question sont les puits Bandol-1, Emerillon C-56, East Wolverine G-37 et Heron H-73. Nous élargissons le plan stratigraphique des phénomènes précédemment créé pour la marge de Scotian, au large des côtes de la Nouvelle-Écosse, aux nouveaux secteurs à l'est le long de la zone méridionale des Grands bancs, où nous reconnaissons quatre nouveaux phénomènes stratigraphiques séquentiels dans les diagraphies des puits et nous modifions la définition d'une surface régionale antérieurement reconnue. Les nouvelles surfaces régionales modifiées sont la discordance de l'Albien précoce, la surface d'inondation maximale (SIM) du Bathonien tardif, la SIM du Bajocien tardif (SIM du Bathonien/Bajocien rebaptisée), la discordance bajocienne?/toarcienne et la SIM du Pliensbachien tardif. Nous reconnaissons la « discordance d'Avalon » et la « discordance de base-tertiaire » d'études antérieures en tant que regroupements de plusieurs discordances d'échelle plus modeste et nous déterminons leur âge de façon plus précise dans les puits étudiés. Une amélioration notable par rapport à nos plans antérieurs des phénomènes survenus dans la marge de Scotian est l'élargissement de la stratigraphie des phénomènes au cours du Jurassique précoce au moyen de repères stratigraphiques marins. Nous comparons le plan des phénomènes du Jurassique précoce au site 547B du projet de forage en eau profonde sur la marge marocaine conjuguée pour mieux limiter les intervalles éventuels de roche mère et les débuts de l'océan Atlantique central.

[*Traduit par la redaction*]

doi:10.4138/atlgeo.2023.009
2564-2987|23|0183–0239$9.55|0
Copyright © Atlantic Geoscience, 2023

INTRODUCTION

The Scotian Margin Play Fairway Analysis (PFA) project was a multidisciplinary study (under the auspices of the Offshore Energy Technology Research Association of Nova Scotia; OERA 2011) that examined the petroleum potential and exploration risk of the Mesozoic–Cenozoic Scotian Basin of offshore Nova Scotia. The project involved a government, industry, and academic partnership that integrated geophysical and geological data across the region, building on decades of prior studies (e.g., Wade and MacLean 1990), to understand the Scotian Margin tectonics, depositional history, and petroleum systems. The results had value for both applied exploration work and broader scientific inquiry about the history of the central Atlantic Ocean and the conjugate northwestern African margin (Sibuet *et al.* 2012). Follow-up studies (OERA 2016, 2019) refined the PFA work and extended the approach to adjacent areas, such as Georges Bank (OERA 2015) and the Paleozoic Sydney Basin (OERA 2017). The present paper focuses on the Laurentian Subbasin (OERA 2014; MacLean and Wade 1992), located at the northeastern extremity of the Scotian Basin, which makes up much of the passive Scotian Margin where it transitions to the southern Grand Banks of Newfoundland across the Newfoundland Transform Zone (Fig. 1).

As with the original Scotian Margin PFA work and other follow-up studies, the Laurentian Subbasin study involves well-based biostratigraphy from predominantly three fossil groups, palynomorphs, microfossils, and nannofossils. (The terms microfossils and micropaleontology in this study refer to larger inorganic-walled groups, mainly foraminifera, but also ostracods.) The biostratigraphic results from the original PFA study (OERA 2011) were presented in a detailed synthesis of the regional event stratigraphy in Weston *et al.* (2012). In the present study, new biostratigraphic analyses and re-evaluations of existing data from wells in the Laurentian Subbasin were used to constrain stratigraphic interpretations, age and paleoenvironments. The biostratigraphic interpretation was closely coordinated with a seismic-stratigraphic study of the region, especially when identifying major unconformities and maximum flooding surfaces (MFSs) of regional significance.

In this paper we present new biostratigraphic interpretations from four wells located within the Laurentian Subbasin — Bandol-1, East Wolverine G-37, Emerillon C-56, and Heron H-73 — and one from the conjugate Moroccan Margin, Deep Sea Drilling Project Leg 79 Site 547B (henceforth DSDP Site 547B; Fig. 1). In addition, we incorporate data released from the southern Grand Banks area following the original Laurentian PFA study (OERA 2014). We also extend the event stratigraphy of the Scotian Margin PFA and Weston *et al.* (2012) onto the southern Grand Banks and add new events that are not represented in wells studied on the Scotian Margin; this is especially pertinent for the Lower Jurassic part of the succession (Fig. 2). For clarity, the terms Scotian Margin and Grand Banks refer to geographic areas. The Scotian Basin, of which the Laurentian Subbasin is part, is a structural feature. The Scotian Basin underlies the outer part of the Scotian Margin and a southern part of the Grand Banks, with the Laurentian Subbasin underlying the geographic transition between the two geographical areas.

BACKGROUND AND TECTONIC SETTING

The Scotian Margin of offshore Nova Scotia and the eastern margin of the Grand Banks of Newfoundland are distinct zones of passive margin development, with the Scotian Margin representing extension between North America and western Africa and the eventual formation of the central Atlantic Ocean; the Newfoundland Margin represents extension between North America and Iberia and eventual formation of the North Atlantic (Srivastava *et al.* 2000; Tucholke *et al.* 2007; Labails *et al.* 2010; Sibuet *et al.* 2012). Although initial rifting began in both areas at a similar time, with syn-rift sedimentation occurring by the Late Triassic, seafloor spreading commenced off the Scotian Margin during the Early Jurassic (Labails *et al.* 2010; Sibuet *et al.* 2012), whereas it did not begin between the Grand Banks and Iberia until the Early Cretaceous after a second, Late Jurassic–Early Cretaceous rift phase (Sinclair 1995; Tucholke and Sibuet 2007). This difference in Mesozoic tectonic history has led to somewhat different stratigraphic successions in the two areas. Though Grand Banks stratigraphy was initially treated as a simple extension of the earlier-established Scotian Margin stratigraphy (McIver 1972; Jansa and Wade 1975), the stratigraphic scheme for the Grand Banks subsequently diverged for some intervals as differences became better understood (Grant and McAlpine 1990; McAlpine 1990; MacLean and Wade 1993; Fig. 2). However, the extensive hydrocarbon exploration and production in the Jeanne d'Arc Basin has biased stratigraphic studies towards the eastern Grand Banks and much less work has been published on the southern Grand Banks adjacent to its transition to the Scotian Margin.

The southern margin of the Grand Banks is marked by a now-inactive major transform zone, the Newfoundland Transfer Zone (Fig. 1), which offsets the passive margins to the north and south (MacLean and Wade 1992; Pe-Piper and Piper 2004). The Laurentian Subbasin straddles this structural transitional zone and consequently its stratigraphic nomenclature incorporates a mix of Scotian-Margin and Grand Banks terminology. Thus, clastic-dominated units such as the Missisauga and Logan Canyon formations (Fig. 2), the type areas for which are on the Scotian Margin, are still used in this area even though similar, roughly coeval clastic-dominated units within the Jeanne d'Arc Basin have different names (for example the Hibernia and Avalon formations; MacLean and Wade 1992; Grant and McAlpine 1990; McAlpine 1990). Structurally, the outboard portion of the southern Grand Banks defines the eastern extremity of the Scotian Basin, within the Laurentian Subbasin (Fig. 1), which encompasses all the western Atlantic wells studied here. Farther inboard on the southern

Copyright © Atlantic Geoscience, 2023

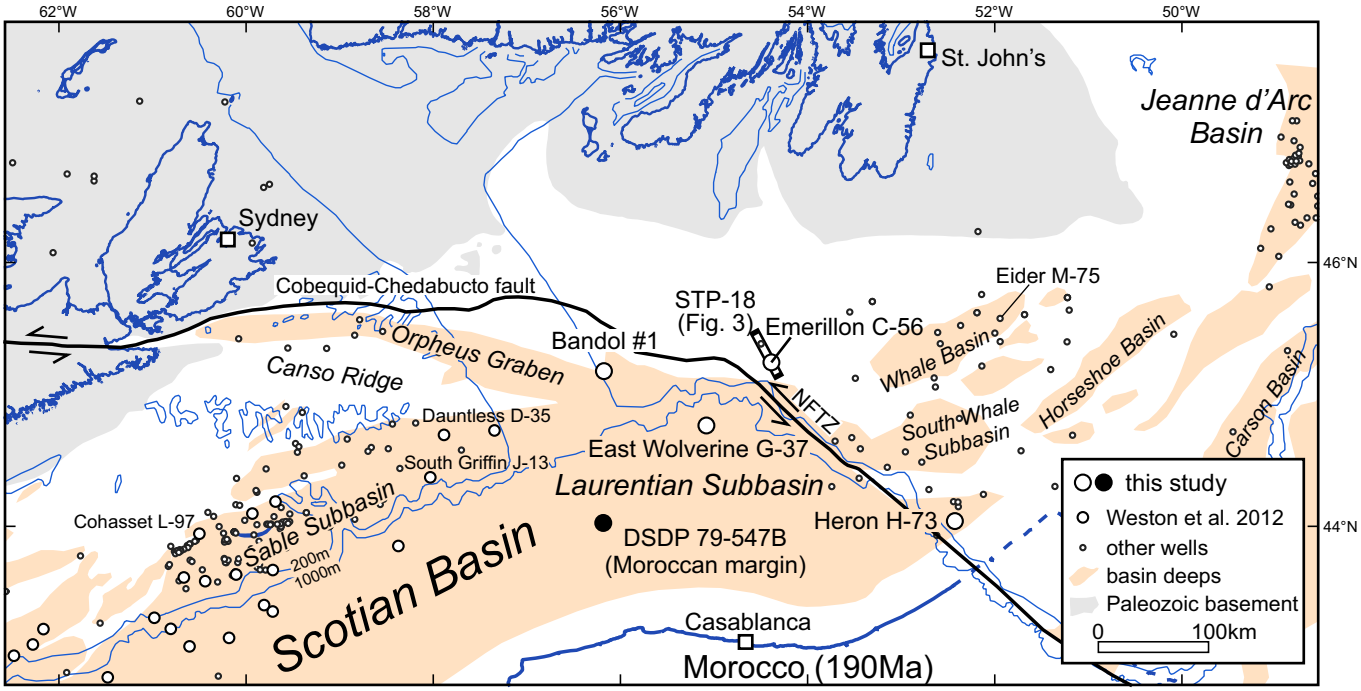

Figure 1. Location map for the Laurentian Subbasin and adjacent areas of the Scotian Margin and Grand Banks of Newfoundland showing well locations, including wells studied by Weston *et al.* (2012) and in the present study. Deeper basinal areas are shaded (generally >4 km), simplified from Williams and Grant (1998). The reconstructed position of the conjugate Moroccan Margin and the projected location of Deep Sea Drilling Project Leg 79, borehole 547B (filled well circle) are shown for 190 Ma (approximately the Pliensbachian/Sinemurian boundary) based on the rotation poles of Sibuet *et al.* (2012). The location of seismic line STP-18 provided in Figure 3 is also shown. NFTZ = Newfoundland Transfer Zone.

Grand Banks, the South Whale, Whale and Horseshoe basins possess similar stratigraphic successions to that of the Laurentian Subbasin. Relatively few published studies have focussed primarily on the southern Grand Banks, but Balkwill and Legall (1989), Enachescu (1988), Sinclair (1988), and MacLean and Wade (1992) are notable earlier studies, and stratigraphic correlations were proposed by McAlpine *et al.* (2004). The Laurentian PFA (OERA 2014) is one of the most recent integrations of tectonic, structural, and stratigraphic work in the area, although Cawood *et al.* (2022) recently examined the tectonic history in additional detail.

Although the focus of the present work is on the Mesozoic–Cenozoic succession, significant Devonian–Carboniferous basins also occur on the southern Grand Banks, and in some areas, structures formed from Carboniferous salt have impacted younger strata (Wade and MacLean 1990; MacLean and Wade 1993; Pascucci *et al.* 1999; Fig. 3). Late Triassic and Early Jurassic salt tectonics related to the two Mesozoic rift phases are also a major structural influence in the region (Balkwill and Legall 1989; McAlpine 1990; Hanafi *et al.* 2022).

A prominent feature of Grand Banks stratigraphy is a geographically and temporally extensive hiatus, the Avalon Unconformity that, at its maximum duration, extends from the Early Jurassic to the Late Cretaceous (Fig. 2; Jansa and Wade 1975; Grant and McAlpine 1990). Over much of the Grand Banks, this break occurs as an angular unconformity placing Upper Cretaceous strata above Jurassic strata (e.g., Fig. 3), but toward depocentres such as the Jeanne d'Arc Basin it separates into three to four individual unconformities (Grant and McAlpine 1990).

Biostratigraphic works on the southern Grand Banks have been mostly in the context of broader studies across offshore eastern Canada, such as Barss *et al.* (1979) on palynology and Ascoli (1990) on foraminifera, ostracods and calpionellids; study of calcareous nannofossils has been limited to the Upper Cretaceous (Doeven 1983). Williams *et al.* (1990) summarized the biostratigraphic results for offshore eastern Canada. Additional unpublished reports on analyses by industry exist but usually represent studies conducted following initial drilling, with only a limited number of more recent (post-1980s) studies. Notable exceptions include studies of the Bandol-1, East Wolverine G-37 and Emerillon C-56 wells, which are included and referenced in the present study (Fig. 4).

The conjugate Moroccan margin (Fig. 1) has also been the subject of industry and academic borehole studies. Although the detailed tectonic and stratigraphic context of the Moroccan margin is beyond the scope of this study, we have compared results from the Laurentian Subbasin wells with those from the Lower Jurassic of the cored section from DSDP Site 547B on the Mazagan Plateau (Hinz *et al.* 1984). Based on the plate reconstructions of Labails *et al.* (2010) and Sibuet *et al.* (2012), DSDP Site 547B projects to a

Copyright © Atlantic Geoscience, 2023

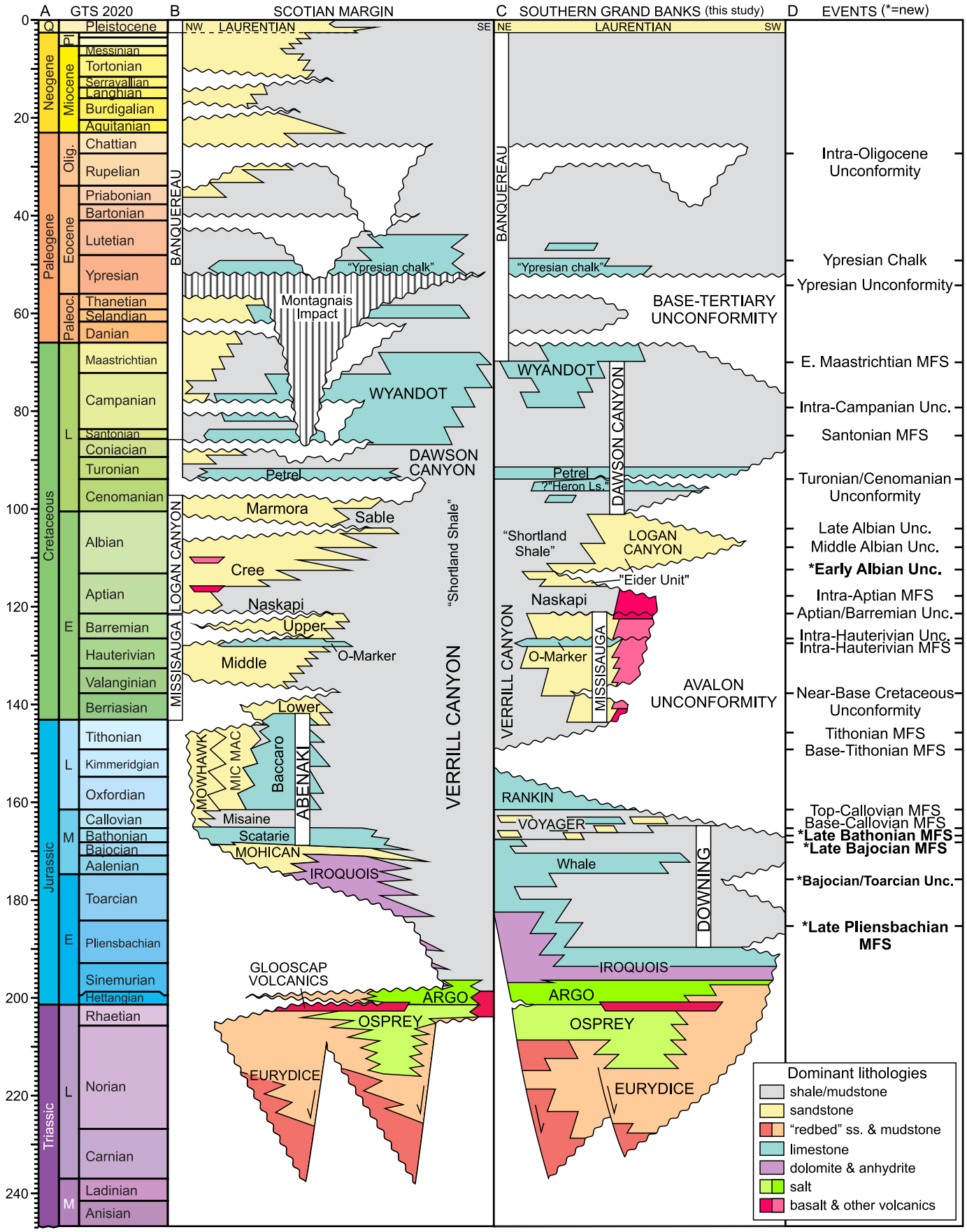

Copyright © Atlantic Geoscience, 2023

location only a few hundred kilometres away from some of the other wells examined herein, and it was adjacent to the Laurentian Subbasin during the rifting and earliest spreading phases of the central Atlantic Ocean (Fig. 1).

MATERIALS AND METHODS

Well selection

We selected wells primarily on the basis of stratigraphic penetration, availability of related seismic lines, and availability of existing data. The localities chosen represent the westernmost wells on the southern Grand Banks (Fig. 1) except for Heron H-73, which lies farther east and was picked because of its relatively deep stratigraphic penetration (to the Argo Formation salt), presence of post-salt Lower Jurassic strata, and its distal shelf-margin location, permitting ties with available seismic data to more westerly wells in the study.

For the wells Emerillon C-56 and Heron H-73, the original drilling parameters are quoted in feet in data sources used by this paper (e.g., Ascoli 1986; Barss *et al.* 1979), whereas the original drilling parameters are in metres for the wells Bandol-1 and East Wolverine G-37. When discussing the biostratigraphy of Emerillon C-56 and Heron H-73, we discuss depths first in feet, with a conversion to metric to facilitate later use of the interpretations in correlations and seismic mapping.

Biostratigraphic approach

Biostratigraphic methods in this study parallel those of Weston *et al.* (2012), to which the reader is referred for greater detail. As in that study, we rely on integration of several biostratigraphic disciplines: calcareous microfossils (foraminifera and ostracods), palynomorphs (dinoflagellates, acritarchs, and pollen and spores—collectively miospores), and nannofossils (mainly coccoliths). The biostratigraphic data evaluated in this study consist mainly of pre-existing data of various vintages, supplemented by targeted new analyses (Fig. 4). Our data sources are outlined in the following over-view.

(1) The BASIN database contains exhaustive geological, geophysical and engineering information, mostly generated by government scientists working on materials derived from petroleum exploration activities, primarily from offshore eastern Canada. A version of the database is available publicly (https://basin.gdr.nrcan.gc.ca/index_e.php). An internal restricted-access version of this database is available only within the Geological Survey of Canada (GSC), but contains information for Emerillon C-56 and Heron H-73 that were available to us via co-authors at GSC Atlantic. This data includes sample by sample taxon lists that provide invaluable information for assessing taxon distribution, especially last downhole occurrences. Data from this source are acknowledged in the results section below by reference to the respective author "in the BASIN database".

(2) Recent industry reports for Bandol-1 and East Wolverine G-37 that include quantitative data and full range charts; these are directly referenced as appropriate herein.

(3) A recent publication by Ainsworth *et al.* (2016), including biostratigraphic-event data for East Wolverine G-37 and Emerillon C-56.

(4) New quantitative micropaleontological and nannofossil preparations and analyses undertaken by us for this project for Bandol-1, East Wolverine G-37 and Heron H-73 using cuttings samples. For methodology, see Weston *et al.* (2012); and for full results of analyses, see the Supplementary Data associated with this paper.

(5) A review of pre-existing palynological slides held at the Canada–Newfoundland and Labrador Offshore Petroleum Board (C-NLOPB) for Heron H-73 (https://home-cnlopb.hub.arcgis.com/) and at Geological Survey of Canada (Atlantic) for Emerillon C-56.

In addition to the four wells from offshore eastern Canada for which we undertook new analyses, we also analyzed new nannofossil and palynological samples from conventional core in the Early Jurassic interval of DSDP Site 547B on the Mazagan Plateau of Morocco. The aim of the analyses from the DSDP site is to clarify and compare the ages and depositional settings of potential source rock horizons to Lower Jurassic source horizons in Heron H-73 (see OERA 2014, pl. 5.4.8). A plate reconstruction using the Euler rotation poles of Labails *et al.* (2010) and Sibuet *et al.* (2012) and rendered with GPlates (https://www.gplates.org/) is used in Figure 1 to show the relative positions of the Heron H-73 well and the reprojected DSDP Site 547B at about 190 Ma (Sinemurian–Pliensbachian).

Figure 2. (previous page) Wheeler diagram showing lithostratigraphy (B and C) and biostratigraphic events (D) on the Scotian Margin (B) in comparison to the southern Grand Banks area of this study (C). Scotian Margin chart is modified from Weston *et al.* (2012) and Deptuck and Altheim (2018); it does not show post-depositional salt tectonic movement. Grand Banks chart is modified from Sinclair (1988), McAlpine (1990), and MacLean and Wade (1992). Age of volcanic rocks is based on Pe-Piper and Jansa (1987) and Bowman *et al.* (2012). Timescale (A) is from Gradstein *et al.* (2020). Two colour shades for "redbeds" refer to sandstone and mudstone-dominated lithologies, respectively, and the two shades for volcanic rocks refer to basalts and to other types of volcanic rocks, respectively. Formation labels are in upper case, members are lower case. Informal units are in quotation marks. Abbreviations: ls. = limestone; ss. = sandstone; Unc. = unconformity; MFS = maximum flooding surface; Pl. = Pliocene; Olig. = Oligocene; Paleoc. = Paleocene; E. = Early; M. = middle; L. = Late.

Copyright © Atlantic Geoscience, 2023

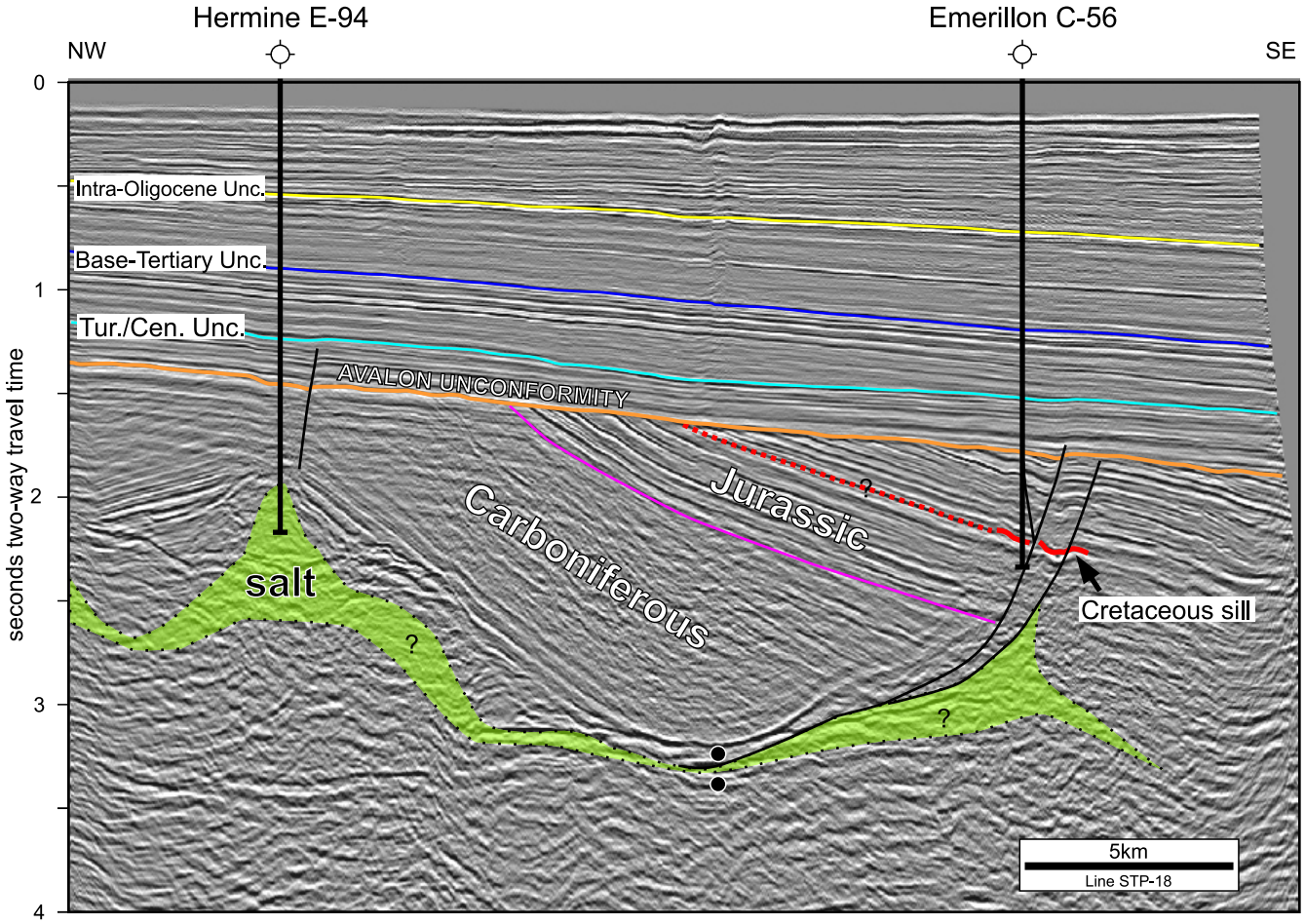

Figure 3. Interpretation of seismic line STP-18 (Geological Survey of Canada, St. Pierre Survey of 1983), which passes through Hermine E-49 and Emerillon C-56 (see Fig. 1 for location). The seismic event corresponding to the Avalon Unconformity forms a prominent angular unconformity in most of the region and is well expressed here, truncating both the Paleozoic and Mesozoic sections. Emerillon C-56 penetrates a Cretaceous sill (Bowman *et al.* 2012; red line) and the well may also cross at least one fault in the Middle or Early Jurassic part of the succession, depending on the exact well tie. Carboniferous salt is penetrated at Hermine E-94 and salt-related structures at depth likely include a salt weld (paired black dots) or similar structure. Interpretation modified from Pascucci *et al.* (1999), OERA (2014), and Bowman (2010). Tur./Cen. Unc. = Turonian/Cenomanian Unconformity.

While the focus of this study is biostratigraphy, we have closely integrated the biostratigraphic results with lithostratigraphy, wireline geophysical logs, and seismic stratigraphy. Rather than traditional zone-based biostratigraphy (e.g., Williams *et al.* 1990), we have relied on individual biostratigraphic well events and their association with lithostratigraphic and geophysical log signatures that indicate regional sequence stratigraphic surfaces; sequence boundaries and maximum-flooding surfaces. The latter are recognizable as peaks in abundance and diversity of marine forms within sedimentary successions (Armentrout 1996; Emery and Myers 1996), ideally identified from sample-by-sample quantitative data at tens-of-metres scale. In marine shelf settings these peaks are commonly associated with fine-grained sediments, higher gamma-ray log signatures and more abundant carbonate deposition. In a shelf setting, maximum flooding surfaces contrast with intervals that are dominated by coarse-grained clastic sediments and terrestrial palynomorphs in contrast to typical marine biotas, which are concomitantly absent or low in abundance and diversity. The latter intervals are typically where sequence boundaries are located, often in association with the development of a significant unconformity. By using sample-by-sample quantitative data through a well section, major changes in biostratigraphic assemblage compositions can be related to stratigraphic hiatuses and shifts in depositional environments that represent major sequence boundaries (Emery and Myers 1996). The potential well-log sequence stratigraphic events recognized within the biostratigraphic data are integrated with lithofacies and wireline log evidence to provide a single depth for the surface within a well section. Across multiple wells, these surfaces are checked by seismic mapping, which allows recognition of the most laterally extensive, time-significant surfaces, be they MFSs or sequence

Copyright © Atlantic Geoscience, 2023

Well Name	New Samples Analysed			Biostratigraphic Data Reviewed		Interval	
	Micropalaeo	Nannopalaeo	Palynology			metres	feet
Bandol-1	64	64	0	Davies and Huang (2001)	P	1000–4045	
East Wolverine G-37	0	23	0	Rutledge (2010); Ainsworth *et al.*(2016)	M, N, P	2920–6857	
Emerillon C-56	0	0	0	Ascoli (1981, 1986); Williams (1979); Ainsworth *et al.* (2016)	M, P	435.9–3276.6	1430–10 750
Heron H-73	0	16	77	Gradstein (1977); Williams (1978,1979)	M, P	469.4–3657.6	1550–11 970
DSDP 547B	0	6	4	Riegraf *et al.* (1984)	M	847.55–905.2	

M = Micropalaeontology
N = Nannopalaeontology
P = Palynology

Figure 4. Summary of the new and pre-existing biostratigraphic data on which this study is based, listing the sources of information consulted and the disciplines involved.

boundaries. This facilitates division of the section into useful seismic sequence stratigraphic units for more detailed study. For the wells studied here, seismic mapping was completed by Beicip-Franlab (OERA 2014).

STRATIGRAPHY

Lithostratigraphic framework

In general, we have followed the lithostratigraphic terminology used by McAlpine (1990), Wade and MacLean (1990), and MacLean and Wade (1992, 1993) for Emerillon C-56 and Heron H-73; but as the study area straddles the boundary between the Scotian Margin and Grand Banks, stratigraphic nomenclature of both areas can be, and has been, applied by different authors. We provide both alternatives where possible, although we routinely display only the Scotian Margin terminology on the Summary Logs in the Supplementary Data, following MacLean and Wade (1993) and because these wells are within the Scotian Basin. For example, we use the informal term "Eider unit" within the Logan Canyon Formation as in MacLean and Wade (1992, 1993) rather than the formalized Eider Formation (McAlpine 1990) because of uncertainties about correlations from our study area to the Eider Formation type section farther northwest (Eider M-79; Fig. 1), and also because of the lack of an equivalently-defined Naskapi Member subdivision within the Eider Formation. In places we have modified individual well lithostratigraphic picks based on wireline geophysical logs and using biostratigraphic guidance. For wells drilled since earlier lithostratigraphic studies (Bandol-1 and East Wolverine G-37), we revised operator terminology or well picks from the C-NLOPB as necessary. A more detailed account of regional lithostratigraphy can be found in the above references and Weston *et al.* (2012).

Chronostratigraphy

Chronostratigraphic units and numerical ages are based on the Geological Time Scale (GTS; Gradstein *et al.* 2020). This time scale is significantly different from that used in Weston *et al.* (2012), in which they relied on earlier versions of the GTS (primarily Gradstein *et al.* 2005 and Ogg *et al.* 2008), with some modifications. However, many of the changes in the 2020 GTS are more compatible with our preferred usage (see comments in Weston *et al.* 2012, p. 1423). Whereas our sequence and biostratigraphic events have been recalibrated to the 2020 timescale, the original timescale used in the Laurentian PFA (OERA 2014) reflects the older timescale (Gradstein *et al.* 2005); thus, numerical ages associated with the seismic events in that study do not correspond chronostratigraphically to the present time scale.

Biostratigraphy

The stratigraphic ranges of the calcareous microfossils (mainly foraminifera and ostracods) are based on those defined in Ohm (1967), Ascoli (1976, 1988, 1990), Bartenstein (1979), Kennett and Srinavasan (1983), Robaszynski *et al.* (1984), Bolli *et al.* (1985), Boudagher-Fadel *et al.* (1997), Olsson *et al.* (1999), Premoli Silva and Verga (2004), Pearson *et al.* (2006), Wade *et al.* (2011, 2018), and Gradstein *et al.* (2017a, b). Planktonic foraminiferal ranges in the Tertiary are based on the zonation schemes of Blow (1969) and Wade *et al.* (2011) (see Wade *et al.* 2011 for correlation of these zonation schemes). The stratigraphic ranges of the nannofossils are based on Martini (1971), Thierstein (1973), Perch-Nielsen (1985a, b), and papers in Bown (1998). The ranges of the dinocysts and miospores are based on Williams (1975), Bujak and Williams (1977), Thusu (1978), Woollam and Riding (1983), Riding (1984), Williams and Bujak (1985), Powell (1992), Stover *et al.* (1996), Williams *et al.* (1999, 2004), Poulsen and Riding (2003), and Fensome *et al.* (2008, 2009).

We have generally recorded events as first downhole occurrences (FDOs) and last downhole occurrences (LDOs) — equivalent to last appearance datums (LADs) and first appearance datums (FADs) respectively. The nature of cuttings samples derived from well sections means that FDO events are generally more reliable and used most extensively, although the potential for reworking and the occurrence of downhole caving can complicate interpretation, as can the introduction of exotic drilling mud. The issue of sample

Copyright © Atlantic Geoscience, 2023

contamination due to caving means that a progressively "downhole" approach to interpretation works most reliably and, therefore, as is the common convention when dealing with well sections, the stratigraphy in wells is discussed from youngest to oldest. The naming of biostratigraphic events reflects this convention by placing the name of the younger age ahead of the older age where appropriate (e.g., Albian–Aptian); this is consistent with OERA (2011) and Weston *et al.* (2012). The terms Early/Lower, Middle, Late/Upper for units above age/stage level begin with upper case letters where formal and lower-case initial letters where they are informal. For simplicity and to avoid confusion, similar terms at stage/age level are given lower case initial letters throughout, even though some are formally defined.

Taxonomic treatment follows the works cited by Weston *et al.* (2012) with the addition of more recent taxonomy for dinoflagellates (Fensome *et al.* 2019), nannofossils (Young *et al.* 2017) and planktonic foraminifera (Gradstein *et al.* 2017a, b; Wade *et al.* 2018). For a list of taxa cited in this study with full names and authorships, see Appendix A. For data newly generated, we use a question mark before a species name (e.g., ?*Zeugrhabdotus streetiae*) to indicate questionable species identifications; a question mark immediately after the genus name (e.g., *Adnatosphaeridium*? *chonetum*) indicates questionable generic assignment. For reviewed data from other authors, we cite a name incorporating a question mark as used by that author due to our uncertainty of their usage.

Detailed well summary charts and biostratigraphic range charts in the Supplementary Data are plotted with the StrataBugs™ program by StrataData Ltd. (https://www.stratadata.co.uk). Page-size well-plot figures were generated by a custom program by one of us (lithplot3 by AM).

RESULTS

The overall event stratigraphy used in this study is summarized in Figures 5 to 8. Whereas changes from the schemes in Weston *et al.* (2012) are minimal for the Cenozoic and Cretaceous, significant refinements have been made in the scheme for the Middle and Early Jurassic (Fig. 7).

We provide simplified page-sized summary charts and tables showing diagnostic biostratigraphic criteria, major stratigraphic and well-log sequence-stratigraphic interpretations for each of the four wells in Figures 9 to 15, with more detailed summary charts shown in Supplementary Data 1–4. Similar data for the section analyzed from DSDP Site 547B is shown in Figures 16 to 17 and Supplementary Data 5. Range charts for new biostratigraphic analyses and the pre-existing palynological data from Bandol-1 are provided in Supplementary Data 1.

Bandol-1

Our evaluation of Bandol-1 (Figs. 4, 9 to 11a) is based on palynological data published as species lists in the report by Davies and Huang (2001). These data are from 185 cuttings samples and 26 sidewall core samples. Additionally, we undertook 64 new micropaleontological and 64 new nannofossil analyses from cuttings samples collected from the Bureau Exploration-Production des Hydrocarbures (BEPH) in Paris, France. Occasional nannofossil "tops" (i.e., FDOs) were provided by Jiang in Davies and Huang (2001, their Appendix A). We reviewed the interval 1060–4045 m. A summary stratigraphic plot for this well is provided as Figure 11a (with legend in Fig. 10), and the interpreted stratigraphic breakdown is summarized in Figure 9. A more detailed summary chart and range charts of newly generated micropaleontological and nannofossil data are shown in Supplementary Data 1.

Occurrences of the dinocysts *Pentadinium laticinctum* subsp. *laticinctum* from 1060 m, *Pentadinium laticinctum* subsp. *granulatum* and *Palaeocystodinium* spp. from 1080 m and the top of persistent recovery of the dinocyst *Cleistosphaeridium ancyreum* (as *Systematophora ancyrea*) from 1100 m indicate an age no younger than intra-Tortonian at and below 1060 m. A distinct change in composition of the dinocyst flora occurs at 1280 m, associated with the FDO of *Spiniferites pseudofurcatus*, implying penetration of strata no younger than Serravallian from 1280 m. The sole occurrence of the dinocyst *Achomosphaera andalousiensis* at 1340 m suggests that strata between 1280 and 1340 m are of late Serravallian age. A slight positive downhole shift in the gamma-ray log at 1277 m may represent the position of the Tor1 sequence boundary of Hardenbol *et al.* (1998) that approximates to the Tortonian/Serravallian boundary (Ogg *et al.* 2016). Palynofloral assemblages are consistent with a broad Miocene age down to 1390 m, whereas the shallowest sample analyzed micropaleontologically, at 1360 m, yields a poor calcareous benthic foraminiferal assemblage consistent with a Neogene age.

Jiang in Davies and Huang (2001) noted a major change in nannofossil recoveries in the sample 1380–1390 m, with the FDOs of *Chiasmolithus bidens, Fasciculithus* spp., *Placozygus sigmoides* and *Ellipsolithus distichus*. These occurrences indicate penetration of strata of Thanetian to Selandian age by 1390 m, an interpretation supported by the occurrence of the Paleocene calcareous benthic foraminiferid *Bulimina* aff. *plena* at 1390 m. We therefore place a major unconformity between the Miocene and the Paleocene just above 1390 m, at sharp negative shifts (downhole) in the gamma-ray and sonic logs at 1388 m (i.e., faster sonic velocity). This hiatus correlates to the major Intra-Oligocene Unconformity of Weston *et al.* (2012). A Thanetian age equivalent to Martini nannofossil subzone NP9a was determined in the new nannofossil data beneath this unconformity, indicated by the FDOs of the Thanetian-restricted nannofossils *Fasciculithus alanii* and *Fasciculithus clinatus* at 1410 m; these occurrences occur within a rich, typically Thanetian to Selandian nannofossil assemblage. A distinct change in the composition of the micropaleontological assemblage occurs downhole at 1420 m, with the top of persistent common to abundant radiolaria (mainly *Cenosphaera* spp.). This

Copyright © Atlantic Geoscience, 2023

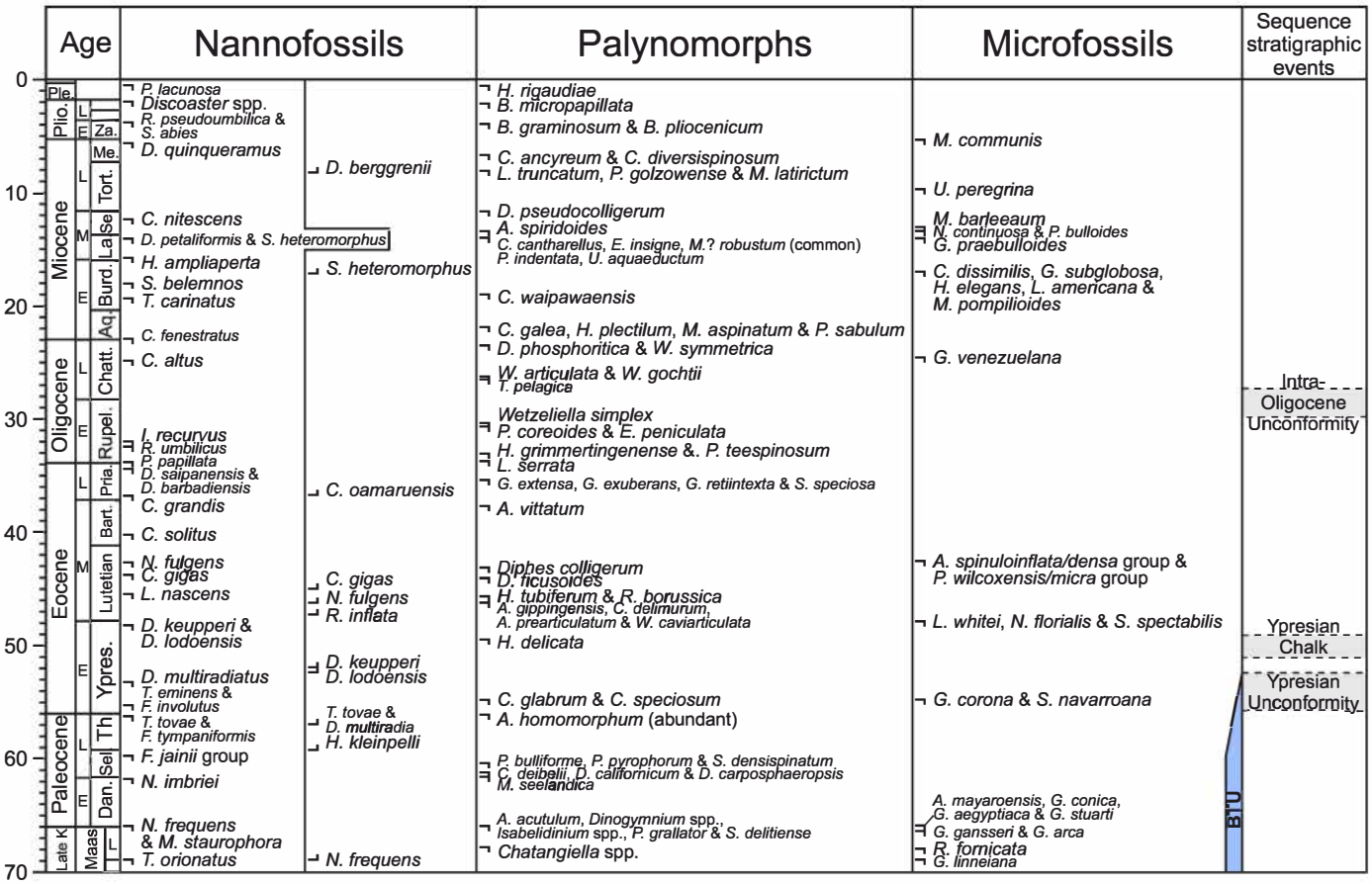

Figure 5. Key biostratigraphic events used for the Cenozoic in the present study, together with important sequence-stratigraphic events. Timescale is from Gradstein *et al.* (2020). New events in this study that were not recognized in Weston *et al.* (2012) are indicated in blue. Timescale abbreviations: Aq. = Aquitanian; Bart. = Bartonian; BTU = Base-Tertiary Unconformity; Burd. = Burdigalian; Chatt. = Chattian; Dan. = Danian; E = Early; L = Late; La = Langhian; Late K. = Late Cretaceous; M = Middle; Me. = Messinian; Ple. = Pleistocene; Plio. = Pliocene; Pria. = Priabonian; Rupel. = Rupelian; Se. = Serravallian; Sel. = Selandian; Th. = Thanetian; Tort. = Tortonian; Ypres. = Ypresian; Za = Zanclean. A listing of taxon names in full is provided in Appendix A.

event is associated with the FDO of the planktonic foraminiferid *Subbotina triloculinoides* at 1420 m, which implies a Selandian to Danian age, equivalent to Blow zones P4a–P1b. An age no younger than Selandian is confirmed by the FDOs of the dinocysts *Palaeoperidinium pyrophorum* at 1420 m and *Trithyrodinium* spp. at 1470 m. Nannofossil assemblages are dominated by *Coccolithus pelagicus* and *Toweius* spp., associated with relatively common *Fasciculithus tympaniformis* down to 1500 m, which indicates an age no older than Martini nannofossil zone NP5 of the Selandian to this depth. However, the FDO of the dinocyst *Trithyrodinium evittii* at 1500 m suggests penetration of strata of Danian age. The Selandian/Danian boundary is defined at the Sel1 sequence boundary of Hardenbol *et al.* (1998), as shown in Gradstein *et al.* (2020); we therefore interpret the Selandian/Danian boundary as being just above 1500 m, at the overall change in wireline log signature at 1489 m, associated with negative shifts in the density and resistivity logs and a positive shift in the sonic log downhole. The FDO of the dinocyst *Tanyosphaeridium xanthiopyxides* at 1580 m suggests an age no younger than intra-Danian, whereas the radiolarian *Cenosphaera* spp. and the nannofossil *Coccolithus pelagicus* characterize micropaleontological and nannofossil assemblages, respectively throughout the Paleocene interval from 1420 to 1630 m. A consistent common recovery of typical Late Cretaceous nannofossils and rare Cretaceous planktonic foraminifera occur through this interval, which we attribute to reworking.

A sharp downhole increase in the abundance of Late Cretaceous nannofossils occurs at 1640 m, which we attribute to penetration of in situ Upper Cretaceous strata. The FDOs of the nannofossils *Hexalithus gardetiae* and *Eiffellithus eximius* at 1640 m indicate that the top of the Cretaceous section in Bandol-1 is Campanian; thus we interpret a Danian/Campanian unconformity in this well to be at 1636 m, at the sharp negative spikes in the gamma-ray and sonic logs and the changes in trends of the sonic and neutron logs. We use the term Base-Tertiary Unconformity (BTU) here following previous work (e.g., MacLean and Wade 1993;

Copyright © Atlantic Geoscience, 2023

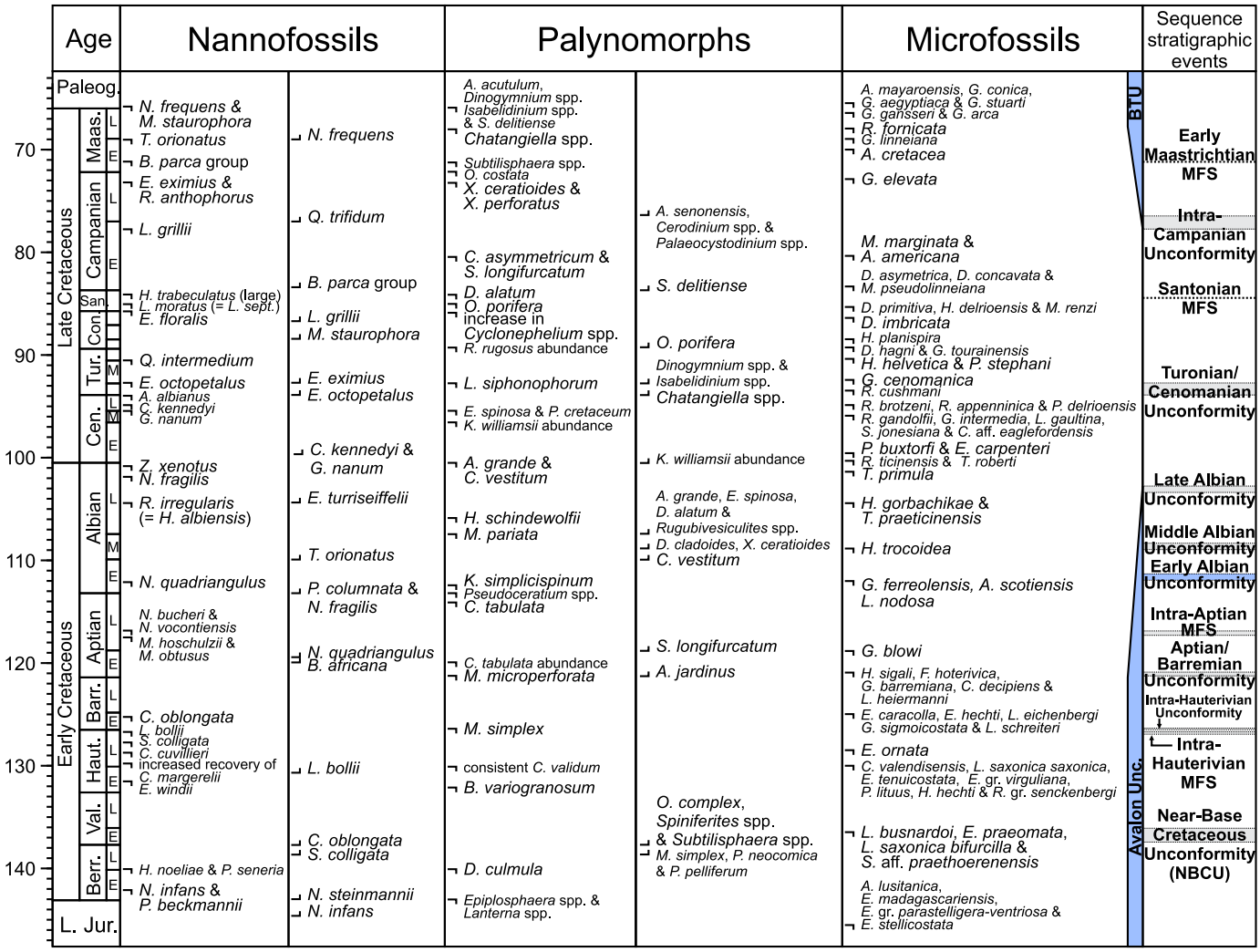

Figure 6. Key biostratigraphic events used for the Cretaceous in the present study, together with important sequence-stratigraphic events. In the case of some unconformity events, the event is placed at the smallest hiatus interval for the relevant unconformity, but at many locations on the southern Grand Banks in the Late Jurassic through Cretaceous, multiple unconformities are amalgamated into a single "Avalon Unconformity" of variable age (see text and Fig. 2). New events in this study that were not recognized in Weston *et al.* (2012) are indicated in blue. Timescale is from Gradstein *et al.* (2020). Abbreviations: Barr. = Barremian; Berr. = Berriasian; Cen. = Cenomanian; Con. = Coniacian; E = Early; Haut. = Hauterivian; L = Late; L. Jur. = Late Jurassic; M = Middle; Maas. = Maastrichtian; MFS = maximum flooding surface; Paleog. = Paleogene; San. = Santonian; Tur. = Turonian; unc. = unconformity; Val. = Valanginian. A listing of taxon names in full is provided in Appendix A.

equivalent to the Fox Harbour Unconformity of Deptuck *et al.* 2003). Another distinct change in the composition of the nannofossil assemblages occurs in the sample at 1650 m, which contains the FDOs of species such as *Broinsonia enormis* and *Lithastrinus grillii.* These species are indicative of an age no younger than early Campanian, a determination supported by the FDO of the planktonic foraminiferid *Marginotruncana marginata* at 1650 m. It is notable that palynological assemblages show a consistent change in composition downhole from 1660 m, suggestive of a marked change in depositional conditions from 1660 m downhole. In combination therefore, these three datasets suggest that another unconformity surface lies between 1640 m and 1650 m, equating with the Intra-Campanian Unconformity of Weston *et al.* (2012). We place this hiatus at the strong downhole negative shifts in gamma-ray, sonic, and neutron log responses at 1644 m; such shifts are typical of penetration of the chalks of the Wyandot Formation.

The FDO of the dinocyst *Odontochitina porifera* at 1660 m indicates an intra-Santonian to Coniacian age. The FDO of the planktonic foraminiferid *Marginotruncana pseudolinneiana* at 1670 m confirms that the age is no younger than Santonian, whereas the sole occurrence of the calcareous benthic foraminiferid *Stensioina granulata polonica*, also at

Copyright © Atlantic Geoscience, 2023

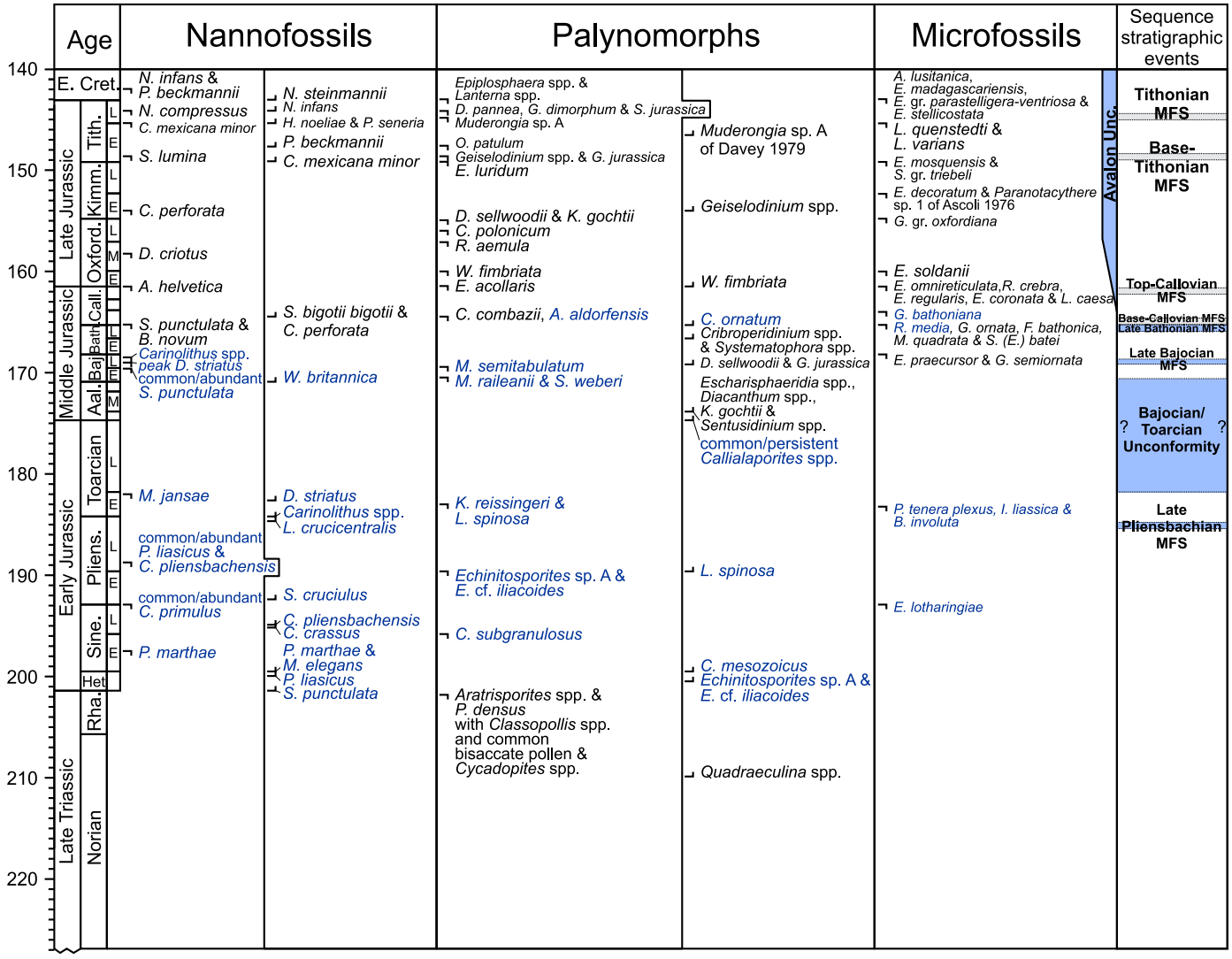

Figure 7. Key biostratigraphic events used for the Jurassic and Late Triassic in the present study, together with important sequence-stratigraphic events. In the case of some unconformity events, the event is placed at the smallest hiatus interval for the relevant unconformity, but at many locations on the southern Grand Banks in the Late Jurassic through Cretaceous, multiple unconformities are amalgamated into a single "Avalon Unconformity" (see text and Fig. 2). New events in this study that were not recognized in Weston *et al.* (2012) are indicated in blue. Timescale is from Gradstein *et al.* (2020). Abbreviations: Aal. = Aalenian; Baj. = Bajocian; Bath. = Bathonian; Call. = Callovian; E = Early, E. Cret. = Early Cretaceous; Het. = Hettangian; Kimm. = Kimmeridgian; L = Late; M = Middle; MFS = maximum flooding surface; Oxford. = Oxfordian; Pliens. = Pliensbachian; Rha. = Rhaetian; Sine. = Sinemurian; Tith. = Tithonian; Unc. = Unconformity. A listing of taxon names in full is provided in Appendix A.

1670 m, implies a restricted Santonian age. The gamma-ray and sonic logs show increasing up-hole trends (increasing gamma-ray and slower sonic) from around 1670 m to coincident positive spikes at 1654 m, whereas a peak in nannofossil density occurs around 1650–1670 m. The increasing uphole trends in the wireline data are typical of a marine transgression, and the positive spikes in the gamma ray and sonic logs and the peak in nannofossil density are characteristic of a condensed interval related to a maximum flooding surface. We infer that the Santonian MFS, defined in Weston et al. (2012), lies at the positive spikes in the gamma-ray and sonic logs at 1654 m in Bandol-1.

The sole occurrence of the planktonic foraminiferid *Marginotruncana schneegansi* at 1675 m implies an age no younger than early Santonian from that depth, whereas the peak in abundance of the dinocyst *Odontochitina porifera* between 1700 and 1720 m is characteristic of a Coniacian age. The LDO of the calcareous benthic foraminiferid *Stensioina exsculpta* at 1755 m and occurrences of the calcareous benthic foraminiferid *Stensioina granulata* at 1755 m and 1785 m are typical of the Coniacian. The LDO and base of persistent recovery of the nannofossil *Lithastrinus grillii* at 1780 m implies an age no older than late Coniacian to this depth, whereas

Copyright © Atlantic Geoscience, 2023

Event name in this paper	Name in OERA (2014) and associated seismic horizon	OERA (2014) plate number & description, or other source
Intra-Oligocene Unconformity	Mid Oligocene Unconformity (T29)	pl. 7-3-2
Ypresian Chalk		see Weston *et al.* 2012
Ypresian Unconformity	Base Ypresian Chalk (T50)	pl. 7-3-4
Base-Tertiary Unconformity	Intra-Campanian Unc. (K78) to Ypresian Unc. (T50) (merged)	pl.4-3-1 and 4-4-1; top Cretaceous-base Tertiary (TK) event of MacLean & Wade 1992
Early Maastrichtian MFS		see Weston *et al.* 2012
Intra-Campanian Unconformity	Intra-Campanian Unc. (K78)	see Weston *et al.* 2012
Santonian MFS		see Weston *et al.* 2012
Turonian/Cenomanian Unconformity	Cenomanian Turonian Unconformity (K94)	pl. 7-3-6
Late Albian Unconformity	Late Albian Unconformity (K101)	pl. 7-3-8
Early Albian Unconformity (new)	Early Albian Unconformity (above K112)	defined herein, also pl. 4-4-1 & 4-4-2
Intra-Aptian MFS	Intra Aptian MFS (above K125)	see Weston *et al.* 2012
Aptian/Barremian Unconformity	Aptian/Barremian Unconformity (K125)	see Weston *et al.* 2012
Intra-Hauterivian MFS	Hauterivian MFS (K130)	pl. 7-3-10
Near-Base Cretaceous Unconformity (NBCU)	Berriasian / Valanginian Unconformity (K137)	pl. 7-3-12
Avalon Unconformity	Cretaceous/Jurassic Unc. (diachronous K147 & K137 + others)	pl. 4-1-1, 4-3-1, 4-3-2, & 7-3-12; see MacLean & Wade 1992
Tithonian MFS	Tithonian MFS (just above J150 seismic horizon)	pl. 7-3-14
Base-Tithonian MFS	Near Tithonian MFS (just below J150 seismic horizon)	pl. 7-3-14
Top-Callovian MFS	Near Callovian MFS (above J163 seismic horizon)	pl. 7-3-16
Base-Callovian MFS	Near Callovian MFS (below, diachronous with J163)	pl. 7-3-16
Late Bathonian MFS (new)	Bathonian MFS (J166)	defined herein
Late Bajocian MFS (renamed)	Late Bajocian MFS	see Bathonian/Bajocian MFS of Weston et al. 2012
Bajocian/Toarcian Unconformity (new)	Bajocian/Toarcian Unconformity (J170)	pl. 4-1-1, 4-2-1, and 4-3-1
JPl8 sequence boundary of Haq (2018)	not recognized	tentative - see Haq (2018)
Late Pliensbachian MFS (new)	Pliensbachian MFS (J186)	pl. 4-1-1, 4-2-1, and 4-3-1

Figure 8. Sequence-stratigraphic events recognized in this study using biostratigraphy, and the equivalent or approximately equivalent seismic horizons in the Laurentian PFA study (OERA 2014; Weston *et al.* 2012, or other sources if relevant). Some events are new in the present study (in bold) and were not fully defined in detail in OERA (2014) and are defined here. The Avalon Unconformity is an amalgamated event that encompasses a variable number of other events depending on location and is thus highly diachronous (see Figs. 2, 6, and 7). Seismic horizon names (e.g., J186, K137) are the original designations in OERA (2014) and are not recalibrated to the Gradstein *et al.* (2020) timescale. Abbreviations: MFS = Maximum Flooding Surface; Unc. = Unconformity.

there is also the base of persistent common to abundant recovery of the nannofossil *Micula staurophora* at 1780 m, confirming an age no older than intra-Coniacian at 1780 m. The persistent occurrence of the dinocyst *Odontochitina porifera* to at least 1790 m also suggests a Coniacian age. The interval 1644–1790 m is therefore considered to be early Campanian to Coniacian.

A sharp change in the composition of the nannofossil assemblages occurs at 1810 m, associated with the FDO of *Rhagodiscus achlyostaurion*. This event indicates an age no younger than middle Turonian at 1810 m and suggests that the Coniacian/Turonian boundary lies between 1790 and 1810 m. The sole occurrence of the planktonic foraminiferid *Marginotruncana sinuosa* at 1815 m suggests that strata from

Copyright © Atlantic Geoscience, 2023

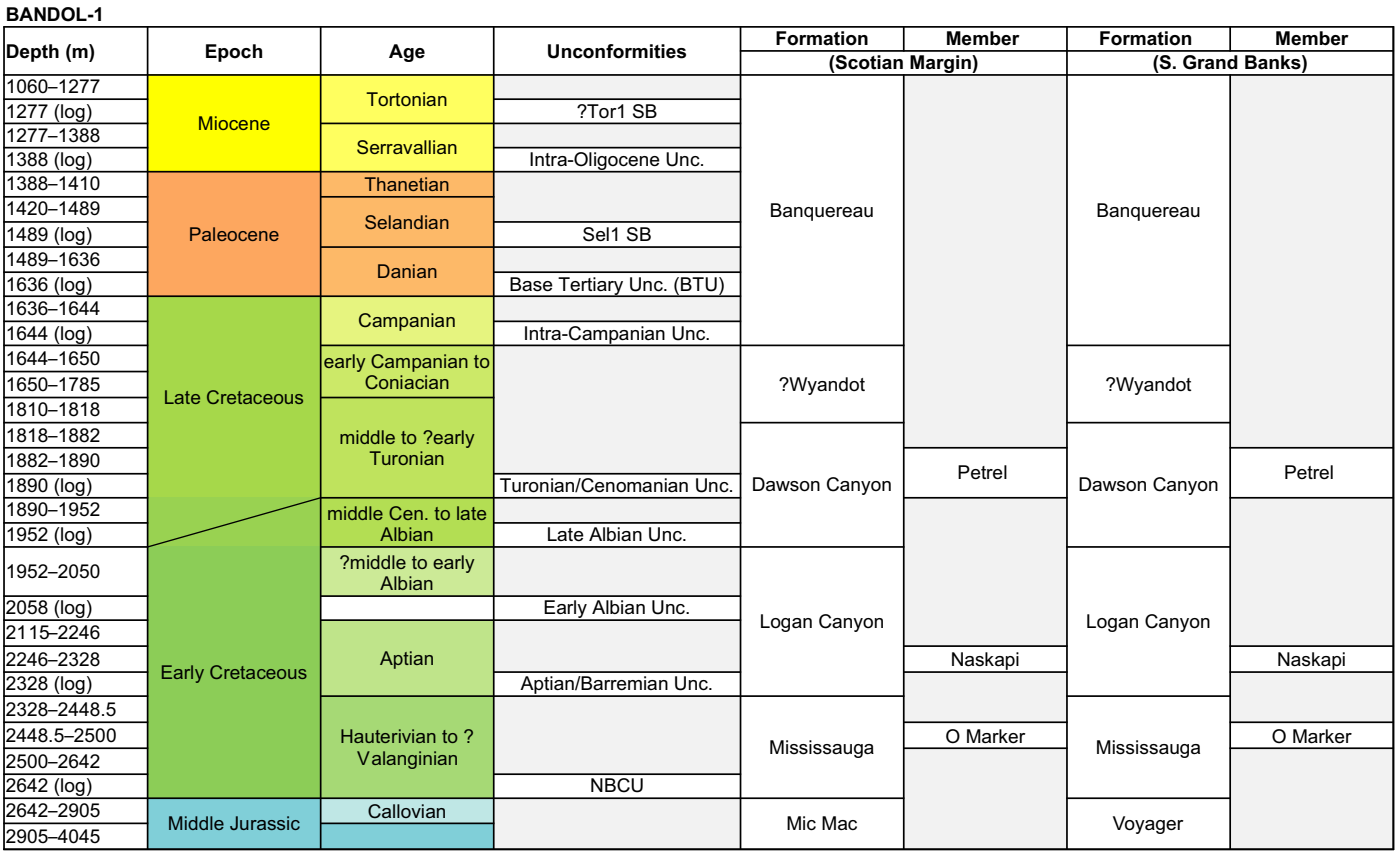

Figure 9. Stratigraphic summary of age, sequence stratigraphic events, and lithostratigraphic units in Bandol-1. Depths annotated with "(log)" were adjusted using the combination of biostratigraphic data and geophysical logs. Abbreviations: Unc. = unconformity; NBCU = Near-Base Cretaceous Unconformity; S. = south.

1810 to 1815 m are later middle Turonian. Occurrences of the nannofossil *Quadrum intermedium* at 1840 and 1870 m are indicative of a middle to early Turonian age, whereas the FDO of the nannofossil *Corollithion achylosum* at 1840 m supports an age no younger than middle Turonian. The base of persistent recovery of the nannofossil *Eiffellithus eximius* at 1870 m and of dinocysts of the genus *Isabelidinium* at 1875 m suggest an age no older than middle Turonian to that depth.

A major downhole decrease in nannofossil recovery occurs at 1900 m, but this is associated with the FDOs of the Cenomanian marker species *Microstaurus chiastius* and *Rhagodiscus asper*. We therefore place the Turonian/Cenomanian boundary between 1875 and 1900 m, at the subtle but sharp downhole increases in the gamma ray, sonic and bulk density logs at 1890 m. It is notable that biostratigraphic events typical of the early Turonian are missing and we infer that the Turonian/Cenomanian boundary in Bandol-1 is equivalent to the Turonian/Cenomanian Unconformity of Weston *et al.* (2012). This event occurs within a limestone interval that likely includes the Petrel Member of the Dawson Canyon Formation. We attribute a narrow interval (1882–1890 m) to the Petrel Member based on the gamma-ray and sonic wireline signature; but a broader and thicker than typical interval (extending into the Cenomanian) on the Scotian Margin could be chosen based on the cuttings log (as deep as 1905 m). Alternatively, the lower limestone unit of Cenomanian age could be assigned to the informal "Heron limestone" found on the southern Grand Banks farther east (Swift *et al.* 1975; see Heron H-73 below).

The FDO of the planktonic foraminiferid *Praeglobotruncana delrioensis* at 1905 m indicates an age no younger than middle Cenomanian, whereas an influx of dinocysts of the genus *Epelidosphaeridia* and the FDO of the nannofossil *Staurolithites aenigma* at 1930 m are characteristic of the early Cenomanian. The sole occurrence of the nannofossil *Corollithion kennedyi* at 1930 m confirms the Cenomanian age, supported by the sole occurrence of the middle to early Cenomanian restricted nannofossil *Gartnerago nanum* at 1930 m. The LDO of the planktonic foraminiferid *Praeglobotruncana delrioensis* at 1935 m implies an age no older than intra-late Albian.

Marked changes in the compositions of the nannofossil and palynological assemblages occur at 1960 and 1965 m, respectively, and the lithofacies become less calcareous at and below 1960 m. These changes suggest a marked landward shift in depositional conditions downhole around 1960 m. The nannofossil assemblage at 1960 m contains the FDOs of *Nannoconus fragilis* and *Staurolithites canthus*, indicating an age no younger than middle Albian. We infer that the change

Copyright © Atlantic Geoscience, 2023

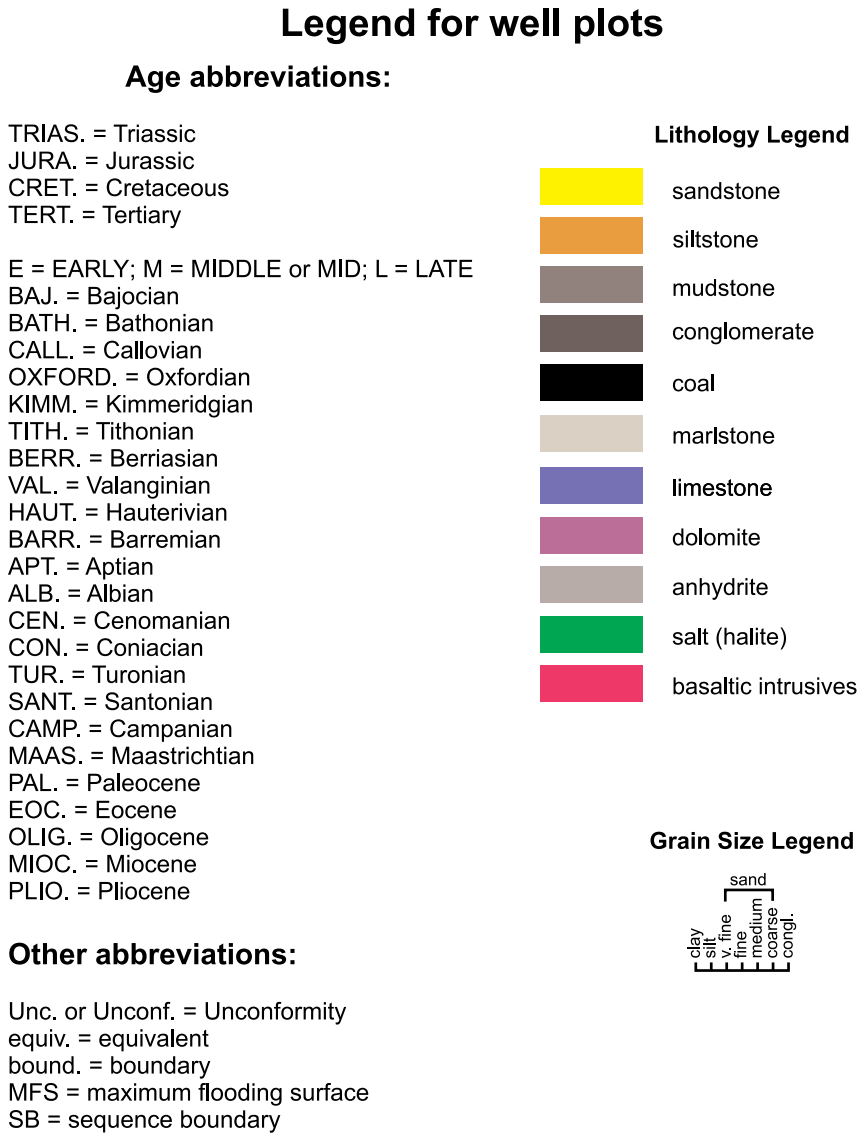

Figure 10. Legend for Figures 11, 14, and 17. Lithology and grain size (when available) were obtained from well history reports completed by the well operator. These have been modified with additional information from geophysical logs. Original data obtained from Bureau Exploration-Production des Hydrocarbures (BEPH) and the Canada–Newfoundland and Labrador Offshore Petroleum Board (C-NLOPB). Gamma-ray geophysical plots were obtained by digitizing paper logs or from the C-NLOPB's Data and Information Hub (https://home-cnlopb.hub.arcgis.com/). Wells are presented at the same vertical scale in metres or feet in measured depth below kelly bushing (MD KB).

in depositional conditions between 1930 and 1960 m and the stratigraphic break suggested by the nannofossil evidence are representative of an unconformity, which we place at the major positive shifts in the gamma-ray, sonic and neutron logs at 1952 m. We correlate this boundary to the Late Albian Unconformity of Weston *et al.* (2012) and here treat it as a proxy for the boundary between the Dawson Canyon and Logan Canyon formations.

A marked reduction in marine microfossils occurs from 1965 m downhole, and the palynofloras become strongly dominated by miospores from this depth. The sole occurrence of the nannofossil ?*Zeugrhabdotus streetiae* at 2050 m suggests that strata are no older than early Albian to at least 2050 m, an interpretation consistent with the FDO of the earliest Albian or older dinocyst *Kleithriasphaeridium simplicispinum* at 2035 m. However, within the lower part of this interval, older Cretaceous (Aptian–Barremian) calcareous benthic foraminifera such as E*pistomina hechti* at 2025 m and *Epistomina caracolla*, *Gavelinella barremiana* and *Lenticulina heiermanni* at 2055 m are present; we suggest that these are reworked. Major downhole negative shifts in the gamma-ray, sonic, neutron and resistivity logs occur at 2058 m, marking a sharp transition to more arenaceous lithologies. This transition is coincident with an overall change in palynofloras between 2055 and 2090 m, perhaps marking another major boundary or unconformity at 2058 m. An influx of nannofossils beneath this wireline event at 2080 m includes the FDOs of *Rucinolithus irregularis,*

Copyright © Atlantic Geoscience, 2023

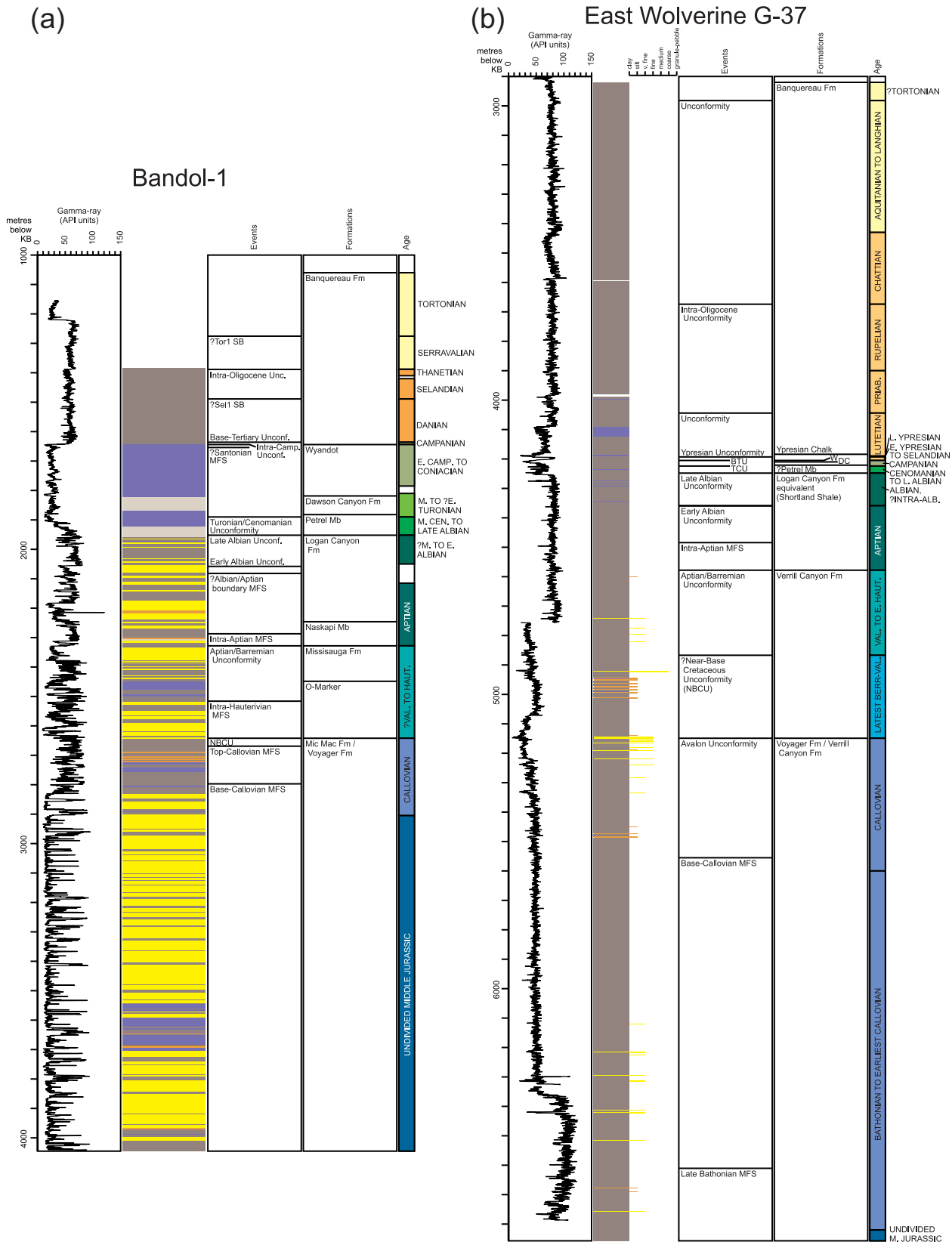

Figure 11. (a) Reduced-scale summary plot for Bandol-1 well. "Events" refers to sequence stratigraphic events (Figs. 8 and 18). Expanded-scale plots with additional geophysical logs and biostratigraphy data are presented in Supplementary Data 1. (b) Reduced-scale summary plot for East Wolverine G-37 well. Abbreviations: BTU = Base-Tertiary Unconformity; DC = Dawson Canyon Formation; fm = formation; mb = member, NBCU = Near-Base Cretaceous Unconformity; Sel1 SB = Sel1 sequence boundary of Hardenbol *et al.* (1998); TCU = Tor1 SB = Tor1 sequence boundary of Hardenbol *et al.* (1998); Turonian/Cenomanian Unconformity; W = Wyandot Formation. See Figure 10 for legend.

Copyright © Atlantic Geoscience, 2023

Hemipodorhabdus gorkae and *Tegumentum stradneri*. The latter two species range throughout the Early Cretaceous, but *Rucinolithus irregularis* is restricted to the earlier late Albian to latest Barremian. A peak in dinocyst recovery at 2115 m includes the FDOs of the typical Aptian markers *Cerbia tabulata* and *Aptea* cf. *polymorpha* of Davies and Huang (2001). The combination of wireline and biostratigraphic data (Fig. 11) suggests the presence of a sequence boundary that we term here the Early Albian Unconformity at 2058 m, which overlies a condensed interval related to a maximum flooding surface, most probably the Albian/Aptian boundary MFS of Weston *et al.* (2012). We place this maximum flooding surface close to the peak in nannofossil recovery, at 2082 m, where positive spikes in the gamma-ray and sonic logs coincide, associated with maximum separation of the neutron-density logs indicative of more argillaceous lithologies. The sole occurrence of the dinocyst *Aptea polymorpha* at 2220 m and the LDO of *Aptea* cf. *polymorpha* of Davies and Huang (2001) at 2260 m confirm an Aptian age below 2115 m, and the FDO of the dinocyst *Pseudoceratium pelliferum* at 2260 m is typical of an Aptian age. The LDO of the nannofossil *Eprolithus floralis* at 2260 m indicates that strata at this depth are no older than intra-early Aptian. Nannofossil recoveries increase between 2260 m and 2320 m, and the lithofacies are more argillaceous within this part of Bandol-1 than above; in addition, peaks in nannofossil and dinocyst recoveries occur at 2290 and 2310 m, respectively. In association with the lithofacies data, we suggest that a condensed interval related to a maximum flooding surface lies between 2260 and 2320 m, and so we place it at 2287 m, at the positive inflection on the gamma-ray curve that is coincident with a sharp positive spike on the sonic log (i.e., slower velocity) and maximum separation of the neutron-den-sity logs. The correlation of this event with the LDO of the nannofossil *Eprolithus floralis* at 2260 m and the FDO of the early Aptian or older nannofossil *Nannoconus bonetii* at 2320 m suggest that this is the Intra-Aptian MFS of Weston *et al.* (2012), which lies within the regionally recognized argillaceous Naskapi Member of the Logan Canyon Formation. Also notable is the LDO of the nannofossil *Rhagodiscus angustus* at 2320 m; this species does not range below the latest Barremian. We therefore assign the more argillaceous interval between 2246 and 2328 m to the Naskapi Member.

A sharp change in the composition of the palynoflora occurs between 2330 and 2365 m, although the FDO of the dinocyst *Dingodinium cerviculum* at 2365 m implies only an Aptian or older age. However, just below, in the sidewall core at 2379 m, Davies and Huang (2001) recorded the top of persistent recovery and first in situ downhole occurrence of the Hauterivian to latest Berriasian marker dinocyst *Muderongia simplex*. We therefore infer that the sharp change in palynofloral composition between 2330 m and 2365 m reflects transition across the regional Aptian/Barremian Unconformity of Weston *et al.* (2012), which we place at the overall change in wireline log signature (particularly major downhole negative shifts in the resistivity, density and gamma-ray logs) at 2328 m, reflecting penetration of a thick sandstone. We suggest that this is the boundary between the Logan Canyon and Missisauga formations in Bandol-1 and that the unconformity marks a sharp transition from the Aptian into the Hauterivian.

Palynofloras typical of the Early Cretaceous persist downhole to 2650 m, where the base of persistent recovery of the dinocysts *Muderongia perforata* and *Subtilisphaera* spp. indicate an age no older than Valanginian. Within this interval, a peak in recovery of dinocysts of the genus S*ubtilisphaera* occurs at 2490–2520 m, associated with an influx of typical earliest Aptian to Berriasian nannofossils, such as *Nannoconus steinmannii* and *Micrantholithus hoschulzii*, at 2530 m. The sole in situ occurrence of the calcareous benthic foraminiferid *Lenticulina heiermanni* at 2535 m suggests that this peak in recovery of marine forms is no older than late Hauterivian (Jenkins and Murray 1989). The peak in *Subtilisphaera* and the late Hauterivian age determination are characteristic of the condensed interval related to the regional Intra-Hauterivian MFS of Weston *et al.* (2012), which we thus place at the coincident positive spikes in the gamma-ray, sonic and neutron logs at 2516 m. The limestone lithofacies above this Intra-Hauterivian MFS between 2448.5 m and 2500 m are characteristic of the O-Marker within the Missisauga Formation. On the Scotian Margin, the Intra-Hauterivian MFS is sometimes found above, within, or below the O-Marker limestone depending on the extent of limestone development (Weston *et al.* 2012).

As noted above, typical Early Cretaceous palynofloras persist downhole to 2650 m. However, the cuttings sample at that depth also yields the FDOs of the typical Jurassic dinocysts *Ctenidodinium continuum*, *Dichadogonyaulax sellwoodii* and *Korystocysta pachyderma*. These occurrences indicate that strata no younger than earliest Oxfordian, and probably of Callovian or older age, have been penetrated by 2650 m. We therefore infer that the Cretaceous/Jurassic boundary lies around 2650 m and represents a major unconformity between strata of Hauterivian/?Valanginian and probable Callovian age; we attribute this to the Near-Base Cretaceous Unconformity (NBCU) of Weston *et al.* (2012), although here the unconformity is more extensive than in many Scotian Margin sections, reflecting proximity to the Avalon Uplift (Jansa and Wade 1975). We place the NBCU at the sharp downhole increases of the gamma-ray and sonic logs and consistent increased separation of the neutron-density logs downhole at 2642 m, near the base of an interval with relatively thick sandstone units. These wireline features reflect the penetration of an interval of more argillaceous strata downhole.

Typical Jurassic dinocyst floras characterized by *Meiourogonyaulax* spp., *Sentusidinium* spp. and *Systematophora* spp., and including *Dichadogonyaulax sellwoodii* and *Korysto-*

Copyright © Atlantic Geoscience, 2023

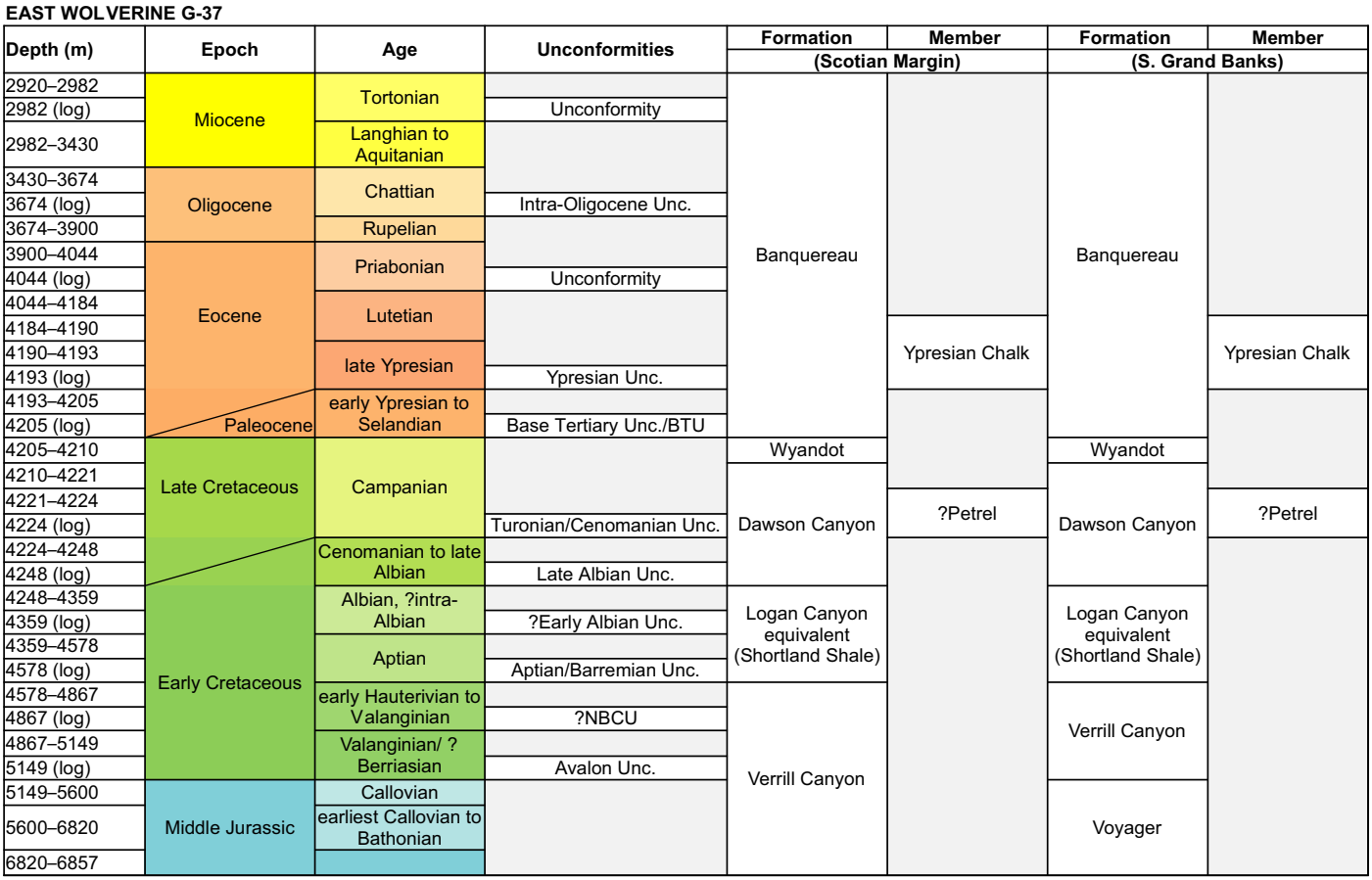

Figure 12. Stratigraphic summary of age, sequence stratigraphic events, and lithostratigraphic units in East Wolverine G-37. Additional information shown in Supplementary Data 2. Depths annotated with "(log)" were adjusted using the combination of biostratigraphic data and geophysical logs. Abbrevia-tions: NBCU = Near-Base Cretaceous Unconformity; S = south; Unc. = unconformity.

cysta pachyderma, persist downhole below 2650 to 2905 m. These dinocyst assemblages also include persistent *Ctenidodinium ornatum* between 2675 and 2905 m and *Durotrigia filapicata* (as *Diacanthum filapicatum*) between 2780 and 2905 m, confirming a Callovian age. The sole occurrence of the calcareous benthic foraminiferid *Ophthalmidium strumosum* at 2685 m provides further evidence for a Callovian age; Ascoli (1976) showed this species to be typical of the Callovian, although Ascoli (1988) and Grigelis and Ascoli (1995) indicated that it ranges up into the Oxfordian. The sole occurrence of the calcareous benthic foraminiferid *Epistomina* cf. *nuda* of Coleman (1981) at 2745 m is also typical of the Middle Jurassic (Callovian to Bajocian), whereas the sole occurrence of a poorly preserved specimen of the nannofossil ?*Stephanolithion bigotii* subspecies *bigotii* at 2770 m supports an age no older than Callovian. The base of persistent recovery of the dinocyst *Ctenidodinium ornatum* in the sidewall core sample at 2796 m also indicates an age no older than Callovian.

Within this Callovian interval between 2642 and 2905 m are two peaks in dinocyst abundance and diversity. The first is at the top of the interval at 2675 m and is associated with small influxes of typical Jurassic nannofossils at 2680 m and Jurassic calcareous benthic foraminifera at 2685 m. We infer that these increases in marine microfossils reflect proximity to a maximum flooding surface, which we place within the more argillaceous interval from 2642 to 2688 m at the coincident positive spikes in the gamma-ray and sonic logs at 2669 m, representing positive inflections in these curves. We suggest that this is the Top-Callovian MFS of Weston *et al.* (2012) from the position of this event within the Bandol-1 section and correlation to West Esperanto B-78 in Weston *et al.* (2012). The second peak in dinocyst abundance and diversity is within the interval 2800–2825 m, with the maximum abundance recorded at 2815 m and maximum diversity at 2825 m. However, poor nannofossil and micropaleontological recoveries occur at 2770–2800 and 2775 m, respectively, whereas samples are barren of foraminifera and nannofossils from 2805 m downhole. We suggest that an older Callovian MFS, the Base-Callovian MFS of Weston *et al.* (2012), lies within the interval 2790–2798 m, which shows high gamma-ray and sonic values associated with maximum separation of the neutron-density logs, suggestive of the most argillaceous lithofacies. We place this MFS at the coincident positive inflections of the gamma-ray and sonic logs at 2797 m. Although assigned

Copyright © Atlantic Geoscience, 2023

EMERILLON C-56

Depth (ft)	Depth (m)	Epoch	Age	Unconformities	Formation (Scotian Margin)	Member (Scotian Margin)	Formation (S. Grand Banks)	Member (S. Grand Banks)
1430–2566	435.9–782	Miocene to ? Oligocene			Banquereau		Banquereau	
2566 (log)	782 (log)			Intra-Oligocene Unc.				
2566–3014	782–918.7	Eocene	?Priabonian					
3014 (log)	918.7 (log)			Unconformity				
3014–3634	918.7–1107.6		early Lutetian to ? Ypresian					
3634 (log)	1107.6 (log)			?Ypresian Unc.				
3634–3746	1107.6–1141.8	Paleocene	?Thanetian					
3746 (log)	1141.8 (log)			?Base Tertiary Unc./BTU				
3746–3792	1141.8–1155.8	Late Cretaceous	Maastrichtian					
3792 (log)	1155.8 (log)			Unconformity				
3792–4147	1155.8–1264		Campanian		Wyandot		Wyandot	
4147 (log)	1264 (log)			Intra-Campanian Unc.				
4147–5060	1264–1542.3		Santonian to Coniacian		Dawson Canyon		Dawson Canyon	
5060–5300	1542.3–1615.4		Turonian					
5300–5400	1615.4–1645.9					Petrel Limestone		Petrel Limestone
5400 (log)	1645.9 (log)			Turonian/Cenomanian Unc.				
5400–5582	1645.9–1701.4		Cenomanian to ? late Albian					
5582 (log)	1701.4 (log)			?Late Albian Unc.				
5582–5858	1701.4–1785.5	Early Cretaceous	Albian					
5858 (log)	1785.5 (log)			?Early Albian Unc.				
5858–6380	1785.5–1944.6		Aptian		Logan Canyon	Eider unit	Logan Canyon	Eider unit
6380–6482	1944.6–1975.7					Naskapi		Naskapi
6482 (log)	1975.7 (log)			Aptian/Barremian Unc.				
6482–6847	1975.7–2087		Barremian		Mississauga		Mississauga	
6847 (log)	2087 (log)			Avalon Unc.				
6847–7150	2087–2179.3	Middle Jurassic	early Callovian		Verrill Canyon		Voyager	
7150–7160	2179.3–2182.4		early Callovian to late Bathonian					
7160–7640	2182.4–2328.7				?Mic Mac		Downing	
7640–8400	2328.7–2560.32		Bathonian					
8400 (log)	2560.32							
8400–8450	2560.32–2575.6							Whale
8450–9230	2575.6–2813.3		Bathonian to Bajocian					
9230–9400	2813.3–2865.1							
9400–9650	2865.1–2941.32				?Mohican Equiv.			
9650-9740	2941.32-2968.75							
9740–9816	2968.75–2991.9					Cret. intrusive		Cret. intrusive
9816-9550	2991.92-2910.84							
9550–10 150	2910.84–3093.7		?Bajocian					
10 150–10 214	3093.7–3113.2							
10 214 (log)	3113.2 (log)			?Bajocian/Toarcian Unc.				
10 214–10 520	3113.2–3206.5				?Iroquois		?Iroquois	
10 520–10 750	3206.5–3276.6	Early Jurassic	earliest Toarcian-late Sinemurian					

Figure 13. Stratigraphic summary of age, sequence stratigraphic events, and lithostratigraphic units in Emerillon C-56. Depths annotated with "(log)" were adjusted using the combination of biostratigraphic data and geophysical logs. Abbreviations: Unc. = unconformity; NBCU = Near-Base Cretaceous Unconformity; S. = south; equiv. = equivalent.

to the Mic Mac Formation, the interval of mudstone and minor carbonate rocks between these two MFSs is probably approximately correlative to the Misaine Member of the Abenaki Formation, which is penetrated in numerous wells on the Scotian Margin.

From 2925 to 4045 m — the latter being the base, or total depth (TD), of Bandol-1 — the palynofloras recorded by Davies and Huang (2001) comprise almost exclusively rich miospore assemblages dominated by *Classopollis torosus* (as *Corollina torosa*) and *Callialasporites* spp. The latter suggests an age no older than Middle Jurassic, an interpretation supported by the presence of rare nannofossils including *Watznaueria barnesae* and *Watznaueria britannica* at 4030 m. These nannofossils do not range older than the Bajocian. Rare dinocysts are also present within cuttings and sidewall core samples from the more argillaceous rocks at the base of the well (3961–4030 m). These include *Dichadogonyaulax sellwoodii* and *Escharisphaeridia pocockii* in the relatively rich marine assemblage recovered from the sidewall core at 4022 m. The LDOs of these species at 4022 m imply an age no older than late Bajocian, but the co-occurrence of these species with *Ctenidodinium ornatum* in the cuttings sample at 4020 m and the sidewall core at 4022 m is problematic. As noted above, *Ctenidodinium ornatum* does not range below the Callovian and, if in situ, this occurrence indicates that the whole of the Jurassic section from the NBCU at 2642 m to the base of Bandol-1 at 4045 m is of Callovian age. Such a substantial thickness of lowest Callovian strata is not typical of the Scotian Margin and southern Grand Banks. Davies and Huang (2001) dated strata below 3215 m as late to middle Bathonian, which fits better into the regional context. Given the uncertainties associated with a review of pre-existing biostratigraphic data, we thus attribute the section below 2905 m to a broad Middle Jurassic age within the Mic Mac Formation.

Copyright © Atlantic Geoscience, 2023

East Wolverine G-37

Our evaluation of East Wolverine G-37 (Figs. 11b and 12) is based on multidisciplinary quantitative biostratigraphic data displayed as range charts in Rutledge (2010). These data are derived from 144 quantitative micropaleontological analyses, 310 quantitative nannofossil analyses and 114 quantitative palynological analyses through the interval from 2920 m to the well's TD at 6857 m. These data are supplemented by biostratigraphic events summarized in the East Wolverine G-37 Stratigraphic Summary Log in Ainsworth *et al*. (2016), which are taken from 197 micropaleontological and palynological analyses over the same interval as that studied by Rutledge (2010). New nannofossil analyses were undertaken by one of us (MKEC) on 23 cuttings samples supplied by C-NLOPB through the interval 4250–6857 m. A summary stratigraphic plot of this well is provided as Figure 11b and in Supplementary Data 2, and the stratigraphic breakdown is summarized in Figure 12. Full digital wireline data are not available for display on the charts in Supplementary Data 2, so comments on wireline characteristics below reflect observations on available wireline data displayed in charts from Rutledge (2010) and OERA (2014).

Biostratigraphic data from both reviewed studies commence downhole just beneath the casing shoe, the highest cuttings sample being at 2920 m. Rutledge (2010) noted that this sample contains reworked Campanian and caved Pleistocene nannofossils, together with the sole occurrence of the intra-Tortonian to latest Serravallian restricted nannofossil *Discoaster bollii*. In the first sample analyzed palynologically at 2930 m, occurrences of the dinocysts *Pentadinium laticinctum* subspecies *laticinctum*, *Pentadinium laticinctum* subspecies *granulatum* and *Cleistosphaeridium ancyreum* (as *Systematophora ancyrea*) confirm an age no younger than intra-Tortonian. Also at 2930 m, Rutledge (2010) noted the presence of the early Tortonian or older nannofossil *Discoaster exilis*. We therefore suggest that the shallowest samples analyzed from East Wolverine G-37 at 2920–2930 m are intra-Tortonian in age.

Distinct changes in the compositions of the benthic foraminiferal assemblages occur between 2960 and 3005 m and in the palynofloral assemblages between 2990 and 3050 m. These observations suggest that a sharp change in depositional conditions, possibly an unconformity, lies between 2990 and 3005 m. Nannofossil assemblages from 3000 m downhole show the persistent recovery of the Middle Miocene and older species *Cyclicargolithus floridanus*, and the FDO of the nannofossil *Sphenolithus heteromorphus* occurs at 3000 m. *Sphenolithus heteromorphus* is restricted to the Langhian to late Burdigalian Martini nannofossil zones NN5–NN4. We therefore infer that an unconformity between the Tortonian and Langhian lies above 3000 m and place it at a negative spike and overall change in the trend of the sonic log at 2982 m. Rare specimens of the nannofossil *Cyclicargolithus floridanus* at 2925 and 2930 m in Rutledge (2010) and an occurrence of the dinocyst ?*Unipontidinium aquaeductus* at 2970 m in Ainsworth *et al*. (2016) likely represent reworking of older Miocene forms into the Tortonian.

Support for a Langhian age below 3000 m is provided by the sole occurrences of a specimen of the dinocyst *Unipontidinium aquaeductus* at 3050 m and of the nannofossil *Discoaster petaliformis* at 3070 m: both species are restricted to the Langhian. The FDO of the nannofossil *Helicosphaera ampliaperta* at 3080 m implies an age no younger than early Langhian and Martini nannofossil zone NN4; and at 3100 m, Ainsworth *et al.* (2016) recorded the FDO of the planktonic foraminiferid *Globorotalia* ?*zealandica*, which supports an age no younger than earliest Langhian Blow zone N8/Wade *et al.* zone M5 (Kennett and Srinivasan 1983). It is not possible to determine the position of the Langhian/Burdigalian boundary in East Wolverine G-37, but the FDO of the dinocyst *Cordosphaeridium cantharellus* at 3170 m in both datasets indicates an age no younger than Burdigalian. This event coincides with the base of persistent common recovery of the nannofossil *Sphenolithus heteromorphus* at 3170 m, which indicates an age no older than Martini zone NN4 of the late Burdigalian. Immediately below, at 3180 m, a change in the composition of the nannofossil assemblages occurs, including the FDOs of the intra-Burdigalian Martini zone NN3 marker species *Sphenolithus belemnos* and *Sphenolithus disbelemnos*. Rutledge (2010) recorded a further occurrence of the Martini-zone-NN3-restricted nannofossil *Sphenolithus belemnos* at 3210 m, whereas Ainsworth *et al.* (2016) recorded the FDO of the planktonic foraminiferid *Ciperoella ciperoensis* (as *Globigerina ciperoensis*) at 3200 m. This species does not range younger than the early Burdigalian (Blow zone N5/Wade *et al.* zone M2) (Kennett and Srinivasan 1983) and so supports the intra-Burdigalian age derived from the nannofossil data around this depth. The FDO of the nannofossil *Triquetrorhabdulus carinatus* at 3260 m indicates an age no younger than Martini zone NN2 of early Burdigalian to Aquitanian age, whereas the sole occurrence of the nannofossil *Discoaster druggii* at 3270 m implies an age no older than intra-Aquitanian Martini zone NN2. A small influx of planktonic foraminifera at 3400 m includes the FDOs of *Globoquadrina dehiscens* and *Paragloborotalia continuosa* (as *Globorotalia continuosa*), which do not range below Blow zone N4b and Wade *et al*. zone M1b in the Aquitanian (Wade *et al*. 2011; Wade et al. 2018). An influx of the dinocyst *Homotryblium floripes* at 3410 m in both datasets and an increase in the abundance of the nannofossil *Cyclicargolithus floridanus* at 3420 m are characteristic of the Aquitanian. The interval 2982 to 3420 m therefore comprises what appears to be a conformable section of intra-Middle to Early Miocene, Langhian to Aquitanian age.

Ainsworth *et al*. (2016) recorded the top of common specimens of the dinocyst genus *Chiropteridium* at 3430 m, the shallowest evidence for an Oligocene age; we therefore place the top of the Chattian at 3430 m. This age is confirmed by the FDOs of the dinocysts *Chiropteridium dispersum* and *Chiropteridium lobospinosum*, with the top

Copyright © Atlantic Geoscience, 2023

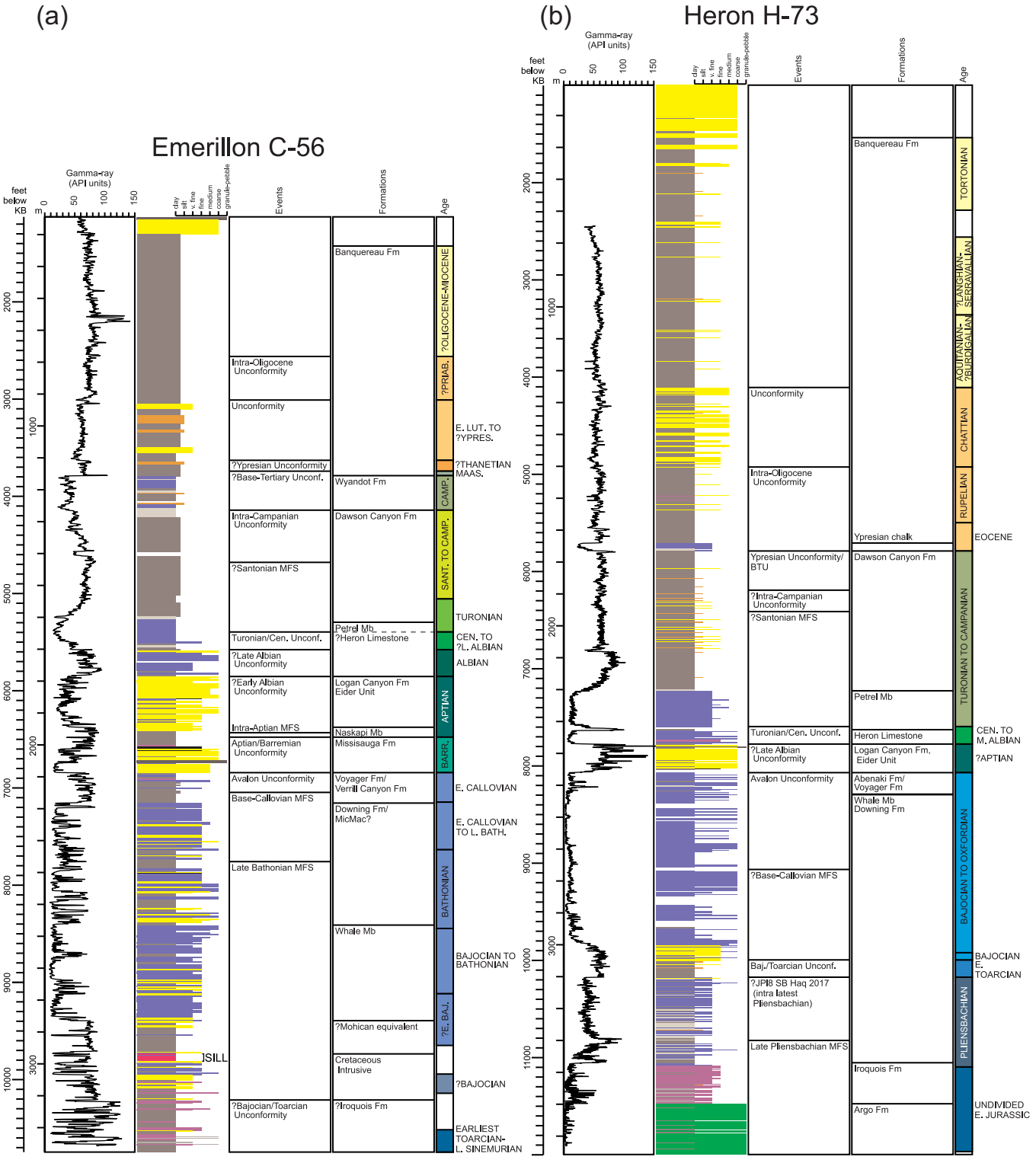

Figure 14. (a) Reduced-scale summary plot for Emerillon C-56 well. "Events" refers to sequence stratigraphic events (see Figs. 8 and 19). Expanded-scale plots with additional geophysical logs and biostratigraphy data are presented in Supplementary Data 3. (b) Reduced-scale summary plot for Heron H-73 well. Measurements in feet (original units) and metres are provided. Abbreviations: Fm = Formation; Mb = Member. See Figure 10 for legend.

Copyright © Atlantic Geoscience, 2023

of common and persistent recovery of the dinocyst *Chiropteridium mespilanum* at 3470 m according to Rutledge (2010). (*Chiropteridium dispersum* and *Chiropteridium mespilanum* are listed as synonyms of *Chiropteridium galea* in Fensome *et al.* 2019.) The Chattian nannofossil *Sphenolithus ciperoensis*, restricted to Martini zones NP25–NP24, is recorded in the interval 3570–3625 m, whereas the FDO of the nannofossil *Chiasmolithus altus* at 3600 m implies an age no younger than intra-Chattian. At 3650 m, the FDO of dinocysts of the genus *Wetzeliella* indicates an age no younger than early Chattian, an age which is supported by the FDO of the nannofossils *Sphenolithus distentus, Sphenolithus predistentus* and *Helicosphaera compacta* at 3655 m. The base of persistent recovery of the nannofossil *Cyclicargolithus abisectus*, also at 3655 m, suggests that strata to this depth are no older than early Chattian and Martini zone NP24.

Rutledge (2010) reported a marked change in the composition of the palynofloras between 3630 and 3700 m, whereas Ainsworth *et al.* (2016) recorded the FDO of the Rupelian or older dinocyst *Enneadocysta magna* at 3690 m. We therefore suggest that the Chattian/Rupelian boundary lies between 3655 and 3690 m, placing it at 3674 m, where small positive downhole shifts in the gamma-ray and density logs occur, coincident with a negative spike in the sonic log (i.e., reflecting faster velocity). We attribute this boundary to the Intra-Oligocene Unconformity of Weston *et al.* (2012). The FDOs of the planktonic foraminifera *Turborotalia increbescens* (as *Globorotalia increbescens*) at 3720 m in Ainsworth *et al.* (2016) and *Turborotalia ampliapertura* (as *Globigerina ampliaperta*) at 3760 m in Rutledge (2010) confirm an age no younger than Rupelian, but suggest that the Rupelian interval is truncated by the Intra-Oligocene Unconformity, as both of these species have their stratigraphic tops within the lower part of the Rupelian Blow zone P19/Wade *et al.* zone O2; that of *Turborotalia increbescens* is in the lower part of these biozones (Wade *et al.* 2018). A broad Rupelian age is further confirmed by the FDO of the nannofossil *Markalius inversus* at 3780 m, whereas the FDO of the dinocyst *Enneadocysta arcuata* at 3810 m and the common occurrence of *Enneadocysta arcuata* at 3830 m support an intra-Rupelian or older age. We interpret the occurrence of the dinocyst *Diphyes colligerum* at 3830 m as reworked because its range top is in the Lutetian on the Scotian Margin (Fensome *et al.* 2008). The FDO of the planktonic foraminiferid *Chiloguembelina ototara* at 3880 m is suggestive of an age no younger than the earliest Rupelian equivalent to Blow zone P18/Wade *et al.* zone O1.

The FDO of planktonic foraminifera of the *Subbotina linaperta* group at 3900 m indicates an age no younger than Eocene (Blow zone P17/Wade *et al.* zone E16). Nannofossil recovery at 3900 m is relatively poor, but at 3920 m there is a sharp change in the composition of nannofossil assemblages, associated with the FDOs of *Coccolithus formosus, Corannulus germanicus* and *Isthmolithus recurvus.* The presence of *Coccolithus formosus* indicates an age no younger than earliest Oligocene (Martini zone NP21), whereas *Isthmolithus recurvus* is restricted to the Rupelian to intra-Priabonian (Martini zones NP22–NP20/19). *Corannulus germanicus* is restricted to the Priabonian, within Martini zones NP21–NP17. In combination, then, these downhole incomings at 3920 m indicate a latest Priabonian age equivalent to Martini zones intra-NP21–NP20/19 at 3920 m. We therefore infer that the Oligocene/Eocene boundary is around 3900 m in East Wolverine G-37 and that this boundary is conformable, with no evident stratigraphic break.

An Eocene age is supported by the FDOs of the dinocyst *Areosphaeridium diktyoplokum* at 3940 m and the nannofossil *Reticulofenestra reticulata* (as *Cyclicargolithus reticulatus*) at 3960 m. Notably, *Reticulofenestra reticulata* shows a peak in abundance at 3980 m, where it is associated with the FDO of the nannofossil *Neococcolithes dubius*; these events are characteristic of the early Priabonian Martini nannofossil zone NP18. Relatively abundant recovery of *Reticulofenestra reticulata* persists downhole to 4030 m, where the FDO of the nannofossil *Sphenolithus obtusus* occurs; the latter species also has its stratigraphic top in the earliest Priabonian (intra-Martini zone NP18). We suggest that the interval 3980–4030 m is early Priabonian, equivalent to Martini zone NP18. Ainsworth *et al.* (2016) recorded common Middle to Early Eocene (Lutetian to Ypresian) planktonic foraminifera in the micropaleontological assemblages from the interval 3980–4020 m, but the species they listed are stratigraphically mixed and include forms restricted to the Middle Eocene (e.g., *Globigerinatheka subconglobata*) together with Early Eocene taxa (e.g., *Acarinina soldadoensis soldadoensis, Acarinina soldadoensis angulosa*). We interpret these planktonic foraminifera to be reworked into lower Priabonian strata. According to Rutledge (2010), rare reworked Middle to Early Eocene nannofossils are present at 4000 m.

A sharp change in the composition of the nannofossil assemblages occurs at 4050 m, associated with the FDO and top of persistent recovery of the Lutetian restricted nannofossil *Sphenolithus spiniger*. Rutledge (2010) also noted a marked change in the planktonic foraminiferal assemblages at 4060 m, where the downhole incomings of *Acarinina bullbrooki, Acarinina spinuloinflata* and *Globigerinatheka subconglobata subconglobata* support an intra-Middle Eocene age no younger than Blow zone P12/Wade *et al.* zone E10. These data suggest an unconformity between the Priabonian and Lutetian between 4030 and 4050 m, potentially correlative with the Pr1 sequence boundary of Hardenbol *et al.* (1998). We place this unconformity at the strong downhole negative shifts in the gamma-ray and sonic logs at 4044 m; these shifts are associated with slight but distinct positive shifts in the density and resistivity logs.

Further support for an intra-Middle Eocene or older age below 4050 m is provided by the FDOs of the nannofossil *Sphenolithus furcatolithoides* at 4070 m, the planktonic foraminiferid *Turborotalia cerroazulensis frontosa* at 4090 m and the dinocyst *Diphyes ficusoides* at 4110 m. The persistent recoveries of the Middle Eocene restricted planktonic foraminiferid *Globigerinatheka subconglobata subconglobata* through the interval 4060–4150 m and the Lutetian restricted

Copyright © Atlantic Geoscience, 2023

HERON H-73

Depth (ft)	Depth (m)	Epoch	Age	Unconformities	Formation (Scotian Margin)	Member (Scotian Margin)	Formation (S. Grand Banks)	Member (S. Grand Banks)
1540–2290	469.4–697.99	Miocene	Tortonian		Banquereau		Banquereau	
2560–3330	780.29–1014.98		Serravallian-? Langhian					
3330–4110	1014.98–1252.73		?Burdigalian-Aquitanian					
4110 (log)	1252.7 (log)			Unconformity				
4110–4928	1252.7–1502	Oligocene	Chattian					
4928 (log)	1502 (log)			Intra-Oligocene Unc.				
4928–5500	1502–1676.4		Rupelian					
5500–5710	1676.4–1740.4	Eocene						
5710–5792	1740.4–1765.4					Ypresian Chalk		Ypresian Chalk
5792 (log)	1765.4 (log)			Ypresian Unc.				
5792–6195	1765.4–1888.2	Late Cretaceous	Campanian to Turonian		Dawson Canyon		Dawson Canyon	
6195 (log)	1888.2 (log)			?Intra-Campanian Unc.				
6195–6420	1888.2–1956.82							
6420 (log)	1956.82							
6420-7230	1956.82-2203.7							
7230–7598	2203.7–2315.9					Petrel Limestone		Petrel Limestone
7598 (log)	2315.9 (log)			Turonian/Cenomanian Unc.				
7598–7630	2315.9–2325.6		Cenomanian to late Albian					
7630–7778	2325.6–2370.7					Heron Limestone		Heron Limestone
7778 (log)	2370.7 (log)			?Late Albian Unc.				
7778–8072	2370.7–2460.4	?Early Cretaceous	?Aptian		Logan Canyon	Eider unit	Logan Canyon	Eider unit
8072 (log)	2460.4 (log)			Avalon Unc.				
8072–8296	2460.4–2528.6	early-Late to Middle Jurassic	Oxfordian to Bajocian		Abenaki		Voyager	
8296–9792	2528.6–2984.6						Downing	Whale
9792–9930	2984.6–3026.66				Mohican Equiv.			
9930–9998	3026.66–3047.39		Bajocian					
9998 (log)	3047.4 (log)			Bajocian/Toarcian Unc.				
9998–10 176	3047.4–3101.6	Early Jurassic	early Toarcian					
10 176 (log)	3101.6 (log)			?JPl8 SB Haq				
10 176–11 056	3101.6–3369.9		Pliensbachian			Limestone Facies		
11 056–11 100	3369.9–3383.3				Iroquois		Iroquois	
11 100–11 478	3383.3–3498.5							
11 478–11 970	3498.5–3648.5				Argo		Argo	
11 970–12 000	3648.5–3657.6							

Figure 15. Stratigraphic summary of age, sequence stratigraphic events, and lithostratigraphic units in Heron H-73. Additional information shown in Supplementary Data 4. Depths annotated with "(log)" were adjusted using the combination of biostratigraphic data and geophysical logs. Abbre-viations: JPl8 = Jurassic Pliensbachian sequence boundary 8 of Haq (2018); Unc. = unconformity; S. = south; equiv. = equivalent.

nannofossil *Sphenolithus spiniger* through the interval 4050–4175 m indicate an intra-Lutetian age for the interval 4044–4175 m. At 4185 m, the FDO of the nannofossil *Rhabdosphaera inflata* indicates an earliest Lutetian age equivalent to Martini nannofossil zone NP14b, whereas the FDO of the nannofossil *Discoaster kuepperi* at 4190 m indicates a late Ypresian age, equivalent to Martini nannofossil zones NP14a–NP12. We attribute the light-grey to light-bluish-grey limestone noted at 4185–4195 m on the East Wolverine G-37 master log (ConocoPhillips 2010) to the regional Ypresian Chalk and place the top of this unit at the sharp downhole negative shifts in the gamma-ray and sonic logs at 4184 m. The presence of additional shallower/younger chalk units in the Lutetian, above the more widespread Ypresian Chalk, is consistent with the pattern seen in other wells on the Scotian Slope (e.g., Shubenacadie H-100; see Weston *et al.* 2012).

A sharp change in the composition of the nannofossil assemblages occurs at 4195 m, involving the incoming of abundant *Toweius* spp. and *Sphenolithus primus*, together with the FDOs of *Discoaster diastypus* and *Discoaster multiradiatus*. The occurrence of these species indicates penetration of the earliest Ypresian equivalent to Martini zones NP11-NP10 by 4195 m. We thus suggest that the regional Ypresian Unconformity of Weston *et al.* (2012) lies between 4190 m and 4195 m. We place this hiatus at the negative spike in the gamma-ray log and base of the off-scale sonic and neutron responses at 4193 m. The FDOs of the nannofossils *Fasciculithus tympaniformis* and *Heliolithus riedelii* and the planktonic foraminiferid *Morozovella velascoensis* at 4200 m indicate a Thanetian age equivalent to Martini zone NP8/7 and equivalent to, or older than, Blow zone P5, whereas the FDOs of the nannofossils *Neochiastozygus perfectus* and *Neochiastozygus modestus* at 4205 m indicate a Selandian age equivalent to Martini zones NP5-top NP4. We therefore infer the presence of a relatively complete, but condensed, section of early Ypresian to Selandian age between the Ypresian Unconformity (at 4193 m) and 4205 m.

A sharp change in the composition of the nannofossil assemblages occurs at 4210 m, from domination by the typical Cenozoic *Coccolithus pelagicus* with the Paleocene *Prinsius martinii* at 4205 m to abundances of the typical Late Cretaceous species *Micula staurophora* and *Watznaueria barnesae* at 4210 m. However, although dominated by Cenozoic nannofossils, the assemblage at 4205 m contains the top of persistent recoveries of the Cretaceous nannofossils *Arkhangelskiella cymbiformis* and *Broinsonia*

Copyright © Atlantic Geoscience, 2023

parca subspecies *constricta*. These data suggest that an unconformity between the Selandian and Campanian lies around 4205 m if the Cretaceous taxa are in situ. We place this unconformity at the negative inflections in the gamma-ray and sonic logs coincident with positive downhole shifts in the density and resistivity logs at 4205 m and we attribute it to the Base-Tertiary Unconformity (BTU) here. Penetration of a thin chalk of the Wyandot Formation is represented by the lower gamma-ray and higher sonic velocities between 4205 and 4210 m.

As noted above, Late Cretaceous nannofossils become more abundant at 4210 m with the FDOs of *Reinhardtites levis* and *Quadrum gothicum* implying an age no older than late Campanian. The sole occurrence of the nannofossil *Quadrum trifidum* at 4220 m and the base of persistent recovery of the nannofossil *Reinhardtites levis* at 4225 m support an age no older than late Campanian down to 4225 m, although the FDO of the nannofossil *Lithastrinus ?grillii* at 4225 m suggests a possible early Campanian to latest Coniacian age. This co-occurrence may reflect the presence of the Intra-Campanian Unconformity of Weston *et al.* (2012) between 4220 and 4225 m, but it cannot be confirmed with the current resolution of the biostratigraphic data derived from cuttings samples and the wireline data.

Sharp reductions in the abundances of the Maastrichtian to intra-Coniacian nannofossil *Micula staurophora* and the Campanian nannofossil *Broinsonia parca* subspecies *constricta* occur at 4230 m, associated with the FDO of the middle to early Cenomanian restricted nannofossil *Gartnerago nanum* and the sole occurrence of the Cenomanian-restricted nannofossil *Corollithion kennedyi*. We therefore infer the presence of an unconformity between the Campanian and Cenomanian between the samples at 4225 and 4230 m, which we place at the downhole positive shifts in the gamma-ray and sonic logs at 4224 m. We consider this to be the Turonian/Cenomanian Unconformity of Weston *et al.* (2012). The LDO of the Cenomanian nannofossil *Gartnerago nanum* occurs at 4240 m, but Rutledge (2010) recorded the sole occurrences of the dinocysts *Litosphaeridium arundum*, *Litosphaeridium conispinum* and *Palaeohystrichophora infusorioides* at 4240 m and Ainsworth *et al.* (2016) recorded an abundance of the planktonic foraminiferid *Rotalipora subticinensis* at the same depth. These occurrences indicate a late Albian age. We therefore infer that the Cenomanian/Albian boundary lies within the interval of the cuttings sample at 4240 m (i.e., between 4235 and 4240 m).

Major downhole positive shifts in the gamma-ray and sonic logs occur at 4248 m, coincident with sharp negative shifts in the density and resistivity logs. These wireline features are characteristic of the distal, correlative boundary between the Dawson Canyon Formation and the distal equivalent to the Logan Canyon Formation (i.e., the Shortland Shale) on the Scotian Margin. In combination with the biostratigraphic data from 4240 m, we attribute these wireline features to the Late Albian Unconformity of Weston *et al.* (2012). The nannofossils *Nannoconus fragilis* and R*ucinolithus irregularis* have their FDOs at 4250 m, immediately beneath this event. *Nannoconus fragilis* is restricted to the Albian and was recorded persistently through the interval 4250–4260 m by Rutledge (2010), whereas Ainsworth *et al.* (2016) recorded a planktonic foraminiferal assemblage characterized by the FDOs of the planktonic foraminifera *Ticinella praeticinensis*, *Ticinella raynaudi*, *Ticinella roberti* and common *Ticinella primula* at 4260 m, suggesting a tentative early-late to middle Albian age. The FDO of the planktonic foraminiferid *Hedbergella aptiana* in the same sample is ambiguous; most authors consider this species to be restricted to the Aptian to Barremian, although Boudagher-Fadel *et al.* (1997) indicated that *Hedbergella aptiana* ranges up into the Albian. It is notable that Rutledge (2010) recorded abundant *Muricohedbergella planispira* (as *Hedbergella planispira*) with common *Muricohedbergella delrioensis* (as *Hedbergella delrioensis*) at 4300 m, implying an age no older than Albian to at least this depth. Further support for an age no older than Albian is the LDO of the nannofossil *Nannoconus fragilis* at 4290 m, and the FDO of the agglutinated benthic foraminiferid *Dorothia gradata* at 4320 m; neither of these range older than Albian. At 4340 m is the FDO of the early Albian to late-early Aptian nannofossil *Nannoconus quadriangulus*. Rare questionable records of the Aptian or older marker dinocysts *Dingodinium albertii* at 4270 m and 4290 m and *Cerbia tabulata* at 4310 m in Ainsworth *et al.* (2016) are likely reworked, along with the Barremian–Hauterivian benthic foraminiferid *Gavelinella sigmoicostata* that these authors recorded as reworking at 4280 m. The specimens of the planktonic foraminiferid *Hedbergella aptiana* recorded by Ainsworth *et al.* (2016) from 4260 m may also be reworked, as the FDO of this species was placed at 4390 m by Rutledge (2010).

An influx of miospores at 4350 m was reported by Ainsworth *et al.* (2016), whereas nannofossil assemblages show a sharp increase in abundance and a change in overall composition immediately below that horizon, at 4360 m. The FDOs of the dinocysts *Cerbia tabulata* and *Pseudoceratium pelliferum* occur at 4360 m according to Rutledge (2010), indicating penetration of the intra-late Aptian. The micropaleontological assemblages reported by Rutledge (2010) also show a major change in composition between 4360 and 4390 m. This evidence suggests a sharp basinward shift in deposition downhole around 4360 m, which we attribute to the presence of a major sequence boundary that may reflect erosion of the youngest Aptian strata. We place this event at the negative spikes in the gamma-ray and sonic logs at 4359 m, which are coincident with a broader positive downhole shift in the gamma responses and a negative downhole shift in the resistivity logs. This event is termed the Early Albian Unconformity here and may correspond to a similar event within the lower part of the Albian section in Bandol-1. We therefore suggest that the Albian/Aptian boundary potentially coincides with the Early Albian Unconformity in East Wolverine G-37, placed above at 4359 m. The first recorded downhole occurrence

Copyright © Atlantic Geoscience, 2023

of the planktonic foraminiferid *Globigerinelloides ferreolensis* at 4380 m in Ainsworth *et al.* (2016) and the sole recorded occurrence of *Globigerinelloides ferreolensis* at 4390 m in Rutledge (2010) indicate a late Aptian age, whereas the FDO of the nannofossil *Zebrashapka vanhintei* at 4400 m confirms that the age is no younger than Aptian.

The FDO and top of persistent recovery of the calcareous benthic foraminiferid *Gavelinella barremiana* at 4460 m indicates an early Aptian to Barremian age. The top of persistent recovery of the nannofossil *Nannoconus bucheri* at 4510 m and the FDO of the nannofossil *Micrantholithus hoschulzii* at 4520 m support an intra-Aptian age assignment, whereas a minor influx of the dinocyst *Cerbia tabulata* at 4540 m, associated with the sole occurrence of the miospore *Afropollis zonatus* and the first definite downhole occurrence of the dinocyst *Dingodinium albertii*, confirm an early Aptian age. Further support for an age no younger than early Aptian is the FDO of the dinocyst *Ctenidodinium elegantulum* at 4550 m. Peaks in nannofossil abundance and diversity occur at 4490 m, associated with subtle positive inflections of the gamma-ray and sonic log curves at 4484 m. Based on the combination of these observations, we infer a condensed interval related to a maximum flooding surface around 4490 m and place the Intra-Aptian MFS of Weston *et al.* (2012) at 4484 m.

Major changes in the composition of the micropaleontological assemblages occurred between 4570 and 4600 m, in the nannofossil assemblages between 4570 and 4580 m, and in the palynomorph assemblages between 4540 and 4600 m (Rutledge 2010). Ainsworth *et al.* (2016) recorded the top of persistent pyritized specimens of the radiolarian *Praeconocaryomma* spp. and bivalve spat from 4580 m downhole. The FDOs and top of persistent recoveries of the dinocysts *Muderongia simplex* (as *Muderongia endovata*) and *Cymososphaeridium validum* at 4600 m indicate that strata beneath 4580 m are early Hauterivian to Valanginian in age. The changes in assemblage composition denote a sharp change in depositional conditions between 4570 m and 4580 m, whereas the evidence for a stratigraphic break between Aptian and lower Hauterivian strata indicates an unconformity, specifically the Aptian/Barremian Unconformity of Weston *et al.* (2012), which we pick at 4578 m. The interval above this depth is the shale-dominated distal equivalent of the Logan Canyon Formation, the Shortland Shale (Jansa and Wade 1975; Wade and MacLean 1990).

The top of persistent recovery and first in situ downhole occurrence of the nannofossil *Calcicalathina oblongata* (which ranges from early Barremian to Valanginian) at 4600 m is consistent with an early Hauterivian to Valanginian age, whereas the FDOs of the calcareous benthic foraminifera *Epistomina ornata* and in situ *Gavelinella sigmoicostata* at 4600 m (Rutledge 2010) imply an age no older than Hauterivian (Ascoli 1976; Bartenstein 1976). The recorded FDOs of the calcareous benthic foraminifera *Conorboides hofkeri* at 4620 m and *Epistomina caracolla* and *Lenticulina ouachensis* at 4630 m in Rutledge (2010) confirm the Barremian to Hauterivian age (Ascoli 1976; Bartenstein 1976), Bartenstein 1976), although the latter two species were noted higher in the section (at 4540 m) by Ainsworth *et al.* (2016), where we suggest they are reworked. The FDO of the nannofossil *Cruciellipsis cuvillieri* at 4670 m supports a Hauterivian or older age, whereas a persistent increase in the abundance of the nannofossil *Cyclagelosphaera margerelii* at 4770 m and the FDO of the calcareous benthic foraminiferid E*pistomina tenuicostata* at 4780 m confirm an age no younger than early Hauterivian (Ascoli 1988). The sole record of the Hauterivian-restricted nannofossil *Lithraphidites bollii* at 4790 m suggests that the whole of the interval 4578–4790 m is of early Hauterivian age. The FDO of the Valanginian marker calcareous benthic foraminiferid *Lenticulina busnardoi* recorded by Ainsworth *et al.* (2016) within this interval at 4640 m is thus attributed to reworking. Occurrences of the nannofossil E*iffellithus windii* at 4827 and 4860 m and the sole occurrence of the calcareous benthic foraminiferid *Lenticulina saxonica* at 4840 m are consistent with an early Hauterivian to Valanginian age (Ascoli 1976; Bartenstein 1976), whereas the LDOs of the nannofossils *Calcicalathina oblongata* at 4865 m and *Nannoconus bucheri* at 4870 m suggest an age no older than Valanginian to at least this depth.

A sharp reduction in nannofossil recovery occurs at 4880 m, whereas the micropaleontological assemblages show a distinct change in composition at 4875 m, with the FDOs of the calcareous benthic foraminifera *Conorboides valendisensis* and *Planularia crepidularis* (as *Lenticulina crepidularis*). The change in micropaleontological composition suggests that a sequence boundary lies above 4875 m, and we thus place this event at the downhole positive shift in the gamma-ray log at 4867 m, where the mud log indicates that it is overlain by a thin (~4 to 10 m thick) sandstone. Both *Conorboides valendisensis* and *Planularia crepidularis* have their stratigraphic tops in the Hauterivian on the Scotian Margin, according to Ascoli (1988), but Ascoli (1976) showed that *Conorboides valendisensis* is characteristic of the early Valanginian on the Scotian Shelf. We suggest that the sequence boundary identified at 4867 m represents an intra-Valanginian event, potentially the lateral equivalent of the Near-Base Cretaceous Unconformity (NBCU) of Weston *et al.* (2012), here not amalgamated into the Avalon Unconformity.

Conorboides valendisensis was recorded persistently in the interval 4875–4930 m by Rutledge (2010), and he also recorded the sole occurrence of the early Valanginian to late Berriasian nannofossil ?*Kokia curvata* at 4950 m. The FDOs of the calcareous benthic foraminiferid *Lenticulina saxonica bifurcilla* at 4990 m and the nannofossil *Cyclagelosphaera deflandrei* at 5120 m support an age no younger than Valanginian, whereas the LDOs of the nannofossil *Zeugrhabdotus trivectis* at 5120 m, the dinocysts *Cymososphaeridium validum*, *Muderongia simplex* (as *Muderongia endovata* in Rutledge 2010) and *Pseudoceratium pelliferum* at 5140 m and the nannofossil *Micrantholithus hoschulzii* at 5145 m imply that strata to at least 5145 m are no older than Early Cretaceous and probably Valanginian to latest Berriasian. The sole occurrences of the nannofossils *Polycostella beck-*

Copyright © Atlantic Geoscience, 2023

mannii at 5090 m and *Hexalithus strictus* at 5140 m are likely reworked as these species are restricted to the early Berriasian to Tithonian.

Ainsworth *et al.* (2016) indicated that the base of Cretaceous microfaunas is at 5140 m, and they recorded typical Jurassic dinocysts *Ctenidodinium/Dichadogonyaulax* sp. and *Lithodinia* sp. at 5150 m. Rutledge (2010) confirmed the penetration of Jurassic at 5155 m through the downhole incoming of a typical Callovian dinocyst association, including common *Dichadogonyaulax sellwoodii* and *Sentusidinium* spp. and the occurrence of *Gonyaulacysta jurassica*. The nannoflora at 5155 m shows a complete change from the assemblages recorded at and above 5150 m: above 5150 m the nannofloras are dominated by *Nannoconus* spp., which is typical of the Early Cretaceous, and from 5155 m downhole they are dominated by *Watznaueria barnesae*, associated with relatively common *Watznaueria britannica* (as *Ellipsagelosphaera britannica*) and *Watznaueria fossacincta* (as *Ellipsogelosphaera fossacincta*), which is typical of the Late to Middle Jurassic. Also, the FDO of the Oxfordian or older nannofossil *Lotharingius crucicentralis* occurs at 5155 m. We therefore infer that the Cretaceous/Jurassic boundary occurs at around 5150 m and that a major stratigraphic break occurs across this boundary — between the Valanginian and latest Berriasian–Callovian. We attribute this stratigraphic break to the Avalon Unconformity (Fig. 2), which we place at the downhole positive shifts in the gamma-ray and sonic logs at 5149 m.

Rutledge (2010) recorded the typical Middle Jurassic calcareous benthic foraminiferid *Lenticulina argonauta* at 5160 m, whereas Ainsworth *et al.* (2016) noted an influx of planktonic foraminifera at 5160 m, including *Globuligerina* ?*balakhmatovae* (as *Conoglobigerina* ?*balakhmatovae*), abundant *Globuligerina bathoniana* ("*Globuligerina bathonica*" in the report is assumed to be a misspelling) and *Globuligerina* ?*oxfordiana*. All these species range from the early Kimmeridgian to the Bajocian (Gradstein *et al.* 2017a, b), but on the Scotian Margin, Ascoli (1976, 1988) indicated that *Globuligerina bathoniana* is characteristic of the early Callovian to the Bathonian, whereas *Globuligerina oxfordiana* is restricted to the Oxfordian–Callovian interval. This evidence tentatively suggests an early Callovian age at 5160 m, an assignment supported by the FDO of the dinocyst *Meiourogonyaulax caytonensis* (as *Lithodinia caytonensis*) at 5170 m (Ainsworth *et al.* 2016). The biostratigraphic data therefore suggest that the Avalon Unconformity has truncated the Jurassic strata down to within the lower Callovian.

The FDO of the nannofossil *Cyclogelosphaera tubulata* at 5210 m confirms a broad Late to Middle Jurassic age. The FDO of the calcareous benthic foraminiferid *Lenticulina quenstedti* at 5300 m and further occurrences of this species throughout the interval from 5500 to 5600 m suggest an age no older than Callovian and that a relatively thick interval of lower Callovian strata is present. This interpretation is supported by the persistent occurrence of the dinocyst *Ctenidodinium ornatum* throughout the interval from 5425 to 5625 m (with an abundance peak at 5625 m). The FDOs of the dinocysts *Aldorfia aldorfensis* at 5310 m, ?*Ctenidodinium combazii* at 5550 m, and definite Ctenidodinium combazii at 5625 m indicate an earliest Callovian age at and below 5310 m. The sole occurrences of the nannofossils *Stephanolithion speciosum* subspecies *speciosum* and *Biscutum dorsetensis*, associated with the FDO of the nannofossil *Ansulasphaera helvetica* in our new data at 5540 m, indicate an early Callovian to late Bathonian age, whereas the FDO of the nannofossil *Tetrapodorhabdus shawensis* at 5600 m (Rutledge 2010) suggests an age no younger than Bathonian, and hence proximity to the Callovian/Bathonian boundary around this depth. Peaks in nannofossil abundance and in dinocyst abundance and diversity occur at 5550–5600 m and at 5550–5575 m respectively, and the interval from 5475 to 5600 m is characterized by relatively rich benthic foraminiferal faunas. In combination, these data suggest an increased open marine influence in the interval 5550–5600 m, which is likely an expression of a maximum flooding surface. We thus place an MFS at 5556 m, at the coincident positive spikes in the gamma-ray and sonic logs within broader positive inflections in these curves, and we correlate this event to the Base-Callovian MFS of Weston *et al.* (2012).

Marine biostratigraphic recoveries all show a marked decrease from 5625 m downhole and no new marker taxa are recorded until 6175 m, where the FDO of the nannofossil *Pseudoconus enigma* confirms a Middle Jurassic age no younger than early Callovian. The LDOs of the dinocysts *Gonyaulacysta jurassica* at 6317 m and *Dichadogonyaulax sellwoodii* at 6395 m imply an age no older than latest Bajocian to at least this depth, whereas the base of persistent recovery of dinocysts of the genus *Systematophora* at 6345 m suggests an age no older than late Bathonian. Between 6370 and 6695 m, persistent and occasionally common specimens of the planktonic foraminiferid *Globuligerina bathoniana* were recovered. As noted above, *Globuligerina bathoniana* is relatively long-ranging, but has an acme in the Bathonian (Ascoli 1988; Gradstein *et al.* 2017b). The top of common recovery of *Globuligerina bathoniana* at 6370 m is associated with the FDO of the ostracod *Praeschuleridea subtrigona*, a species restricted to the Bathonian to Bajocian in north-western Europe (e.g., Whittaker and Hart 2009). Further support for a Bathonian age is provided by the FDO of the Callovian to Bathonian calcareous benthic foraminiferid *Reinholdella crebra crebra* at 6400 m, the sole occurrence of the Bathonian calcareous benthic foraminiferid *Reinholdella media* at 6570 m, and sole occurrences of the nannofossils *Biscutum novum* at 6595 m and *Biscutum intermedium* at 6620 m, which have their extinctions in the Bathonian. The LDO of the nannofossil *Cyclagelosphaera margerelii* at 6620 m indicates an age no older than the Bathonian/Bajocian boundary. The Bathonian-restricted ostracod *Micropneumatocythere quadrata* occurs within the interval 6620–6695 m, whereas the sole occurrences of the Bathonian ostracods

Copyright © Atlantic Geoscience, 2023

Micropneumatocythere subconcentrica and ?*Schuleridea (Eoschuleridea) trigonalis* occur at 6730 m, the LDO of the ostracod *Praeschuleridea subtrigona* occurs at 6740 m, and the LDO of the calcareous benthic foraminiferid *Reinholdella crebra* occurs at 6820 m. The typical Middle Jurassic nannofossil *Lotharingius contractus* occurs at 6730 and 6760 m. We therefore infer a definitive Bathonian age for strata between 6370 and 6820 m, whereas the ostracod fauna reported by Rutledge (2010) between 6620 m and 6730 m is most typical of the late Bathonian in northwestern Europe. We thus suggest that the interval 6370–6730 m is probably of late Bathonian age. Influxes of both planktonic foraminifera and nannofossils occur within the lower part of this interval, at 6620 m, and we interpret a maximum flooding surface to be present around this depth. We place it at the coincident positive spikes in the gamma-ray, sonic and neutron logs at 6611 m and designate it here as the Late Bathonian MFS.

Little biostratigraphic data has been reported from 6820 m to TD at 6857 m. However, the persistent occurrence of low numbers of the nannofossils *Watznaueria barnesae* and *Watznaueria britannica* down to the TD sample at 6857 m suggests a Middle Jurassic age no older than Bajocian for the base of this well section.

Emerillon C-56

Our evaluation of Emerillon C-56 (Figs. 13 and 14a) is based on unpublished information from work undertaken by personnel at GSC Atlantic, together with biostratigraphic events marked on the Stratigraphic Summary Log for this well in Ainsworth *et al.* (2016). The interpretation of the Cenozoic interval is based on a qualitative reconnaissance study of 27 pre-existing palynological preparations held at GSC Atlantic from cuttings samples at 90 ft (27.43 m) intervals between 1160 and 3740 ft (353.57 and 1139.95 m) by one of us (RAF), together with a single sample analyzed micropaleontologically at 3710–3740 ft (1130.81–1139.95 m) (Ascoli 1986). Data from the Cretaceous and Jurassic intervals are more extensive and include a large dataset of semi-quantitative micropaleontological data from 49 composite cuttings samples (samples containing material from all cuttings samples for that interval), mainly at 100 ft (30.48 m) intervals, held in the internal GSC version of the BASIN database and partially documented in the unpublished reports of Ascoli (1981, 1986). The internal GSC version of the BASIN database also includes unpublished data from palynological preparations from 16 sidewall core samples analyzed by one of us (GLW) and partially reported in Williams (1979). The events shown in Ainsworth *et al.* (2016) for Emerillon C-56 are derived from 108 micropaleontological and 108 palynological analyses of cuttings samples through the interval 4070–10 740 ft (1240.54–3273.55 m). No nannofossil data were available for this well. A summary stratigraphic plot of this well is provided in Figure 14a and Supplementary Data 3, and the stratigraphic breakdown is summarized in Figure 13.

Palynological recoveries from the upper part of Emerillon C-56 are poor, but the occurrence of the dinocyst *Reticulatosphaera actinocoronata* at 1410–1430 ft (429.77–435.87 m) implies an age no younger than Miocene from at least this depth downhole. Dinocysts consistent with an age no younger than Miocene are recorded down to 2510–2540 ft (765.05–774.19 m). There is a distinct change in the palynological recovery at 2600–2630 ft (792.48–801.62 m), where occurrences of the dinocysts *Lentinia serrata* and ?*Glaphyrocysta extensa* imply an age no younger than Priabonian. We infer the presence of an intra-Cenozoic unconformity between 2540 and 2630 ft (774.19 and 801.62 m) and place this horizon at the sharp downhole negative shifts in the gamma-ray and resistivity logs at 2566 ft (782.12 m); we suggest that this hiatus is correlative to the Intra-Oligocene Unconformity of Weston *et al.* (2012). An Eocene age below 2566 ft (782.12 m) is supported by the consistent presence of the dinocyst *Glaphyrocysta extensa* from 2840 ft (865.63 m), whereas the sole occurrence of the dinocyst *Axiodinium* sp. at 3020–3050 ft (920.5–929.64 m), associated with a questionable specimen of *Cordosphaeridium delimurum* at the same depth, suggests an early Lutetian to Ypresian age from 3050 ft (929.64 m) downhole. It is notable that a sharp change in the wireline log trends coincident with major negative spikes in the gamma-ray, sonic and resistivity logs occurs at 3014 ft (918.67 m), suggesting an unconformity between the ?Priabonian and intra-Lutetian at 3014 ft (918.67 m).

Dinocyst assemblages from samples from 3020–3050 ft (920.5–929.64 m) downhole are more diverse than those above, and include typical early Lutetian to Ypresian species such as *Areoligera circumsenonensis*, ?*Axiodinium prearticulatum*, and definite *Cordosphaeridium delimurum* from 3230 ft (984.5 m). A sharp change in the composition of the palynofloras occurs at 3620–3650 ft (1103.38–1112.52 m), with an influx of areoligeracean dinocysts, particularly *Glaphyrocysta divarica*. This palynoflora is characteristic of a Paleocene, probably Thanetian, age. We therefore suggest the presence of another unconformity between the Eocene and Paleocene between the samples at 3530 and 3650 ft (1075.94 and 1112.52 m), an interpretation consistent with major downhole positive shifts in the gamma-ray and sonic logs at 3634 ft (1107.64 m); the latter are coincident with a sharp negative shift in the resistivity log. We suggest that this unconformity is correlative to the Ypresian Unconformity of Weston *et al.* (2012). The Ypresian Chalk that usually drapes this unconformity at most other locations on the Scotian Margin does not appear to be present here. The palynological assemblage at 3710–3740 ft (1130.81–1139.95 m) is very similar to that at 3620–3650 ft (1103.38–1112.52 m), implying continued penetration of Thanetian strata at this depth, an interpretation supported by records of typical Paleocene foraminifera such as *Subbotina* cf. triloculinoides (as Globigerina cf. triloculinoides) and Gavelinella cf. danica at 3710–3740 ft (1130.81–1139.95 m) by Ascoli (1986).

Copyright © Atlantic Geoscience, 2023

A major influx of Late Cretaceous planktonic and benthic foraminifera is recorded by Ascoli (1986) at 3740–3770 ft (1139.95–1149.1 m). These forms include the late Maastrichtian-restricted planktonic species *Contusotruncana contusa* (as *Globotruncana contusa*), with the Maastrichtian taxa *Globotruncanita conica* (as *Globotruncana conica*) and *Gansserina gansseri* (as *Globotruncana gansseri*). The latter species became extinct during the late Maastrichtian. We therefore infer the presence of an unconformity between the Thanetian and intra-late Maastrichtian between 3740 and 3770 ft (1139.95–1149.1 m) and place this event at the sharp downhole positive shift in the sonic log and negative shift in the resistivity logs at 3746 ft (1141.78 m). We correlate this unconformity to the regional Base-Tertiary Unconformity (BTU). Ascoli (1986) records another sharp change in micropaleontological recovery at 3800–3830 ft (1158.24–1167.38 m), where the FDO of the planktonic foraminiferid *Globotruncanita elevata* (as *Globotruncana elevata*) is indicative of an age no younger than Campanian. We suggest that another unconformity lies between the Maastrichtian and Campanian, between 3770 and 3830 ft (1149.1 and 1167.38 m), which we place at 3792 ft (1155.8 m) at major downhole negative shifts in the gamma-ray and sonic logs associated with a downhole transition from claystone of the Banquereau Formation to limestone/marlstone lithofacies typical of the Wyandot Formation. The FDOs of the planktonic foraminiferid *Globotruncana ventricosa* and the calcareous benthic foraminiferid *Stensioina exsculpta gracilis* at 3890–3920 ft (1185.67–1194.82 m) imply an intra-Campanian age, whereas the FDO of the calcareous benthic foraminiferid *Bolivinoides miliaris* and the last downhole and common occurrence of the planktonic foraminiferid *Globotruncana ventricosa* at 4070–4090 ft (1240.54–1246.63 m) support an age no older than middle Campanian to at least 4090 ft (1246.63 m).

Ainsworth *et al.* (2016) recorded the FDO of the dinocyst *Odontochitina porifera* at 4150 ft (1264.92 m), indicating an age no younger than intra-Santonian, an assignment confirmed by the FDOs of the benthic foraminifera *Neoflabellina praerugosa, Neoflabellina suturalis* and *Stensioina* ?*granulata polonica* just below, at 4180 ft (1274.06 m). We suggest that an unconformity is present between the middle Campanian and intra-Santonian, which we place at the downhole positive shifts in the gamma-ray and sonic logs at 4147 ft (1264.0 m), coincident with negative shifts in the resistivity logs. We correlate this unconformity to the Intra-Campanian Unconformity of Weston *et al.* (2012) and suggest that it represents the boundary between the Wyandot and Dawson Canyon formations. Further support for an intra-Santonian age slightly deeper in the section comes from the FDOs of the planktonic foraminiferid *Marginotruncana sigali* and the ostracod *Phacorhabdotus pokornyi* forma A of Ascoli (1976) at 4210–4240 ft (1283.21–1292.35 m) (Ascoli 1981) and the planktonic foraminifera *Archaeoglobigerina bosquensis and abundant Whiteinella baltica, with the benthic foraminifera Stensioina exsculpta exsculpta, Stensioina granulata incondita and Stensioina granulata perfecta* at 4320 ft (1316.74 m) (Ainsworth *et al.* 2016). Ainsworth *et al.* (2016) also recorded the FDO of the Santonian-restricted planktonic foraminiferid *Dicarinella asymetrica* at 4580 ft (1395.98 m) and an abundance of the Santonian or older planktonic foraminifera *Archaeoglobigerina bosquensis* and *Whiteinella baltica* at 4700 ft (1432.56 m), where the FDO of the planktonic foraminiferid *Dicarinella concavata*, a species that became extinct in the Santonian, also occurs. The abundance of planktonic foraminifera recorded by Ainsworth *et al.* (2016) at 4700 ft (1432.56 m) suggests that this sample may reflect a condensed interval related to a maximum flooding surface that we tentatively suggest may be correlative to the Santonian MFS of Weston *et al.* (2012); we place this event at the positive inflections in the gamma-ray, sonic and neutron logs at 4686 ft (1428.29 m). The FDOs of the planktonic foraminifera *Dicarinella primitiva* (as *Globotruncana primitiva*), *Muricohedbergella delrioensis* (as *Hedbergella delrioensis*) and *Whiteinella brittonensis* (as *Hedbergella brittonensis*) at 4720–4760 ft (1438.66–1450.85 m) (Ascoli 1981) indicate an age no younger than earliest Santonian, whereas the FDOs of the dinocyst *Dinopterygium alatum* (as *Xiphophoridium alatum*) at 4780 ft (1456.94 m) and common specimens of the planktonic foraminiferid *Marginotruncana renzi* at 4880 ft (1487.42 m) (Ainsworth *et al.* 2016) confirm the broad Santonian or older age. At 4900 ft (1493.52 m), Ainsworth *et al.* (2016) recorded the FDO of the dinocyst *Scriniodinium campanula*, implying an age no younger than Coniacian, a determination confirmed by the subsequent FDOs of the planktonic foraminifera *Dicarinella imbricata* at 4940 ft (1505.71 m) (Ainsworth *et al.* 2016) and *Clavihedbergella amabilis* (as *Hedbergella amabilis*) and *Muricohedbergella planispira* (as *Hedbergella planispira*) at 4920–4960 ft (1499.62–1511.81 m) (Ascoli 1981). These planktonic foraminifera indicate an age no younger than intra-Coniacian and imply that the Santonian/Coniacian boundary lies somewhere above 4900 ft (1493.52 m); however, we are unable to determine its position accurately from the available data. Ainsworth *et al.* (2016) recorded an increase in the abundance of the dinocyst genus *Cyclonephelium* at 4980 ft (1517.9 m), an event characteristic of Coniacian or older strata on the Scotian Margin (Weston *et al.* 2012).

A distinct change in the composition of the micropaleontological assemblages occurs at 5060 ft (1542.29 m), where both Ascoli (1981) and Ainsworth *et al.* (2016) recorded the first downhole and common occurrence of the calcareous benthic foraminiferid *Gavelinopsis tourainensis*. Ascoli (1981) also recorded the FDOs of the agglutinated benthic foraminiferid *Dorothia* aff. *filiformis* and the ostracod *Veenia* aff. *spoori* at this depth. Ascoli (1988) recognized all of these taxa as markers for the Turonian, and we therefore place the top of the Turonian at 5060 ft (1542.29 m). The presence of abundant to common dinocysts of the genus Chatangiella between 5080 and 5210 ft (1548.38 and 1588.0 m) (Ainsworth *et al.* 2016) is characteristic of an age no older than Turonian, whereas an

Copyright © Atlantic Geoscience, 2023

influx of marginotruncanid planktonic foraminifera, including *Marginotruncana coronata, Marginotruncana marginata, Marginotruncana pseudolinneiana* and *Marginotruncana schneegansi* at 5190 ft (1581.91 m) (Ainsworth *et al.* 2016) indicates an age no older than late-middle Turonian. The latter authors also recorded an influx of *Marginotruncana sigali* at 5240 ft (1597.15 m), associated with the FDO of the planktonic foraminiferid *Praeglobotruncana stephani*; this combination of taxa indicates a definitive middle Turonian age at this depth. The FDO of the calcareous benthic foraminiferid *Stensioina granulata* ?*humilis* at 5300 ft (1615.44 m) (Ainsworth *et al.* 2016) is consistent with a middle Turonian age (Koch 1977), whereas the first recorded downhole occurrences of the planktonic foraminifera *Helvetoglobotruncana helvetica* and *Praeglobotruncana gibba* with the first definite occurrence of *Stensioina granulata humilis* at 5360 ft (1633.73 m) in Ainsworth *et al.* (2016) implies a middle to early (likely middle) Turonian age.

Another major change in the composition of the micropaleontological assemblages was recorded by Ainsworth *et al.* (2016) at 5420 ft (1652.02 m): an influx of rotaliporid and hedbergellid planktonic foraminifera including *Rotalipora cushmani, Rotalipora deeckei* and *Rotalipora greenhornensis*. These taxa indicate a late to late-middle Cenomanian age at 5420 ft (1652.02 m); the Turonian/Cenomanian boundary therefore lies between 5360 and 5420 ft (1633.73 and 1652.73 m). We place this boundary at the sharp downhole positive shifts in the sonic and neutron logs at 5400 ft (1645.92 m), which are coincident with sharp negative shifts in the gamma-ray and resistivity logs. We correlate this boundary to the Turonian/Cenomanian Unconformity of Weston *et al.* (2012), which on the Scotian Margin is usually overlain by the Petrel Member. We have picked the Petrel Member from 5300 to 5400 ft (1615.44 to 1645.92 m) in the interval where mud logs identify limestone; but as seen in some other Grand Banks wells (e.g., Bandol-1 and Heron H-73), limestone continues to be present in the Cenomanian beneath the correlative position of the Turonian/Cenomanian Unconformity. Alternatively, the base of the Petrel Member could be as low as 5508 ft (1678.84 m) if this lower limestone is included (e.g., MacLean and Wade 1993), or the lower limestone interval could be regarded as the informal "Heron limestone" of Swift *et al.* (1975).

Ascoli (1981) recorded *Rotalipora cushmani* together with the FDO of the planktonic foraminiferid *Praeglobotruncana delrioensis*, at 5420–5450 ft (1652.02–1661.16 m); these occurrences indicate a late-middle Cenomanian age. The FDOs of the planktonic foraminifera *Rotalipora globotruncanoides* (as *Rotalipora brotzeni*) at 5480 ft (1670.3 m) and *Rotalipora reicheli* at 5540 ft (1688.59 m) recorded by Ainsworth *et al.* (2016) confirm a middle Cenomanian age. The presence of the planktonic foraminiferid *Rotalipora cushmani evoluta* at 5520–5550 ft (1682.5–1691.64 m) in Ascoli (1981), associated with the ostracod *Neocythere vanveenae* (as *Neocythere vanveeni*), is characteristic of a middle to early Cenomanian age, whereas the common occurrence of the dinocyst *Dinopterygium alatum* (as *Xiphophoridium alatum*) at 5570 ft (1697.74 m) in Ainsworth *et al.* (2016) indicates an age no older than late Albian to that depth.

The dinocyst palynofloras recorded by Ainsworth *et al.* (2016) show a change in overall composition at 5630 ft (1716.02 m). From the sidewall core at 5630 ft (1716.02 m), Williams (1979) recorded a marked increase in miospore recovery, suggestive of a landward shift in depositional setting downhole; he also noted the FDO of the late to middle Albian dinocyst *Chichaouadinium vestitum* (as *Spinidinium vestitum*). On the Scotian Margin, *Chichaouadinium vestitum* has an acme in the middle Albian (Weston *et al.* 2012). The wireline log signature changes sharply at 5582 ft (1701.39 m) and, in light of the variation in palynofloral character between 5570 and 5630 ft (1697.74 and 1716.02 m), we suggest that this reflects an intra-Albian unconformity that we tentatively attribute to the Late Albian Unconformity of Weston *et al.* (2012). The wireline log pattern observed at 5582 ft (1701.39 m) resembles the log event seen at 1952 m in Bandol-1, where it represents a subtle lithofacies transition from the Dawson Canyon Formation to Logan Canyon Formation. In Emerillon C-56, sandstones characteristic of the Logan Canyon Formation are not developed until deeper, at 5858 ft (1785.52 m), implying that the lithostratigraphic boundary is significantly diachronous between Bandol-1 and Emerillon C-56. The FDO of the calcareous benthic foraminiferid *Lingulogavelinella ciryi ciryi* at 5660 ft (1725.17 m) (Ainsworth *et al.* 2016), the first downhole and common occurrence of the calcareous benthic foraminiferid *Epistomina carpenteri* and the ostracod *Schuleridea jonesiana* at 5730 ft (1746.5 m) (Ainsworth *et al.* 2016), and the FDO of the calcareous benthic foraminifera *Epistomina cretosa* and *Berthelina berthelini* (as *Gavelinella berthelini*) at 5720–5750 ft (1743.46–1752.6 m) (Ascoli 1981) confirm the broad Albian age of the section beneath this unconformity at 5582 ft (1701.39 m). Ascoli (1976, 1988) suggested that an assemblage containing common *Epistomina carpenteri* and *Schuleridea jonesiana* is most typical of the early Albian on the Scotian Margin, and strata from at least 5730 ft (1746.5 m) may thus be of early Albian age. An age no younger than early Albian is supported by the FDO of the dinocyst *Kleithriasphaeridium simplicispinum* at 5810 ft (1770.89 m) and the first downhole and common occurrence of the calcareous benthic foraminiferid *Epistomina chapmani* at 5840 ft (1780.03 m) (Ainsworth *et al.* 2016). Ascoli (1981) reported the presence of the calcareous benthic foraminifera *Epistomina spinulifera colomi, Epistomina spinulifera polypioides* and *Epistomina carpenteri* at 5820–5850 ft (1773.94–1783.08 m); these taxa are typical of the Albian on the Scotian Margin.

From 5860 ft (1786.13 m) downhole, the Emerillon C-56 well-history log (Elf Oil Exploration & Production Ltd. 1974) records a transition into poorly sorted sandstone of the Eider unit, the top of which MacLean and Wade (1993) placed at 5858 ft (1785.52 m). Ainsworth *et al.* (2016) noted a major downhole increase in miospore versus

Copyright © Atlantic Geoscience, 2023

dinocyst recovery from 5870 ft (1789.18 m) and a marked downhole decrease in microfaunal recovery from 5900 ft (1798.32 m). This evidence indicates a landward shift in depositional conditions downhole from 5858 ft (1785.52 m). Williams (in the BASIN database) recorded the FDO of the intra-late Aptian or older dinocyst *Cerbia tabulata* in the sidewall core at 5923 ft (1805.33 m), whereas Ainsworth *et al.* (2016) reported the FDOs of the dinocyst *Dingodinium albertii* at 5990 ft (1825.75 m) and the dinocyst *Aptea securigera* at 6110 ft (1862.33 m), implying an age no younger than early Aptian from at least 5990 ft (1825.75 m) downhole. We suggest that the downhole transition from limestone and shale to poorly sorted sandstone at 5858 ft (1785.52 m) represents the boundary between the Albian and Aptian and we thus place this event at the top of the Eider unit sandstone at 5858 ft (1785.52 m). We tentatively call this event the Early Albian Unconformity and correlate it to probable unconformities observed between the lower Albian and Aptian in Bandol-1 and East Wolverine G-37.

Between 6140 ft and 6380 ft (1871.47 an d 1944.62 m), micropaleontological recoveries are very poor (comprising coaly fragments, shelly debris, and charophyte oogonia), whereas palynofloras show increased recovery of spores and plant tissue, accompanied by rare dinocysts of the genus *Subtilisphaera.* These recoveries imply marginal marine depositional conditions. The underlying light-grey, calcareous shales between 6380 and 6480 ft (1944.62 and 1975.1 m), however, yield a moderate micropaleontological assemblage at 6420–6450 ft (1956.82–1965.96 m) that includes the FDO of the calcareous benthic foraminifera *Gavelinella barremiana* (common) and *Lenticulina gaultina* with the LDO of the calcareous benthic foraminiferid *Gavelinella intermedia* (Ascoli 1981). These occurrences indicate an early Aptian age. The shales between 6380 and 6480 ft (1944.62 and 1975.1 m) are therefore attributed to the Naskapi Member of the Logan Canyon Formation, and we attribute the increase in open marine influence observed at 6450 ft (1965.96 m) to the Intra-Aptian MFS of Weston *et al.* (2012). We place this event at the coincident positive spikes in the gamma-ray and sonic logs at 6438 ft (1962.3 m). Reworking of older Lower Cretaceous material into the Naskapi Member is implied by the records of the dinocysts *Muderongia perforata* in the sidewall core at 6390 ft (1947.67 m) (Williams in the BASIN database) and ?*Phoberocysta neocomica* at 6410 ft (1953.77 m) (Ainsworth *et al.* 2016).

Ainsworth *et al.* (2016) recorded the incoming of an abundant agglutinated benthic foraminiferal fauna characterized by species of *Ammobaculites*, *Haplophragmoides* and *Trochammina* at 6500 ft (1981.2 m), with a similar assemblage at 6520–6550 ft (1987.3–1996.44 m) in Ascoli (1981). However, the latter assemblage also includes the ostracod ?*Hutsonia* sp. 3 of Ascoli (1976). This ostracod is a marker for the *Hutsonia* sp. 3 – *Protocythere triplicata* Zone of Barremian age on the eastern North Atlantic margin (Ascoli 1988), and we infer that the Aptian/Barremian boundary lies between 6450 and 6500 ft (1965.96 and 1981.2 m). We place this event at the top of the thin sandstone at 6482 ft (1975.71 m), where downhole negative shifts in the sonic and resistivity logs occur, associated with a sharp negative spike in the gamma-ray log, below which the shales become dark grey to black, micromicaceous and dolomitic. We correlate this boundary to the Aptian/Barremian Unconformity of Weston *et al.* (2012) and suggest that this is the boundary between the Logan Canyon and Missisauga formations. An age no younger than Barremian is supported by the record of the dinocyst *Muderongia perforata* in the sidewall core at 6570 ft (2002.54 m) (Williams in the BASIN database) and the sole occurrence of the agglutinated benthic foraminiferid *Marssonella kummi* at 6620–6650 ft (2017.78–2026.92 m) (Ascoli 1981). Ascoli (1976, 1988) considered *Marssonella kummi* to be indicative of an age no younger than early Barremian on the Scotian Margin. Occurrences of the dinocysts *Palaeoperidinium cretaceum* at 6770 ft (2063.5 m) and *Pseudoceratium retusum* at 6830 ft (2081.78 m) (Ainsworth *et al.* 2016) suggest that strata to at least 6830 ft (2081.78 m) are no older than Barremian, correlating to the Upper Member of the Missisauga Formation on the Scotian Margin. Unlike many other sections through the Missisauga Formation, there is no clear indication of Hauterivian strata or the associated O-Marker.

Ainsworth *et al.* (2016) recorded a sharp change from a typical Early Cretaceous dinocyst assemblage at 6830 ft (2081.78 m) to one including the Jurassic species *Dichadogonyaulax sellwoodii* at 6890 ft (2100.07 m). This implies that a major unconformity between Lower Cretaceous and Juras-sic strata no younger than Oxfordian lies between 6830 and 6890 ft (2081.78 and 2100.07 m). We place this unconformi-ty at the major downhole positive shifts in the gamma-ray and resistivity logs at 6847 ft (2086.97 m). We correlate it to the major unconformity known as the Avalon Unconfor-mity in this region, which is easily mapped on seismic data (see Fig. 3). This unconformity is commonly more expan-sive in time than the NBCU of the Scotian Margin (see Figs. 2, 6, and 7), for example in this well it also encompasses the Intra-Hauterivian Unconformity. A broad Kimmeridgian to Callovian age below this unconformity is supported by the record by Ainsworth *et al.* (2016) of a rich micropaleonto-logical assemblage at 6920 ft (2109.22 m), which includes the calcareous benthic foraminifera *Epistomina parastelligera*, *Lenticulina* ?*quenstedti* and *Planularia tricarinella* (as *Lenticulina tricarinella*). The FDOs of the calcareous benthic foraminifera *Epistomina* cf. *soldanii* and *Lenticulina varians* at 6920–6950 ft (2109.22–2118.36 m) (Ascoli 1981) confirm an age no younger than Oxfordian. The FDO of the dinocyst *Ctenidodinium combazii* at 6950 ft (2118.36 m) (Ainsworth *et al.* 2016) indicates an age no younger than earliest Callovian, whereas the dinocyst and foraminiferal assemblages recorded above by these authors are typical of the early Callovian in this area. We therefore suggest that the Avalon Unconformity at 6847 ft (2086.97 m) truncates the Jurassic in Emerillon C-56 to within the lower Callovian.

Copyright © Atlantic Geoscience, 2023

Ainsworth *et al.* (2016) cited the first downhole and common occurrence of the calcareous benthic foraminifera *Epistomina regularis, Lenticulina quenstedti* and *Ophthalmidium carinatum* at 6980 ft (2127.5 m), and this assemblage is characteristic of a broad Callovian age on the Scotian Margin (Grigelis and Ascoli 1995). The FDO of the dinocyst *Ctenidodinium ornatum* at 7070 ft (2154.94 m) confirms an age no older than Callovian to at least this depth. Ascoli (1981) recorded the FDO of the early Callovian to Bathonian calcareous benthic foraminiferid *Reinholdella crebra* at 7150 ft (2179.32 m), together with the LDO of the calcareous benthic foraminiferid *Lenticulina quenstedti*, which does not range below the Callovian in this area (Grigelis and Ascoli 1995). These observations indicate that strata of early Callovian age are present down to at least 7150 ft (2179.32 m). In the interval from 6847 to 7150 ft (2086.97 to 2179.32 m), Ainsworth *et al.* (2016) noted a local increase in dinocysts and microforaminiferal test linings at 7070 ft (2154.94 m), which they suggested reflects a condensed interval related to a maximum flooding surface. Ascoli's data within the BASIN database also shows that calcareous benthic foraminiferal assemblages are richer and more diverse within the samples at 7020–7050 ft and 7120–7150 ft (2139.7–2148.84 m and 2170.18–2179.32 m), an observation that provides support for an interval of more open, possibly deeper-marine strata between 7020 and 7150 ft (2139.7 and 2179.32 m), potentially related to an MFS. We place this possible MFS within the grey shale around 7050 ft (2148.84 m), at the positive inflections in the gamma-ray and sonic logs at 7048 ft (2148.23 m), and we correlate it to the Base-Callovian MFS of Weston *et al.* (2012). Although the shale-dominated interval between the Avalon Unconformity and the Base-Callovian MFS was assigned questionably to the Verrill Canyon Formation by MacLean and Wade (1993); it also could be regarded, in part, as a lateral equivalent of the Misaine Member of the Abenaki Formation. Alternatively, if using Grand Banks nomenclature, the interval could be assigned to the upper part of the Voyager Formation (McAlpine 1990).

The mixed lithofacies of (sometimes oolitic) limestone, shale, and poorly sorted sandstone from 7160 ft (2182.37 m) downhole yield relatively poor microfaunas and palynofloras. Records in Williams (1979) of the miospore *Circularesporites cerebroides* in and below the sidewall core at 7204 ft (2195.78 m) are consistent with an age no younger than Callovian (Bujak and Williams 1977), whereas the FDO of the dinocyst *Aldorfia aldorfensis* at 7490 ft (2282.95 m) confirms a Middle Jurassic age no younger than early Callovian. Ainsworth *et al.* (2016) recognized an increase in dinocyst recovery, particularly of *Dichadogonyaulax sellwoodii*, from 7610 ft (2319.53 m) downhole, along with a rich ostracod assemblage just below at 7640 ft (2328.67 m). Ostracods recorded by Ainsworth *et al.* (2016) at 7640 ft (2328.67 m) include the FDOs of *Micropneumatocythere ?falcata, Micropneumatocythere subconcentrica*, *Pichottia magnamuris*, *Schuleridea* (*Eoschuleridea*) *batei and Schuleridea* (*Eoschuleridea*)*? bathonica.* Ascoli (1988) considered *Micropneumatocythere falcata, Micropneumatocythere subconcentrica* and *Schuleridea* (*Eoschuleridea*) *batei* to be markers for the *Fabanella batonica – Micropneumatocythere* s.l. Zone of the Bathonian on the North American margin, whereas these species are characteristic of the Bathonian, and particularly the late Bathonian, in northwestern Europe (Ainsworth *et al.* 1998). We therefore conclude that the Callovian/Bathonian boundary lies somewhere within the interval 7150–7640 ft (2179.32–2328.67 m), but we are unable to determine this more precisely with the available data.

The FDO of the dinocyst *Durotrigia filapicata* (as *Diacanthum filapicatum*) in the sidewall core at 7758 ft (2364.64 m) (Williams 1979) is typical of, but not restricted to, a Bathonian age. The Bathonian age is confirmed by an acme of the benthic foraminiferid *Massilina dorsetensis* and ostracods that include the FDO of the Bathonian ostracod *Micropneumatocythere quadrata* in Ainsworth *et al.* (2016) at 7760 ft (2365.25 m). *Micropneumatocythere quadrata* is another marker for the Bathonian *Fabanella batonica – Micropneumatocythere* s.l. Zone of Ascoli (1988) on the North American margin, and it is also typical of the late Bathonian in the United Kingdom and France. Ainsworth *et al.* (2016) recorded common dinocysts (particularly *Dichadogonyaulax sellwoodii* and a granulate form of *Pareodinia*) in samples at 7730 and 7790 ft (2356.1 and 2374.39 m); these abundances of dinocysts, foraminifera and ostracods suggest another condensed interval related to a maximum flooding surface around the acme of *Massilina dorsetensis* and ostracods at 7760 ft (2365.25 m). Dark-grey calcareous shales are recorded on the Elf *et al.* Emerillon C-56 Well History Log at 7740–7770 ft (2359.15–2368.3 m) and we thus place an MFS at 7762 ft (2365.86 m), coincident with positive spikes in the gamma-ray and sonic logs. We correlate this event to the Late Bathonian MFS recognized in the East Wolverine G-37 well in this study, where it is also associated with the FDO of the ostracod *Micropneumatocythere quadrata*.

Ainsworth *et al.* (2016) recorded dinocyst assemblages characterized by *Ctenidodinium continuum*, *Dichadogonyaulax sellwoodii* and *Pareodinia* sp. (including granulate forms) throughout the section down to 8990 ft (2740.15 m); these occurrences indicate an age no older than intra-late Bajocian to at least this depth. Micropaleontological notes in Ainsworth *et al.* (2016) relating to this part of the section are rare, although they did record the ostracod *Pseudomacrocypris atypica* at 8120 ft (2474.98 m) (a species described from the middle Bathonian of France by Sheppard 1981), together with the typical Bathonian ostracods *Darwinula incurva* at 8720 ft (2657.86 m) and *Fabanella bathonica* from 8840 ft (2694.43 m) downhole. Ascoli (1981) recorded the typical Bathonian ostracods *Marslatourella bullata* at 8120–8150 ft (2474.98–2484.12 m) and *Micropneumatocythere brendae* at 8220–8250 ft (2505.46–2514.6 m), with the FDO of *Fabanella bathonica* higher in the section than Ainsworth *et al.*'s. (2016) record at 8320–8350 ft (2535.94–2545.08 m). In the latter sample, *Fabanella bathonica* is associated with the sole

Copyright © Atlantic Geoscience, 2023

occurrence of another typical Bathonian ostracod *Klieana levis* in an assemblage comparable to those described from the middle to lower Bathonian of France (Oertli 1985) and the Anoual Formation (lower Bathonian) in the Eastern High Atlas of Morocco (Haddoumi *et al.* 2008). The LDO of *Fabanella bathonica* according to Ascoli (1981) is at 8420–8450 ft (2566.42–2575.56 m), which suggests that strata to at least 8450 ft (2575.56 m) are no older than Bathonian.

If the record of *Fabanella bathonica* at 8840 ft (2694.43 m) in Ainsworth *et al.* (2016) is in situ, the Bathonian interval could stretch downhole to at least 8840 ft (2694.43 m). However, Ainsworth *et al.* (2016) recorded the FDO of the Bajocian marker dinocyst *Cribroperidinium crispum* (as *Acanthaulax crispa*) at 7910 ft (2410.97 m), as well as questionable specimens of the intra-Bajocian to Pliensbachian dinocyst *Mancodinium semitabulatum* at 8810 and 8930 ft (2685.29 and 2721.86 m). These occurrences indicate an age older than the Bathonian designation provided by the ostracods noted above, and *Mancodinium semitabulatum* does not range as young as the oldest range of the dinocysts *Dichadogonyaulax sellwoodii* and *Ctenidodinium continuum,* which persist downhole to 8990 ft (2740.25 m). We therefore infer that these older dinocysts are probably reworked. At 8990 ft (2740.15 m), Ainsworth *et al.* (2016) recorded the FDOs of the dinocysts *Nannoceratopsis gracilis* and *Gongylodinium erymnoteichon*, the co-occurrence of which indicates an early Bathonian to Bajocian age. Strata between 8450 ft (2575.56 m) and 8990 ft (2740.25 m) are therefore of Bathonian to intra-late Bajocian age.

The top of persistent recovery of questionable specimens of the dinocysts *Mancodinium semitabulatum* and *Scriniocassis weberii* from 9110 ft (2776.73 m) in Ainsworth *et al.* (2016) suggests an age no younger than early Bajocian. Records of definite specimens of the dinocysts *Mancodinium semitabulatum* at 9230 and 9290 ft (2813.3 and 2831.59 m) and *Scriniocassis weberi* at 9650 ft (2941.32 m) by Ainsworth *et al.* (2016) confirm an age no younger than early Bajocian (Woollam and Riding 1983). It is notable that the micropaleontological events in Ainsworth *et al.* (2016) include the FDO of the crinoid *Pentacrinus* spp. from 9380 ft (2859.02 m). *Pentacrinus* spp. was recorded from the well-constrained Bajocian of the Eider M-75 well from the southern Grand Banks (Fig. 1; Ainsworth *et al.* 2016), and we suggest that this event is in the Bajocian in this area. The LDO of the dinocyst ?*Gongylodinium erymnoteichon* at 9410 ft (2868.17 m) in Ainsworth *et al.* (2016) suggests an age no older than Bajocian, whereas their record of the FDO of definite specimens of the dinocyst *Moesiodinium raileanui* at 9530 ft (2904.74 m) supports an age no younger than early Bajocian. Ainsworth *et al.* (2016) recorded the base of persistent recovery of granulate forms of the dinocyst genus *Pareodinia* at 9650 ft (2941.32 m), suggesting an age no older than Middle Jurassic to this depth. Ascoli (1981) recorded the FDOs of the calcareous benthic foraminifera *Reinholdella media* at 9520–9550 ft (2901.7–2910.84 m) and *Garantella ornata* at 9620–9650 ft (2932.18–2941.32 m), and Ascoli (1981) also reported the sole occurrence of the calcareous benthic foraminiferid *Epistomina praecursor* at 9620–9650 ft (2932.18–2941.32 m). Ascoli (in the BASIN database) also recorded occurrences of the calcareous benthic foraminiferid *Epistomina regularis* in both the latter samples. *Reinholdella media* and *Garantella ornata* range from the Bathonian to Bajocian and *Epistomina regularis* from the Callovian to the Bajocian (Gradstein 1978), whereas *Epistomina praecursor* is restricted to the Bajocian (Grigelis and Ascoli 1995; Weston *et al.* 2012). These data therefore imply an age no older than Bajocian down to at least 9650 ft (2910.84 m), with the sample at 9620–9650 ft (2932.18–2941.32 m) being of Bajocian age. Based on the questionable occurrences of *Mancodinium semitabulatum* and *Scriniocassis weberi* from 9110 ft (2776.73 m) and of definite *Mancodinium semitabulatum* from 9230 ft (2813.3 m) and of *Moesiodinium raileanui* from 9530 ft (2904.74 m), we suggest that strata from 9110–9650 ft (2776.73–2941.32 m) are of early Bajocian age. The interval from 7150–9400 ft (2179.32–2865.12 m) is tentatively assigned to the Mic Mac Formation (or its equivalent) due to the presence of sandstone, as suggested by MacLean and Wade (1993); but the amount of limestone could alternatively justify assigning it to the Downing Formation of the Grand Banks area (McAlpine 1990), including the carbonate-rich Whale Member in the lower part of the formation (Fig. 14a).

Between 9740 and 9816 ft (2968.75 and 2991.92 m), MacLean and Wade (1993) and Bowman *et al.* (2012) indicated the presence of a section of Cretaceous intrusive rocks (see caption to Fig. 3); these rocks yielded a K/Ar age of 97.4 ± 3.8 Ma (Cenomanian). In their seismic panel for this well, MacLean and Wade (1993) showed that the Bathonian/Bajocian interval is cut by a fault (Fig. 3; OERA 2014, MacLean and Wade 1993). Without a better well-seismic tie, it is not possible to precisely determine the position of such a fault with the data available to us, but possibly the intrusive rocks have penetrated along the fault. No dinocyst events were recorded by Ainsworth *et al.* (2016) around the position of this intrusive, and the samples beneath it are characterized by prominent woody debris (inertinite) and the miospore *Classopollis* spp. However, Ascoli (1981) reported the sole occurrence of the calcareous benthic foraminiferid *Garantella semiornata* at 10 020–10 050 ft (3054.1–3063.24 m), and Grigelis and Ascoli (1995) and Weston *et al.* (2012) reported that this species is characteristic of the Bajocian on the Atlantic Canadian margin. Ascoli (in the BASIN database) recorded occurrences of the calcareous benthic foraminifera *Epistomina regularis, Garantella ornata* and *Reinholdella media* at 10 120–10 150 ft (3084.58–3093.72 m); all of these species suggest an age no older than Bajocian in offshore eastern Canada and we therefore propose that Bajocian strata lie beneath the Cretaceous intrusives to at least 10 150 ft (3093.72 m), within lithologies that likely correspond to the Mohican Formation or its lateral equivalent (see picks in MacLean and Wade 1993). The FDO of ostracods of the genus *Ektyphocythere* at 10 110 ft (3081.53 m) (Ainsworth *et al.* 2016) is consistent with this age assignment, as this genus ranges through the

Copyright © Atlantic Geoscience, 2023

Middle and Early Jurassic, as are the records of questionable specimens of the dinocyst *Moesiodinium raileanui* at 9950 and 10 010 ft (3032.76 and 3051.05 m).

Biostratigraphic data are very sparse below 10 010 ft (3051.05 m) in Ainsworth *et al.* (2016), but they recorded the FDO of the ostracod *Praeschuleridea arguta arguta* at 10 220 ft (3115.06 m). *Praeschuleridea arguta arguta* was first described from the Aalenian to Toarcian of the Fastnet Basin, offshore southwestern Ireland (Ainsworth 1986), and the taxon has also been recorded from upper Toarcian strata in Portugal (Boomer *et al.* 1998). A major change in overall wireline-log signature occurs at 10 214 ft (3113.23 m), associated with increasing amounts of dolostone and anhydrite interbedded with shale, which MacLean and Wade (1993) attributed to the lithostratigraphic boundary between strata equivalent to the overlying Mohican and deeper Iroquois formations. We suggest that this wireline feature/lithostratigraphic boundary may represent the Bajocian/Toarcian Unconformity recognized in the Heron H-73 well in the present study.

As noted above, biostratigraphic data are sparse within the basal part of the Emerillon C-56 well, although the recovery of common poorly preserved specimens of the ostracod *Ogmoconcha* spp. at 10 520 ft (3206.5 m) (Ainsworth *et al.* 2016) and the sole occurrence of the ostracod *Ektyphocythere lotharingiae* (as *Procytheridea lotharingiae*) at 10 720–10 750 ft (3267.46–3276.6 m) (Ascoli 1981) indicate that the well reached TD within the Lower Jurassic. *Ogmoconcha* spp. is characteristic of an age no younger than Early Jurassic and it can be found in abundance in lower Toarcian and older Jurassic strata (Cabral *et al.* 2020). Gradstein (1979) considered *Ogmoconcha* spp. to be restricted to the *Involutina liassica* zone of approximate Pliensbachian age on the southern Grand Banks. *Ektyphocythere lotharingiae* was described from the upper Sinemurian of France and has been recorded from upper Sinemurian marine faunas of western Portugal and the Fastnet Basin, offshore southwestern Ireland (Cabral *et al.* 2015). We thus suggest that Emerillon C-56 reached TD within strata of Sinemurian, possibly late Sinemurian, age. The interval 10 520–10 750 ft (3206.5–3276.6 m) is therefore earliest Toarcian to late Sinemurian.

Evidence is present of downhole contamination in this basal part of the well, with records of a typical Bajocian epistominid calcareous benthic foraminiferal fauna at 10 520–10 550 ft (3206.5–3215.64 m) (Ascoli in the BASIN database), the Aalenian and late Toarcian ostracod *Praeschuleridea* ?cf. *P. pseudokinkelinella* of Ainsworth (1986) at 10 650 ft (3246.12 m), and specimens of the Late to Middle Jurassic dinocyst genus *Ctenidodinium* in the sidewall core at 10625 ft (3238.5 m) (Williams in the BASIN database).

Heron H-73

Our evaluation of Heron H-73 (Figs. 14b, 15) is partly based on unpublished data from the internal BASIN database. These data include the micropaleontological report of Gradstein (1977) and sample-by-sample palynological data of Williams (in the BASIN database), summarized in Barss *et al.* (1979). These analyses are from the interval 1540–11970 ft (469.39–3648.46 m), primarily from 92 cuttings samples, although data from 61 sidewall cores are also included. In addition, in the interval 7500–11 100 ft (2286–3383.26 m), quantitative nannofossil analyses were undertaken of 16 targeted new spot samples by one of us (MKEC) on cuttings samples supplied by C-NLOPB, and 77 pre-existing palynological slides (mainly from sidewall-core samples) provided by C-NLOPB were re-logged by one of us (DS) to provide new quantitative data over the interval 5785–11 970 ft (1763.27–3648.46 m). A summary stratigraphic plot of this well is provided in Figure 14b and Supplementary Data 4; the stratigraphic breakdown and interpreted depths of well-log sequence-stratigraphic surfaces of Weston *et al.* (2012), as well as additional surfaces recognized in this study, are summarized in Figures 15 and 19.

Occurrences of the dinocysts *Pentadinium granulatum* (as *Pentadinium laticinctum* subspecies *granulatum*) from 1510–1540 ft (460.25–469.39 m) and *Pentadinium laticinctum* from 1690–1720 ft (515.11–524.26 m) indicate an age no younger than Tortonian. The record of the planktonic foraminiferid *Globigerina apertura* at 2260–2290 ft (688.85–697.99 m) implies that strata to this depth are no older than Tortonian (Blow zone N16; Wade *et al.* zone M13a). Penetration of rocks no younger than Serravallian is indicated by the occurrence of the dinocyst *Cannosphaeropsis passio* from 2530–2560 ft (771.14–780.29 m), an age confirmed by the occurrence of the planktonic foraminiferid *Globorotalia praemenardii* at 2830 ft (862.58 m). The Tortonian/Serravallian boundary is therefore between 2290 and 2560 ft (697.99 and 780.29 m). A major change in composition of the micropaleontological assemblages occurs at 3340–3370 ft (1018.03–1027.18 m), with the downhole incoming of coarse arenaceous benthic foraminifera, including *Cyclammina cancellata*. This event characterizes strata of probable Early Miocene age in wells from the Grand Banks (Gradstein 1977) and the boundary between strata of Middle and Early Miocene age may therefore lie around 3340–3370 ft (1018.03–1027.18 m).

The FDO of the dinocyst *Chiropteridium galea* at 4150–4180 ft (1264.92–1274.06 m) indicates an age no younger than Chattian, whereas the in situ occurrence of the planktonic foraminiferid *Paragloborotalia opima opima* (as *Globorotalia opima opima*) from 4240–4270 ft (1292.35–1301.5 m) indicates an intra-Chattian to intra-Rupelian age, implying that the latest Chattian may be absent or condensed. A possible Miocene/Oligocene unconformity occurs around the major shift in the sonic, density and resistivity logs at 4110 ft (1252.73 m), and we propose this depth for the top of the Oligocene. The first in situ downhole occurrence of dinocysts of the genus *Wetzeliella* at 4960–4990 ft (1511.81–1520.95 m) is indicative of an intra-Chattian to Rupelian age. A significant change in sonic and density log signature occurs at 4928 ft (1502.05 m) and the lithofacies becomes

Copyright © Atlantic Geoscience, 2023

notably less arenaceous below this depth. We suggest that these changes reflect the presence of the Intra-Oligocene Unconformity of Weston *et al.* (2012) at 4928 ft (1502.05 m). The occurrence of the planktonic foraminiferid *Turborotalia ampliapertura* (as *Globigerina ampliapertura*) at 5320 ft (1621.54 m) (Gradstein 1977) supports an age no younger than Rupelian below.

The FDOs of the dinocysts *Cordosphaeridium funiculatum* and *Perisseiasphaeridium* spp. in the sidewall core at 5500 ft (1676.4 m) are evidence for penetration of Eocene strata no younger than Priabonian, and we tentatively place the top of the Eocene at 5500 ft (1676.4 m). The FDO of the dinocyst *Diphyes colligerum* at 5680–5710 ft (1731.26–1740.41 m) implies a Lutetian to Ypresian age. Gradstein (1977) noted changes in lithofacies (from clastic to chalky) and faunal composition (from domination by agglutinated benthic foraminifera to predominantly planktonic foraminifera) at 5710 ft (1740.41 m). These planktonic foraminifera include forms such as the *Acarinina bullbrooki* group (as *Globorotalia bullbrooki* group), *Morozovella caucasica* (as *Globorotalia caucasica*) and *Turborotalia cerroazulensis frontosa* (as *Globigerina frontosa*) that do not range below the latest Ypresian. These lithofacies and faunal changes thus represent transition into the regional, seismically recognizable Ypresian Chalk of late Ypresian age (see Weston *et al.* 2012, p. 1451). The top of the Ypresian Chalk is placed at the sharp negative shifts in the gamma-ray and sonic logs at 5710 ft (1740.41 m), which coincide with the incoming of white marlstones. White earliest Ypresian to Thanetian planktonic foraminiferal tests are mixed with grey early? Maastrichtian to Campanian taxa in the micropaleontological preparations at 5770–5800 ft (1758.7–1767.84 m). These stratigraphically mixed assemblages may represent redeposition of reworked/allochthonous sediment equivalent to, but much less extensive than, the major glide blocks observed on the Scotian Margin that were attributed to slope failure related to the Montagnais impact event on the southwestern Scotian Margin (as discussed in Weston *et al.* 2012, p. 1452; see also Deptuck and Campbell 2012). At the base of this interval, sharp downhole positive shifts in the gamma-ray and sonic logs at 5792 ft (1765.4 m) indicate a major lithofacies change, which we attribute to the Ypresian Unconformity of Weston *et al.* (2012).

The presence of the dinocyst *Xenascus ceratioides* in the cuttings sample 5770–5800 ft (1758.7–1767.84 m) tentatively suggests an age no younger than Campanian beneath the Ypresian Unconformity, whereas the sidewall core at 5865 ft (1787.65 m) is characterized by common specimens of the dinocyst genus *Dinogymnium*, typical of a Late Cretaceous, possibly late Campanian, age. The FDO of the dinocyst *Surculosphaeridium longifurcatum* in the sidewall core at 6200 ft (1889.76 m) suggests an early Campanian or older age and we suggest that the regional Intra-Campanian Unconformity of Weston *et al.* (2012) occurs just above this FDO at the changes in the sonic- and bulk-density-log trends and a negative shift in the gamma-ray log at 6195 ft (1888.24 m). The sidewall core at 6450 ft (1965.96 m) contains the FDO of the dinocyst *Senoniasphaera protrusa*, the first downhole evidence for an age no younger than Santonian. This age is confirmed by the presence of the planktonic foraminiferid *Marginotruncana coronata* (as *Globotruncana coronata*) at and below 6610 ft (2014.73 m). Coincident positive inflections in the gamma-ray and sonic logs at 6420 ft (1956.82 m), just above the first evidence for a Santonian age, may represent the position of the Santonian MFS of Weston *et al.* (2012). The FDO of the dinocyst *Odontochitina porifera* in the cuttings sample at 6700–6730 ft (2042.16–2051.3 m) implies an intra-Santonian to Coniacian age, whereas the common occurrence of *Odontochitina porifera* through the interval 7010–7450 ft (2136.65–2270.76 m) is characteristic of a Coniacian age. The interval containing the acme of *Odontochitina porifera* includes the upper part of the Petrel Member limestone, the top of which was placed at 7230 ft (2203.7 m) by MacLean and Wade (1993). Within the lower part of the Petrel Member, the FDO of the dinocyst *Litosphaeridium siphoniphorum* in the sidewall core at 7528 ft (2294.53 m) indicates an age no younger than early Turonian.

Typical middle to early Turonian nannofossils are first recorded in the cuttings sample at 7600 ft (2316.48 m), but the FDOs of the Cenomanian or older taxa *Cyclagelosphaera margerelii* and ?*Rhagodicus asper* are also present in this sample. These occurrences imply an age no younger than middle Cenomanian at 7600 ft (2316.48 m). We therefore place the Turonian/Cenomanian Unconformity of Weston *et al.* (2012), typically associated with the base of the Petrel Member on the Scotian Margin, at the sharp downhole increases in the density and resistivity logs at 7598 ft (2315.87 m). A Cenomanian to late Albian age below 7600 ft (2316.48 m) is confirmed by an abundance of the dinocyst *Chlamydophorella nyei* and the common occurrence of *Litosphaeridium siphoniphorum* in the sidewall core at 7608 ft (2318.92 m) and the FDO of the planktonic foraminiferid *Favusella washitensis* at 7660 ft (2334.77 m), whereas the LDO of *Litosphaeridium siphoniphorum* in the sidewall core at 7690 ft (2343.91 m) implies an age no older than late Albian to at least this depth. The sole occurrence of the dinocyst *Chichaouadinium vestitum* in the sidewall core at 7750 ft (2362.2 m) indicates a late to middle Albian age. The palynological data thus indicate a middle Cenomanian to middle Albian age range for the informal "Heron limestone" unit (Swift *et al.* 1975) between 7630 and 7778 ft (2325.62 and 2370.73 m), as demarcated by MacLean and Wade (1993). There is a sharp change in lithofacies from limestone to coarse- to very coarse-grained sandstone of the Eider unit at and below 7780 ft (2371.34 m). The sidewall core at 7790 ft (2374.39 m) yields the FDO of the dinocyst *Kleithriasphaeridium eoinodes*, indicating an age no younger than late Aptian at 7790 ft (2374.39 m). We therefore infer that the sharp transition from pink to white, micritic to cryptocrystalline limestone of the Heron limestone unit to coarse- to very coarse-grained white sandstone of the Eider unit between the cuttings samples at 7770 to 7780 ft (2368.3 to 2371.34 m) is an unconformity. We place this uncon-

Copyright © Atlantic Geoscience, 2023

formity at the sharp change in wireline-log signature at 7778 ft (2370.73 m) and tentatively attribute it to the Late Albian Unconformity defined by Weston *et al.* (2012), which may be amalgamated with the ?Early Albian Unconformity. Palynofloral recoveries from the Eider unit sandstone are dominated by miospores, particularly fern spores, in the sidewall core at 7810 ft (2380.49 m); FDOs include those of the typical Early Cretaceous miospores *Appendicisporites problematicus* and *Eucommiidites* spp. in the sidewall core at 7830 ft (2386.58 m). Palynofloral recovery is poor at and below 7830 ft (2386.58 m), whereas micropaleontological preparations from this unit are barren.

A further sharp change in lithofacies to creamy or occasionally white limestone occurs at 8080 ft (2462.78 m), whereas the sole in situ occurrences of the dinocysts *Ctenidodinium ornatum* and *Tubotuberella dangeardii* in the sidewall core at 8105 ft (2470.4 m) indicate a Jurassic, Oxfordian to Callovian age for these limestone beds, attributed to the Abenaki Formation by MacLean and Wade (1993), or alternatively Voyager Formation in Grand Banks nomenclature (McAlpine 1990). We interpret the presence of an unconformity at the sharp change from clastic to carbonate lithofacies indicated by the major negative shifts in the gamma-ray and sonic logs associated with major positive shifts in the resistivity logs at 8072 ft (2460.35 m). We correlate this horizon to the regional Avalon Unconformity.

The FDOs of the dinocysts *Gonyaulacysta pectinigera* (as *Leptodinium subtile pectinigerum*) and *Adnatosphaeridium caulleryi* in the sidewall core at 8500 ft (2590.8 m) indicate a Middle Jurassic, Callovian to late Bathonian age, whereas the FDO of the nannofossil *Cyclagelosphaera deflandrei* in the cuttings sample at 8580 ft (2615.18 m) suggests an age no older than Callovian/latest Bathonian. The FDO of the dinocyst *Durotrigia filapicata* (as *Gonyaulacysta filapicata*) in the sidewall core at 9110 ft (2776.73 m) (Williams in the BASIN database) confirms the Callovian to middle Aalenian age, but the species is most typical of the Bathonian. An influx of the benthic foraminiferid *Paalzowella feifeli* in the sidewall core at 9142 ft (2786.48 m) is consistent with a Callovian to Bathonian age, and it is notable that this species has its FDO associated with the Base-Callovian MFS of Weston *et al.* (2012) in other wells in the present study. We thus suggest that the positive inflection in the sonic log just above this FDO at 9070 ft (2764.54 m) represents the Base-Callovian MFS. Limestone beds of the Abenaki Formation persist downhole to 9792 ft (2984.6 m) (MacLean and Wade 1993), below which a major shift in the wireline-log signature occurs, culminating in a change to clastic sedimentary rocks (fine- to very fine-grained, grey sandstone interbedded with white to light brown micritic limestone) downhole at 9850 ft (3002.26 m). These clastic rocks are attributed to an equivalent of the Mohican Formation by MacLean and Wade (1993), and they yield the FDOs of the nannofossils *Carinolithus* spp. and *Podorhabdus grassei* at 9930 ft (3026.66 m) and the sole occurrence of the benthic foraminiferid *Lenticulina dictyodes* at 9990 ft (3044.95 m). These occurrences indicate a Bajocian age for these Mohican/Downing-equivalent strata at 9930–9990 ft (3026.66–3044.95 m), and we assign the interval 8072–9930 ft (2460.35–3026.66 m) to a broad Oxfordian to Bajocian age.

Within the interval attributed to the Mohican equivalent by MacLean and Wade (1993), a sharp lithological change to grey shale with occasional thin interbeds of light-grey to brown limestone occurs at 10 000 ft (3048 m). At 10 020 ft (3054.1 m), these rocks yield the FDO of the early Toarcian to Sinemurian nannofossil *Mitrolithus jansae*. This implies that a Bajocian/intra-Toarcian unconformity occurs at around 10 000 ft (3048 m). We place it at the sharp positive shift in the sonic log and negative shift in the resistivity log at 9998 ft (3047.39 m) and here name it the Bajocian/Toarcian Unconformity. The Early Jurassic age determination below 10 000 ft (3048 m) is confirmed by the FDO of the Toarcian to late Pliensbachian dinocyst *Luehndea spinosa* at 10 060–10 090 ft (3066.29–3075.43 m), within a palynoflora strongly dominated by miospores and particularly by abundant specimens of the pollen *Classopollis torosus* and *Spheripollenites psilatus*. The abundance of *Spheripollenites psilatus* at 10 060–10 090 ft (3066.29–3075.43 m) and also at 10 160–10 190 ft (3096.77–3105.91 m) is suggestive of the earliest Toarcian (Bujak and Williams 1977). Gradstein (1977) recorded the top of his *Involutina liassica* zone at 10 060 ft (3066.29 m), to which he attributed an approximate Pliensbachian age (Gradstein 1978). However, all the taxa cited range up into at least the Toarcian in other areas (Copestake and Johnson 2014); and Boutakiout (1990) showed that such forms have their stratigraphic tops within the earliest Toarcian in Morocco. We therefore suggest that the recognition of the *Involutina liassica* Zone from 10 060 ft (3066.29 m) downhole is consistent with the early Toarcian age indicated by the nannofossil and palynological data from 10 000 ft (3048 m).

A further lithofacies change occurs from 10 176 ft (3101.65 m) downhole, to more thinly interbedded limestone and shale and, at 10 260–10 290 ft (3127.25–3136.39 m), the abundance of *Spheripollenites psilatus* decreases and the palynoflora is strongly dominated by *Classopollis torosus*. This palynofloral change suggests an age no younger than Pliensbachian from 10 260–10 290 ft (3127.25–3136.39 m), based on Bujak and Williams (1977). We tentatively interpret the strong lithofacies change and wireline shift observed at 10 176 ft (3101.65 m) to correlate with the major JPl8 sequence boundary of Haq (2018), and this surface may represent a further, but minor unconformity surface in the well.

A Pliensbachian age for the strata at and below 10 260–10 290 ft (3127.25–3136.39 m) is confirmed by the FDO of the nannofossil *Crepidolithus granulatus* and an abundance of the nannofossil *Lotharingius hauffii* at 10 380 ft (3163.82 m), which together characterize the late Pliensbachian equivalent to the lower part of Bown and Cooper (1998) nannofossil subzone NJ5b plus subzone NJ5a. The persistent occurrence of the dinocyst *Luehndea spinosa* in cuttings samples down to 11 030–11 060 ft (3361.94–3371.09 m) implies

Copyright © Atlantic Geoscience, 2023

that the interval 10 290–11 060 ft (3136.39–3371.09 m) is late Pliensbachian in age, consistent with the record by Gradstein (1977) of the benthic foraminifera *Paralingulina tenera* (as *Lingulina tenera*), *Involutina liassica* and *Berthelinella involuta* down to 10 560 ft (3218.69 m). The top of persistent recovery and first in situ downhole occurrence of the nannofossil *Mitrolithus elegans* at 10 800 ft (3291.84 m) suggests an age no younger than earlier late Pliensbachian (probably Bown and Cooper subzone NJ5a) from that depth, and there is a sharp downhole increase in nannofossil densities at 10 800 ft (3291.84 m) and 10 880 ft (3316.22 m). These two samples are associated with more argillaceous sedimentary rocks, and strong positive curves in the gamma-ray and sonic logs occur through the interval 10 805–10 865 ft (3293.36–3311.65 m). We suggest that these wireline signatures reflect the presence of a major MFS, which we place at the positive inflections in the gamma-ray and sonic logs at 10 830 ft (3300.98 m) and name the Late Pliensbachian MFS here. The occurrence of the miospore *Cadargasporites verrucosus* at 10 930–10 960 ft (3331.46–3340.61 m) is typical of the Pliensbachian or older Jurassic (Bujak and Williams 1977). At the base of the limestone facies attributed to the Mohican equivalent formation by MacLean and Wade (1993), the deepest cuttings sample analyzed for nannofossils at 11 100 ft (3383.28 m) contains the sole occurrence of the nannofossil *Crepidolithus pliensbachensis*, indicating an age no younger than early Pliensbachian and Bown and Cooper nannofossil subzone NJ4a. The co-occurrence of abundant specimens of the nannofossil *Similiscutum cruciulus* to this depth implies an age no older than Pliensbachian and subzone NJ4a within the limestone facies.

The well penetrates dolostone beds of the Iroquois Formation from 11 070 ft (3374.14 m) downhole, with interbedded dolostone and anhydrite from 11 270 ft (3435.1 m). The top of the salt of the Argo Formation is placed on the change in wireline-log signature at 11 478 ft (3498.49 m). These two formations yield palynofloras composed almost exclusively of miospores, predominantly *Classopollis torosus*, which suggest an Early Jurassic age no older than late Hettangian to the bottom of the well at 12 000 ft (3657.6 m) (Bujak and Williams 1977). The sole occurrence of the miospore *Echinitosporites* sp. A of Bujak and Williams (1977) at 11 640 ft (3547.87 m) is consistent with an early Pliensbachian to late Hettangian age.

DSDP Site 547B, Mazagan Plateau, offshore Morocco

As a part of the Laurentian Basin study (OERA 2014), Beicip-Franlab collected seven samples for geochemical analysis from Lower Jurassic cores from DSDP Site 547B (Leg 79) from the Mazagan Plateau, offshore Morocco (Figs. 16–17). Beicip-Franlab's aim was to compare the geochemistry of this well-documented potential source rock interval within the Moroccan Basin (Rullkötter and Mukhopadhyay 1986) to geochemical data from rocks of similar age from offshore eastern Canada, particularly in Heron H-73. Samples were collected from DSDP Site 547B cores 15, 20, and 22, which gave the highest TOC values in the original DSDP studies (Hinz *et al.* 1984); these cores cover the interval from 847.55 to 905.2 m. The Beicip-Franlab sampling locations are shown in OERA (2014, plate 5.4.8) and Figure 17. In order to provide an accurate comparison of the ages and depositional settings of these Moroccan strata from DSDP Site 547B with the Lower Jurassic of Heron H-73, six of the samples from cores 15, 20, and 22 were analyzed for nannofossils and four of the samples from cores 20 and 22 were analyzed palynologically. A summary stratigraphic plot of prior age data (Hinz *et al.* 1984) and new data from these samples is provided in Figures 16 and 17, and a stratigraphic summary and range charts of the new biostratigraphic data and interpretations are recorded in the Supplementary Data 5. The data and interpretations are consistent with those in Robinson *et al.* (2017).

The shallowest sample analyzed, from core 15 section 2 (847.55 m), yielded a rich Early Jurassic nannofossil assemblage dominated by *Schizosphaerella punctulata*, with abundant *Mitrolithus jansae*. The co-occurrence of *Crepidolithus pliensbachensis* and *Similiscutum cruciulus* indicates an early Pliensbachian age equivalent to Bown and Cooper (1998) nannofossil zone NJ4a. *Similiscutum cruciulus* has a well-established inception at the base of the Pliensbachian and zone NJ4a, whereas *Crepidolithus pliensbachensis* ranges from the early Pliensbachian to the Sinemurian (zones NJ4a–NJ2b of Bown and Cooper 1998). This result is consistent with Robinson *et al.* (2017), who reported zone NJ4a from slightly shallower in core 15 (847.53 m), and the start of zone NJ3 slightly deeper (847.66 m). Although core 15 was not sampled for palynology in the present study, Fenton (1984) reported the first downhole occurrence of the miospore *Echinitosporites* cf. *iliacoides* in this core, consistent with an early Pliensbachian age and our observation of this form deeper in core 20 (892.30 m; see below).

A poor nannofossil assemblage is recorded from the top of core 20 section 1 (891.11 m), although the co-occurrence of *Mitrolithus elegans* and *Orthogonoides hamiltoniae* indicates a Pliensbachian to late Sinemurian age. A superabundant nannofossil assemblage is recorded from slightly deeper in core 20 section 1 (892.30 m). This includes the early Pliensbachian to Sinemurian marker *Crepidolithus pliensbachensis*, together with *Crepidolithus crassus* and *Orthogonoides hamiltoniae*, which do not range older than the late Sinemurian and Bown and Cooper (1998) nannofossil zone NJ3. This association therefore indicates an early Pliensbachian to late Sinemurian age, although a high abundance of *Crucirhabdus primulus* suggests a late Sinemurian age and equivalence to nannofossil zone NJ3. Similar, but poorer, nannofloras consistent with an early Pliensbachian to late Sinemurian age were recovered from the other two samples analyzed for nannofossils from section 2 of core 20 (892.79 m and 893.39 m). Palynological preparations from samples in core 20 are dominated by the miospore *Classopollis torosus*, but the first downhole occurrence of the miospore

Copyright © Atlantic Geoscience, 2023

DSDP 547B

Depth (m)	Core	Section	Epoch	Age
847.55	15	2	Early Jurassic	early Pliensbachian
891.11	20	1		early Pliensbachian to late Sinemurian
892.3				early Pliensbachian to late Sinemurian, ?late Sinemurian
892.79–893.39		2		
905.2	22	1		early Pliensbachian to late Sinemurian, ?close to late/early Sinemurian boundary

Figure 16. Summary of age in the sampled portion of DSDP Site 547B.

Echinitosporites sp. A of Bujak and Williams (1977) at 893.01 m (section 2) confirms an Early Jurassic age no younger than early Pliensbachian, consistent with Fenton (1984), who reports the top of the same marker within core 20.

The single sample analyzed from core 22 section 1 (905.20 m) yields a very similar nannofossil assemblage to those from core 20, including *Crepidolithus crassus* and *Orthogonoides hamiltoniae*, which imply an age no older than late Sinemurian and Bown and Cooper (1998) nannofossil zone NJ3. As with samples from core 20, *Crucirhabdus primulus* shows a relatively high abundance and suggests a late Sinemurian age equivalent to zone NJ3. It is notable, however, that a questionable specimen of the early Sinemurian restricted nannofossil *Parhabdolithus marthae* is present in this sample, whereas the palynological assemblage includes a single specimen of the miospore *Cycadopites subgranulosus*, which does not range younger than the early Sinemurian. These occurrences in the sample at 905.20 m tentatively suggest proximity to the upper/lower Sinemurian boundary and the top of nannofossil zone NJ2b (see Fig. 18).

The new analyses provide more stratigraphic resolution than was possible from the original biostratigraphic data in Hinz *et al.* (1984), where cores 15–22 were assigned a broad Pliensbachian to Sinemurian age. Good micropaleontological data from the Jurassic section of DSDP Site 547B were recorded by Riegraf *et al.* (1984), in which cores 15–22 are seen to contain moderate to abundant benthic foraminiferal faunas. A sample from core 15 section 1 at 0–4 cm yielded a moderate assemblage characterized by the *Paralingulina tenera* plexus (as various subspecies of *Lingulina tenera*). Samples from core 20 sections 1 (126–129 cm) and 2 (59–61 cm) yielded abundant and more diverse foraminiferal faunas that include various members of the *Ichthyolaria terquemi* plexus (as subspecies of *Frondicularia terquemi* and including *Frondicularia squamosa*) and the *Paralingulina tenera* plexus, together with numerous nodosariid forms and common agglutinated benthics, particularly *Glomospira pattoni*. A sample from core 22 section 1 (95–98 cm) yielded an impoverished, but similar, benthic foraminiferal fauna. Although all these forms range up into the Toarcian, Copestake and Johnson (2014) indicated that foraminiferal faunas characterized by the *Ichthyolaria terquemi* and *Paralingulina tenera* plexuses, with *Marginulina prima* (present in core 20 section 1) are typical of the Pliensbachian to Hettangian in northwestern Europe. Gradstein (1978, 1979) considered *Paralingulina tenera* (as *Lingulina tenera*) a zonal marker for an approximate Pliensbachian age on the Grand Banks. Occurrences of *Prodentalina integra* (as *Dentalina integra*), *Prodentalina suboligostegia* (as *Dentalina suboligostegia*) and *Prodentalina teutoburgensis* (as *Dentalina teutoburgensis*) in core 20 section 1 (126–129 cm) also support an age assignment no younger than Pliensbachian. Riegraf *et al.* (1984) considered the sole occurrence of *Lingulina acuformis* in core 20 section 2 (59–61 cm) to be diagnostic of the lower Pliensbachian to upper Sinemurian, although Copestake and Johnson (2014) considered *Lingulina acuformis* to be a synonym of *Paralingulina tenera subprismatica* and to range through the Pliensbachian and Sinemurian. In summary, the foraminiferal faunas recorded by Riegraf *et al.* (1984) from cores 15 to 20 in DSDP Site 547B are consistent with the early Pliensbachian to late Sinemurian ages provided by the new nannofossil and palynological data.

The samples analyzed from DSDP Site 547B in this study comprise mudstone and nodular limestone. The nannofossil assemblages recorded indicate deposition occurred under open marine surface water conditions, whereas the foraminiferal assemblages are characteristic of a middle to outer neritic depositional environment (Hylton 1999). The domination of the palynofloras by the gymnosperm pollen Classopollis torosus (including abundant tetrads) suggests deposition occurred in a relatively proximal setting close to a coastal plain.

DISCUSSION

In this section we discuss the consequences of our recognition of new events and significant revisions, especially to the Middle and Early Jurassic stratigraphic breakdown compared to those of Weston *et al.* (2012). We first consider the integration of events in this interval between the four studied Laurentian Subbasin wells before summarizing the event stratigraphy of the entire Mesozoic-Cenozoic interval on the southern Grand Banks. This is followed by a comparison of the Grand Banks, Scotian Margin, and conjugate Moroccan margin, before synthesizing the implications for source rock potential in the central Atlantic in the Early Ju-

Copyright © Atlantic Geoscience, 2023

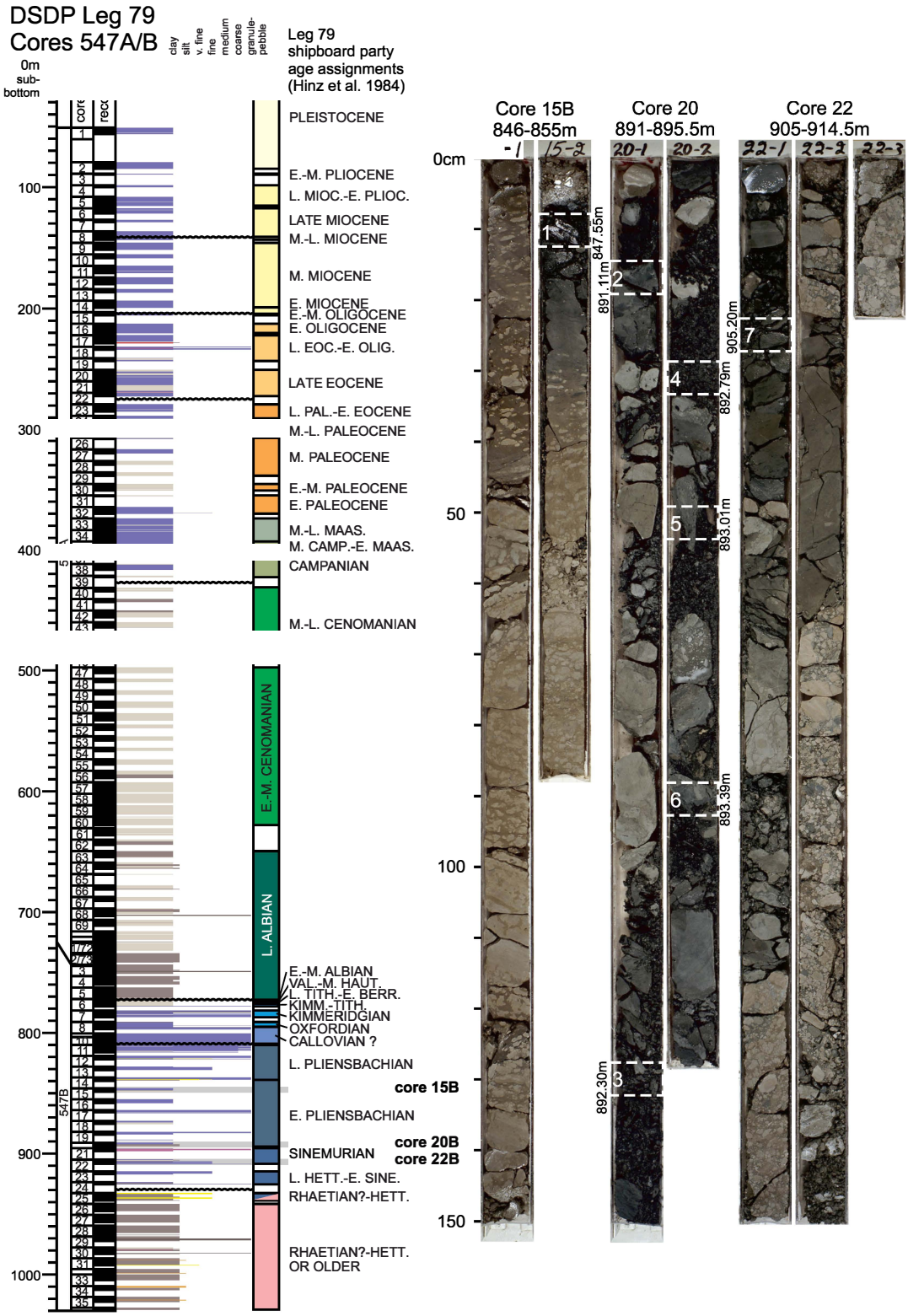

Figure 17. Stratigraphy of Deep Sea Drilling Project Leg 79, Borehole 547A and Site 547B (spliced at approximately 730 m below sea floor), Mazagan Plateau, offshore Morocco. Plate reconstructed position is shown in Figure 1. Coloured bars in lithology column correspond to the lithologies in the legend in Figure 10 and are drawn with vertical thicknesses that represent the recovered intervals. Lithology and the majority of age information from Hinz *et al.* (1984). Samples from this study are recovered from cores 15B, 20, and 22 (photos and sample numbers on right side). See Figure 16 and text for more detailed age results from the studied intervals in the Early Jurassic, and Figure 18 for comparison with Heron H-73. Additional information shown in Supplementary Data 1.

Copyright © Atlantic Geoscience, 2023

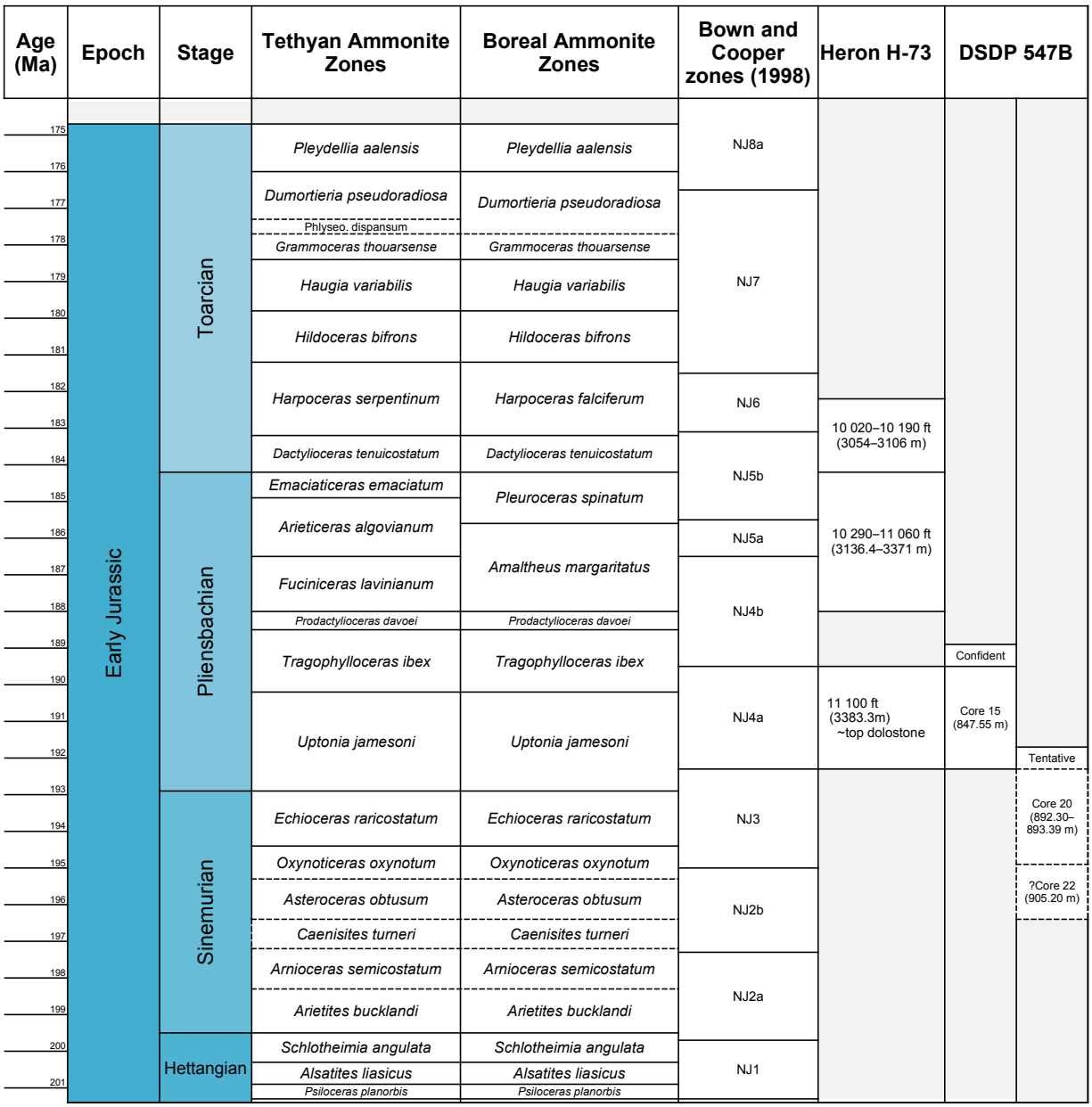

Figure 18. Correlation of Early Jurassic ages with ammonite (Gradstein *et al.* 2020) and nannofossil (Bown and Cooper 1998) zonation schemes showing corresponding intervals within Heron H-73 and the interval of DSDP 547B sampled for this study. The broader context for these wells is plotted in Figures 14b and 17, respectively. Timescale is based on Gradstein *et al.* (2020).

rassic. For helpful cross-sections through all four Laurentian Subbasin wells, see OERA (2014, plates 4-3-1, 4-3-2, 4-4-1, and 4-4-2).

Middle Jurassic biostratigraphic assemblages

Callovian strata in the four wells studied from the Laurentian Subbasin yielded nannofossil and palynological assemblages broadly similar to those described by Weston *et al.* (2012) from wells farther southwest on the Scotian Margin. Major events are shown in Figure 7. The palynomorph assemblages are characterized by *Diacanthum* spp. and *Energlynia acollaris*, and persistent occurrences of species of *Cribroperidinium, Meiourogonyaulax* and *Systematophora*, together with sporadic *Ctenidodinium ornatum*, *Dichadogonyaulax sellwoodii*, *Gonyaulacysta jurassica* and *Korystocysta gochtii*. Although characterized by similar benthic foraminifera to those on the Scotian Margin, Callovian assemblages from the Laurentian Subbasin wells are less dominated by epistominid taxa (especially in the more distal depositional setting of East Wolverine G-37), and they include a diversity of lenticulinid species, particularly *Lenticulina quenstedti*, together with *Paalzowella feifeli* and *Spirillina infima*. Planktonic foraminifera, mainly *Glo-*

Copyright © Atlantic Geoscience, 2023

buligerina bathoniana, are also present occasionally within the lower Callovian. Previously, Gradstein (1978, 1979) indicated a Bathonian stratigraphic top for *Globuligerina bathoniana* on the southern Grand Banks, but the data recovered from these wells are more comparable to that recorded by Ascoli (1976, 1988), who placed the stratigraphic top of this species on the eastern margin of North America in the lower Callovian. Callovian nannofossil assemblages are dominated by watznaueriaceans. In Heron H-73, recovery of nannofossils is poor and no age diagnostic species are recorded. However East Wolverine G-37 yielded Callovian assemblages similar to those described in Weston *et al.* (2012), and these included the age-diagnostic species *Ansulasphaera helvetica* and *Discorhabdus criotus*.

In the wells studied by Weston *et al.* (2012), marine Bajocian to Bathonian strata were poorly represented and only the upper Bathonian could be clearly identified from the palynological data. In the present study, we recorded more extensive pre-Callovian marine forms represented by age-diagnostic assemblages. Bathonian nannofossil assemblages are generally poorer than those from the overlying Callovian, although they are similar in composition and dominated by the genus *Watznaueria*. They are characterized by the FDOs of *Biscutum novum* and *Schizosphaerella punctulata*, and *Pseudoconus enigma* is rare but generally persistent throughout. Dinocyst assemblages are similar to those from the Callovian, but characterized particularly by *Dichadogonyaulax sellwoodii* and species of *Ctenidodinium*. Bathonian micropaleontological assemblages in the four wells studied here are richer and more diverse than those recorded in Weston *et al.* (2012). They are characterized by a diverse ostracod fauna, particularly species of *Micropneumatocythere* and *Schuleridea* (*Eoschuleridea*), with *Fabanella bathonica*, and the benthic foraminifera *Reinholdella crebra*, *Reinholdella media* and *Garantella ornata*. In the more distal depositional setting of East Wolverine G-37, the planktonic foraminiferid *Globuligerina bathoniana* shows an acme in the late Bathonian.

The penetrated Middle Jurassic (undivided or Bathonian–Callovian) is notably thick in Bandol-1, where it consists mainly of sandstone attributable to the Mic Mac Formation, as well as in East Wolverine G-37, where it consists mainly of mudstone of the Verrill Canyon Formation (the distal equivalent of the Mic Mac Formation). In the latter section it is over one kilometre thick despite being truncated at the well's TD. MacLean and Wade (1992, p. 234–235) predicted a greater total thickness of Mic Mac Formation in this area compared to the Scotian Margin, and speculated that the character of reflections would be more consistent with a clastic-dominated, rather than carbonate-dominated succession, which turns out to be the case.

We identified Bajocian strata in Heron H-73 and most likely in Emerillon C-56, although in the latter well the section is complicated by possible faulting and a Cretaceous igneous intrusion (see Fig. 3; MacLean and Wade 1993; Bowman *et al.* 2012; OERA 2014). Nannofossil assemblages from the Bajocian are sparse, dominated by *Schizosphaerella punctulata* and *Schizosphaerella* fragments, and contain consistent occurrences of species of *Crepidolithus* and *Lotharingius*. They also include the FDO of *Carinolithus* spp. Bajocian dinocyst palynofloras are relatively sparse, but include the LDOs of species of *Ctenidodinium*, *Dichadogonyaulax sellwoodii* and *Gongylodinium erymnoteichum* in the uppermost Bajocian and the FDOs of *Mancodinium semitabulatum*, *Moesiodinium raileanu* and *Scriniocassis weberi* in the lower Bajocian. Micropaleontological assemblages are characterized by the FDOs of the benthic foraminifera *Epistomina praecursor*, *Garantella semiornata* and *Lenticulina dictyodes* and the LDOs of the benthic foraminifera *Garantella ornata* and *Reinholdella media*.

No evidence for Aalenian strata was recovered from these wells.

Early Jurassic biostratigraphic assemblages

Lower Jurassic strata were penetrated in Emerillon C-56 and Heron H-73. In Emerillon C-56, potential upper Sinemurian to Toarcian strata are present; and Heron H-73 includes a section of well-constrained Pliensbachian to lower Toarcian strata, overlying a less well-constrained section no older than late Hettangian. In both wells, we interpret a major unconformity between the Lower Jurassic (Toarcian) and the Middle Jurassic (Bajocian), characterized by sharp changes in biostratigraphic recoveries.

Nannofossil recoveries from the shale and limestone of the Pliensbachian to lower Toarcian in Heron H-73 are rich and diverse. The nannofloras are all dominated by *Schizosphaerella punctulata* and *Schizosphaerella* fragments, and species of *Crepidolithus* are important constituents. Other common to abundant nannofossils in the Lower Jurassic include *Lotharingius hauffii* (late Pliensbachian to Toarcian), *Mitrolithus jansae* (Pliensbachian to early Toarcian), *Parhabdolithus liasicus* (Sinemurian to early Pliensbachian) and *Crucirhabdus primulus* (Sinemurian).

Palynofloral recoveries from the Lower Jurassic in Emerillon C-56 appear to be very poor based on the events noted on the Stratigraphic Summary Log in Ainsworth *et al.* (2016); this paucity may reflect the dolomitic and anhydritic lithofacies. The Pliensbachian to lower Toarcian shale and limestone in Heron H-73, by contrast, yield abundant palynofloras strongly dominated by the miospores *Classopollis toro-sus* and *Spheripollenites psilatus*. Occasional rare specimens of the dinocyst *Luenhdea spinosa* are also present. The dolomitic and anhydritic rocks from the older part of the Heron H-73 section yield palynofloras more variable in abundance, but they remain strongly dominated by *Classopollis torosus*. These palynofloras from Heron H-73 in the Laurentian Subbasin are very similar to those recorded from the few new samples analyzed from DSDP Site 547B from the Moroccan Margin and from samples previously reported in Fenton (1984). In both sections, lower Pliensbachian and older strata are dominated by *Classopollis torosus* and characterized by rare occurrences of the miospore *Echinitosporites* sp. A of Bujak and Williams (1977).

Copyright © Atlantic Geoscience, 2023

Event (bolded = new this study)	Bandol-1 (m)	East Wolverine G-37 (m)	Emerillon C-56		Heron H-73	
			(ft)	(m)	(ft)	(m)
Intra-Oligocene Unc. (T29)	1388	3674	2566?	782?	4928?	1502?
Ypresian Chalk	Truncated beneath Unc.	4184	-		5710	1740.4
Ypresian Unc. (T50)	Truncated beneath Unc.	4193	3634?	1107.6?	5792	1765.4
Base-Tertiary Unc. (BTU)	1636	4205	3746	1141.8	-	
Intra-Campanian Unc.	1644	-	4147	1264	6195?	1888.2?
Santonian MFS	1654?	-	4686?	1428.3?	6420?	1956.8?
Turonian/Cenomanian Unc. (K94)	1890	4224	5400	1645.9	7598	2315.9
Late Albian Unc. (K101)	1952	4248	5582?	1701.4?	7778?	2370.7?
Early Albian Unc.	2058?	4359	5858?	1785.5?	-	
Albian/Aptian boundary MFS	2082?	-	-		-	
Intra-Aptian MFS	2287	4484	6438	1962.3	-	
Aptian/Barremian Unc.	2328	4578	6482	1975.7	-	
Intra-Hauterivian MFS (K130)	2516	Truncated beneath Unc.	-		-	
Near-Base Cretaceous Unc./NBCU (K137)	2642	4867?	6847	2087	-	
Avalon Unconformity	-	5149	-		8072	2460.4
Top-Callovian MFS	2669	?Truncated beneath Unc.	?Truncated beneath Unc.		?Truncated beneath Unc.	
Base-Callovian MFS (J163)	2797	5556	7048	2148.2	9070?	2764.5?
Late Bathonian MFS (J166)	-	6611	7762	2365.86	-	
Bajocian/Toarcian Unc. (J170)	-	-	10214?	3113.2?	9998	3047.4
JPl8 SB Haq (2018)	-	-	-		10176?	3101.6?
Late Pliensbachian MFS (J186)	-	-	-		10830	3301
Top Salt	-	-	-		11478	3498.5

Figure 19. Depiction of the depths of existing (Weston *et al.* 2012) and new well-log sequence stratigraphic surfaces within the four wells studied from the Laurentian Subbasin. New or revised surfaces recognized in this study are shown in bold text. Events that have corresponding seismic horizons in the Laurentian PFA are indicated in parentheses (see Fig. 8). Abbreviations: Unc. = unconformity; MFS = maximum flooding surface; JPl8 = Jurassic Pliensbachian sequence boundary 8 of Haq (2018).

Micropaleontological assemblages described by Gradstein (1978, 1979) from the Pliensbachian to lower Toarcian on the southern Grand Banks (including within Heron H-73) are characterized by *Brizalina liassica*, *Involutina liassica* and the *Paralingulina tenera* plexus. Micropaleontological data recorded by Riegraf *et al.* (1984) suggest that foraminiferal assemblages in the upper Sinemurian to lower Pliensbachian cores 15–22 of DSDP Site 547B from offshore Morocco are more diverse than those recorded by Gradstein on the southern Grand Banks. The Moroccan assemblages are characterized by the *Ichthyolaria terquemi* and *Paralingulina tenera* plexuses and various nodosariid/dentalinid forms.

Well-log sequence stratigraphic surfaces

Weston *et al.* (2012) recognized eight major biostratigraphically constrained sequence stratigraphic surfaces across the Scotian Margin. The seismic horizons, and the biostratigraphically-recognized surfaces closely associated with them, are (from youngest to oldest):

T29 (Intra-Oligocene Unconformity)
T50 (Ypresian Unconformity)
K94 (Turonian/Cenomanian Unconformity)
K101 (Late Albian Unconformity)
K130 (Intra-Hauterivian MFS)
K137 (Near-Base Cretaceous Unconformity)
J150 (Tithonian MFS)
J163 (close to Base-Callovian MFS)

In the present work on the four well sections from the Laurentian Subbasin we have recognized the majority of these surfaces, plus other regional biostratigraphically distinct surfaces (Fig. 19). We have verified the surfaces through seismic correlation to wells studied in the original Scotian Margin PFA study, particularly to Dauntless D-35 (see OERA 2011, 2014). Notable differences between surfaces recorded from the Laurentian Subbasin wells and those on the Scotian Margin (Weston *et al.* 2012) are detailed below (see also Fig. 2).

(1) In the present study, we recognized an unconformity between the Upper Cretaceous (Campanian or intra-Maastrichtian) and Paleocene in Bandol-1, East Wolverine G-37 and

Copyright © Atlantic Geoscience, 2023

Emerillon C-56. We term this the Base-Tertiary Unconformity (BTU) here, following the informal usage in previous work (e.g., "Base Tertiary unconformity" of MacLean and Wade 1993). We consider this surface to be equivalent to the Fox Harbour Unconformity of Deptuck *et al.* (2003) in the Jeanne d'Arc Basin. This unconformity is in the lowermost part of the Banquereau Formation in Bandol-1 and Emerillon C-56, but forms the boundary between the Banquereau and Wyandot formations in the more distal East Wolverine G-37 well.

(2) We suggest that an unconformity, the Early Albian Unconformity, is present between the Aptian and lower Albian in Bandol-1, East Wolverine G-37 and Emerillon C-56. This hiatus lies within the Logan Canyon Formation in all three wells, and is at the top of the Eider unit sandstone in Emerillon C-56, though the Eider unit sandstone is often above the equivalent unconformity or the more extensive Avalon Unconformity in other Grand Banks wells (McAlpine 1990). The Early Albian Unconformity appears to reflect a landward shift in depositional conditions downhole at the three well locations and is biostratigraphically constrained by strata that include the FDOs of the early Albian or older markers *Kleithriasphaeridium simplicispinum* (dinocyst) or *Nannoconus quadriangulus* (nannofossil) above and the FDO of the intra-late Aptian and older dinocyst *Cerbia tabulata* below.

(3) Uniquely among the wells studied and rare in the region is a wedge of earliest Cretaceous (Berriasian–?lower Valanginian) strata, beneath the Near-Base Cretaceous Unconformity in East Wolverine G-37. In Weston *et al.* (2012), only Alma F-67 and South Griffin J-13 had representation of these lowermost Cretaceous strata, where they overlie Tithonian rocks. In East Wolverine G-37, these strata overlie Callovian clastics. This earliest Cretaceous package of strata includes occurrences of the benthic foraminifera *Conorboides valendisensis* and *Lenticulina saxonica bifurcilla*, which are typical of an early Valanginian to Berriasian age according to Ascoli (1976); also present is a questionable specimen of the late Berriasian to early Valanginian nannofossil *Kokia curvata*.

(4) The Tithonian MFS and most, if not all, of the Upper Jurassic is absent from all four Laurentian Subbasin well sections due to erosion beneath unconformities. These unconformities are amalgamated as part of the composite Avalon Unconformity of the Grand Banks and northeastern Scotian Margin, which spans an interval as young as Albian–Cenomanian and as old as Kimmeridgian as noted by many workers, including Grant and McAlpine (1990), McAlpine (1990), MacLean and Wade (1992, 1993). In general we have separated sequence stratigraphic events where possible, but the event charts (Figs. 6 and 7) also show the approximate extent of Avalon Unconformity amalgamation seen in the region; this hiatus is generally of greater duration than it is on the Scotian Margin except at the latter's northeastern extremity (Fig. 2).

(5) We refine the definition of the Base-Callovian MFS of Weston *et al.* (2012), which represents a strong increase in open marine influence in all four Laurentian Subbasin wells. It is characterized by the local FDO of the benthic foraminiferid *Paalzowella feifelii*, and the LDOs of the benthic foraminiferid *Lenticulina quenstedti* and the dinocyst *Ctenidodinium ornatum*. In Bandol-1 and East Wolverine G-37, an acme of *Ctenidodinium ornatum* occurs just beneath the Base-Callovian MFS.

(6) In East Wolverine G-37, we recognize a major maximum flooding surface of late Bathonian age, which we term the Late Bathonian MFS. This surface is characterized by an acme of the planktonic foraminiferid *Globuligerina bathoniana* and the FDOs of the ostracod *Micropneumatocythere quadrata* and the nannofossils *Biscutum intermedium* and *Biscutum novum.* We tentatively correlate this surface to Emerillon C-56, where it is also characterized by the FDO of *Micropneumatocythere quadrata*; but in this more proximal well location the micropaleontological recovery is distinguished by an acme of the benthic foraminiferid *Massilina dorsetensis.* The Late Bathonian MFS, which corresponds to seismic horizon J166 in OERA (2014), appears to be younger than the Bathonian/Bajocian MFS recognized in Cohasset L-97 by Weston *et al.* (2012). The Bathonian/Bajocian MFS on the Scotian Margin is characterized by the persistent recovery of the nannofossils *Discorhabdus striatus* and *Schizosphaerella punctulata*; it is reinterpreted here to be an older MFS, probably Bajocian (de Kaenel *et al.* 1996; Mattioli and Erba 1999), and has been accordingly renamed the Late Bajocian MFS.

(7) In Heron H-73, a shallow marine, sand-dominated interval of Bajocian age unconformably overlies a more argillaceous section of early Toarcian age. This section is well-dated by nannofossils, supported by additional micropaleontological and palynomorph data. The palynological data show a major transition downsection across this unconformity from poor assemblages comprising rare dinocysts and microforam test linings to rich assemblages composed mainly of abundant miospores belonging to *Classopollis torosus* and *Spheripollenites psilatus*; the transition represents a major change in depositional conditions within a marine setting, with a sharp increase in terrestrial input below the unconformity. We term this event, which corresponds to seismic horizon J170 in OERA (2014), the Bajocian/Toarcian Unconformity. In Heron H-73, this unconformity lies within a unit equivalent to the Mohican Formation (MacLean and Wade 1993) or the corresponding Downing Formation (McAlpine 1990). We tentatively correlate this surface to Emerillon C-56 at the boundary between the Mohican equivalent and the Iroquois Formation as identified by MacLean and Wade (1993).

(8) In Heron H-73, the upper Pliensbachian comprises interbedded limestone and claystone—equivalent to the Mohican "Limestone facies" of MacLean and Wade (1993) or the Downing Formation of McAlpine (1990). There is a strong shift in wireline signature associated with the change from the more calcareous lithofacies of the upper Pliensbachian to the shale-dominated lithofacies of the lower Toarcian. We suggest that this event on the wireline data repre-

Copyright © Atlantic Geoscience, 2023

sents the major JPl8 sequence boundary of Haq (2018) of latest Pliensbachian age, based primarily on timing (see also Gradstein *et al.* 2020, p. 980).

(9) In Heron H-73, the lower part of the upper Pliensbachian interval yields rich nannofloras dominated by *Schizosphaerella punctulata* and *Schizosphaerella* fragments, associated with abundant *Lotharingius hauffii* and rare but persistent *Mitrolithus elegans*. These are associated with more marly strata that show higher gamma-ray and sonic log responses, interpreted here to reflect a major maximum flooding surface. We term this event the Late Pliensbachian MFS; it is characterized by the FDO of the nannofossil *Mitrolithus elegans*, with an abundance of the nannofossil *Lotharingius hauffii*. This event corresponds to the J186 seismic horizon in OERA (2014).

Early Jurassic comparisons to the Scotian Margin

Weston *et al.* (2012) noted great difficulty in recognizing pre-Bajocian marine biotic indicators on the Scotian Margin and considered that either Lower Jurassic strata in the wells they examined were absent due to erosion, or that marine incursions did not reach far enough landward to influence those well locations at that time. However, Bujak and Williams (1977) and Barss *et al.* (1979) recognized latest Triassic to Early Jurassic non-marine miospore assemblages on the Scotian Margin. Bujak and Williams (1977) assigned the oldest non-marine strata to their *Corollina meyeriana* Peak Zone, which they considered to be of Rhaetian to early Hettangian age; the zone was recognized in Eurydice P-36 and Argo P-38. Sequentially overlying this zone are the Hettangian–Sinemurian *Cycadopites subgranulosus* Assemblage Zone and Sinemurian to early Pliensbachian *Echinitosporites* cf. *iliacoides* Assemblage Zone. Bujak and Williams (1977) recognized Early Jurassic dinocysts only on the Grand Banks, in the *Nannoceratopsis gracilis* Assemblage Zone of Bujak and Williams (1977), originally assigned a Pliensbachian–Toarcian age.

Based on comparison with outcrop sections with ammonite and nannofossil control in Portugal, Davies (1985) modified the ages of the Bujak and Williams (1977) zones, dating the *Corollina meyeriana* Peak Zone as Rhaetian to Hettangian, the *Cycadopites subgranulosus* Assemblage Zone as Sinemurian to early Pliensbachian, and the *Echinitosporites* cf. *iliacoides* Assemblage Zone as late Pliensbachian to early Toarcian. Davies (1985) considered the *Nannoceratopsis gracilis* Zone to be Toarcian to Aalenian.

On the southern Grand Banks, age-diagnostic dinocysts, nannofossils, and foraminifera thus allow confident identification of more extensive Lower Jurassic marine strata (Barss *et al.* 1979; Ascoli 1981; Gradstein 1978; Williams *et al.* 1990; Williams 2006). On the Scotian Margin, post-salt Lower Jurassic non-marine strata of the *Echinitosporites* cf. *iliacoides* Assemblage Zone are identified in the Argo F-38, Eurydice P-36, Hercules G-15, and Iroquois J-17 wells (Bujak and Williams 1977; Barss *et al.* 1979) and, based on the age revisions of Davies (1985), these sections likely include Sinemurian through Toarcian strata, depending on the well. Interestingly, all these wells are either in the Orpheus Graben or on the eastern part of the Scotian Margin closer to the Grand Banks.

Comparison of southern Grand Banks and Moroccan Lower Jurassic sections

We interpret the interval assigned to the Iroquois Formation by MacLean and Wade (1993) in Emerillon C-56 (10 214–10 750 ft; 3113.23–3276.6 m) to be of likely Early Jurassic age, probably late Sinemurian at the base and Toarcian at the top. This interval is composed of dolomitic shale and dolostone, with anhydritic interbeds below about 10 300 ft (3139.44 m). Biostratigraphic recoveries appear poor based on data recorded by Ainsworth *et al.* (2016), Ascoli (1981) and Williams (1979), and suggest deposition in a proximal platform environment throughout.

Lower Jurassic strata in Heron H-73 comprise a relatively thin interval predominantly of shale of early Toarcian age, which overlie a thicker sequence of interbedded shale and limestone of Pliensbachian age. MacLean and Wade (1993) attributed the latter strata to the lower part of the Mohican Formation equivalent. The Mohican-equivalent strata in turn overlie interbedded dolostone and anhydrite of the Iroquois Formation, and the bottom of the well is in evaporites of the Argo Formation. Sedimentary rocks of the Iroquois and Argo formations in Heron H-73 are less well-constrained biostratigraphically than those in the overlying Pliensbachian and early Toarcian intervals, but the palynofloras suggest an Early Jurassic age no older than late Hettangian. Rich miospore assemblages dominated by *Classopollis torosus* (including tetrads) were recovered throughout the Early Jurassic interval in Heron H-73. This abundance/dominance of *Classopollis* pollen suggests deposition proximal to an extensive coastal plain under hot, seasonally arid to semi-arid conditions (Abbink *et al.* 2004; Vieira *et al.* 2021). Micropaleontological and nannofossil assemblages recovered from the Pliensbachian to lower Toarcian (10 020–11 100 ft; 3054.1–3383.26 m) imply deposition in an open marine, probably inner neritic environment, whereas the lithologies and palynofloras of the underlying Iroquois and Argo formations (11 260–11 970 ft; 3432.05–3648.46 m) are indicative of a proximal inner platform setting.

Lower Jurassic samples from cores 15–22 within DSDP Site 547B from offshore Morocco comprise micritic and nodular limestone of late Sinemurian to early Pliensbachian age. The nannofossils indicate open-marine surface-water conditions throughout, whereas the predominance of the miospore *Classopollis torosus* (including abundant tetrads) in cores 20–22 indicates proximity to an adjacent landmass with an extensive coastal plain. Foraminiferal faunas recorded by Riegraf *et al.* (1984) from these cores suggest deposition in a middle neritic setting for core 15 and in a probably deeper, outer neritic setting for cores 20–22.

Copyright © Atlantic Geoscience, 2023

OERA (2014) mapped the top of the dolostone of the Iroquois Formation across the area as the J188 seismic horizon. An age of 188 Ma is approximately consistent with an early Pliensbachian age at the top of the dolostone, as dated by nannofossils in Heron H-73. However, the top of the Iroquois Formation as placed by MacLean and Wade (1993) in Emerillon C-56 is younger, likely Toarcian. We therefore envisage this lithostratigraphic formation top and seismic horizon J188 to be diachronous in the Laurentian Subbasin.

Potential Lower Jurassic source rock

The Lower Jurassic on the Moroccan Margin is usually cited for its hydrocarbon source rock potential. Simoneit *et al.* (1984) showed TOC values ranging up to 8.9% from core 20 of DSDP Site 547B, although such high values were not replicated in the samples studied by Beicip-Franlab (OERA 2014, plate 5.5.10); the highest TOC values recorded in the latter study from core 20 were 2.4–2.9%; and a later study by Robinson *et al.* (2017) yielded values of 0.5–1.8% TOC from core 20. An aim of the present study of Laurentian Subbasin wells was to determine if Lower Jurassic source horizons might be present on the eastern North American margin and, if so, if the age and depositional setting were similar to those of the Moroccan Margin.

The samples studied from DSDP Site 547B on the Moroccan Margin range in age from early Pliensbachian to late Sinemurian, which is older than the lower Toarcian shale and Pliensbachian limestone and shale of Heron H-73 (see Figs. 14b, 17, and 18). The lower Pliensbachian to upper Sinemurian in Heron H-73 (and Emerillon C-56) is characterized by dolomitic, anhydritic, and green–red shale facies of the Iroquois Formation, which represents a different, probably more marginal, lithofacies than is represented at DSDP Site 547B, where anhydrite is absent and nodular limestone and dolostone dominate. Sinclair (1988) postulated that the evaporitic dolostone beds of the Iroquois Formation may be promising source rocks, and Warren (1986) noted the general potential for evaporite-associated environments as source rocks.

The geochemical data from Lower Jurassic samples in Heron H-73 show background TOC values of 1–1.5%, with the highest value of about 2% around 10 830 ft/3300 m, close to the level of the late Pliensbachian MFS (OERA 2014, plate 5.5.11). A conclusion from the Laurentian Subbasin Project was that both DSDP Site 547B and Heron H-73 lay in perched basins that may have developed potential hydrocarbon source rocks at different times, due to local structural and tectonic controls (OERA 2014, plate 5.5.11). In summary, some source rock potential remains within the Lower Jurassic strata of the Laurentian Subbasin and warrants further investigation.

CONCLUSIONS

We have recognized and extended the event stratigraphy of Weston *et al.* (2012) from the Scotian Margin onto the southern Grand Banks using four wells located within the Laurentian Subbasin. The Scotian Margin event scheme for the Middle Jurassic–Cenozoic applies across the new area, with modifications to account for the amalgamation of some events at unconformities (e.g., into the Avalon Unconformity), which is in line with previously published observations.

In addition to previously recognized well-log sequence stratigraphic surfaces, we have recognized four new surfaces, and revised and renamed an existing one:

Early Albian Unconformity
Late Bathonian MFS
Late Bajocian MFS (renamed from Bathonian/Bajocian MFS)
Bajocian/Toarcian Unconformity
Late Pliensbachian MFS

New events in the Middle Jurassic and Early Jurassic part of the succession reflect the more extensive well penetration of marine strata of this age on the Grand Banks, in contrast to penetrations on the Scotian Margin, as well as the presence of age-diagnostic marine microfauna and microflora in that part of the section. This has allowed us to make better age assignments than were possible on the Scotian Margin in Weston *et al.* (2012).

We have also compared Early Jurassic events with those in DSDP Site 547B on the conjugate Moroccan Margin. Lower Jurassic marine strata showing source rock potential are present in both Heron H-73 and DSDP Site 547B; however, those on the Moroccan Margin are Sinemurian to early Pliensbachian, whereas those in Heron H-73 are late Pliensbachian to early Toarcian, indicating a difference in the timing of deposition in the two areas despite their relative proximity at the time.

ACKNOWLEDGEMENTS

We thank all individuals associated with Nova Scotia Offshore Energy Research Association (OERA) for encouraging, facilitating, and in large part funding the initial study and through a grant by the Nova Scotia Department of Natural Resources and Renewables to the Geological Survey of Canada (Atlantic) in part to support the compilation of this article. We would like to thank personnel from the Nova Scotia Department of Natural Resources and Renewables for their support throughout this study, particularly Adam MacDonald for facilitating access to samples and sample preparations. We would also like to thank Rita Parsonage for sampling the Bandol-1 well for this study and to personnel at the Bureau Exploration Production des Hydrocarbures (BEPH) in Paris, France, for facilitating this process for her. We would also like to acknowledge the provision of sample

Copyright © Atlantic Geoscience, 2023

material from East Wolverine G-37 and Heron H-73 and pre-existing sample preparations from Heron H-73 by C-NLOPB. We are grateful to the late Tony King for the new micropaleontological analyses of Bandol-1, and to Fabrizio Tremolada for some nannofossil analyses of Bandol-1.

Our interpretations have benefitted enormously from discussions with personnel from Beicip-Franlab and CNSOPB, and we thank them accordingly. We thank Nikole Bingham Kozlowski, Lynn Dafoe, and Mark Deptuck for their reviews, which have led to significant improvements in the manuscript, and to Atlantic Geoscience co-editor Denise Brushett for helping to steer the manuscript toward publication. This is NRCan Contribution no 20230023.

URL LINKS TO SUPPLEMENTARY DATA:

Supplementary Data Table S1: https://journals.lib.unb.ca/index.php/ag/article/view/33343/1882529549
Supplementary Date Table S2: https://journals.lib.unb.ca/index.php/ag/article/view/33343/1882529550
Supplementary Date Table S3: https://journals.lib.unb.ca/index.php/ag/article/view/33343/1882529551
Supplementary Data Table S4: https://journals.lib.unb.ca/index.php/ag/article/view/33343/1882529553
Supplementary Data Table S5: https://journals.lib.unb.ca/index.php/ag/article/view/33343/1882529554

REFERENCES

Abbink, O.A., Van Konijnenburg-Van Cittert, J., and Visscher, H. 2004. A sporomorph ecogroup model for the northwest European Jurassic–Lower Cretaceous: concepts and framework. Netherlands Journal of Geoscience—Geologie En Mijnbouw, 83, pp. 17–31. https://doi.org/10.1017/S0016774600020436

Ainsworth, N.R. 1986. Toarcian and Aalenian ostracoda from the Fastnet Basin, offshore south-west Ireland. Bulletin of the Geological Survey of Ireland, 3, pp. 277–336, 11 pls.

Ainsworth, N.R., Braham, W., Gregory, F.J., Johnson, B., and King, C. 1998. A proposed latest Triassic to earliest Cretaceous microfossil biozonation for the English Channel and its adjacent areas. *In* Development, evolution and petroleum geology of the Wessex Basin. *Edited by* J.R. Underhill. Geological Society of London, Special Publication 133, pp. 87–102. https://doi.org/10.1144/GSL.SP.1998.133.01.05

Ainsworth, N.R., Riley, L.A., Bailey, H.W., Coles, G.P., and Gueinn, K.J. 2016. Jurassic–Tertiary stratigraphy of the southern Newfoundland Margin. Wells: East Wolverine G-37, Eider M-75, Emerillon M-75 & Narwhal F-99. Riley Geoscience Ltd. report for Nalcor Energy—Oil & Gas, 23 p., 4 encl.

Armentrout, J.M. 1996. High resolution sequence biostratigraphy: examples from the Gulf of Mexico Plio-Pleistocene. *In* High resolution sequence stratigraphy: innovations and applications. *Edited by* J.A. Howell and J.F. Aitken. Geological Society of London, Special Publication 104, pp. 65–86. https://doi.org/10.1144/GSL.SP.1996.104.01.06

Ascoli, P. 1976. Foraminiferal and ostracod biostratigraphy of the Mesozoic–Cenozoic, Scotian Shelf, Atlantic Canada. 1st International symposium on benthonic foraminifera of continental margins: part B: paleoecology and biostratigraphy. Maritime Sediments, Special Publication 1, pp. 653–771.

Ascoli, P. 1981. Report on the biostratigraphy (foraminifera and ostracoda) and depositional environments of the Elf *et al*. Emerillon C-56 well (SW Grand Banks) from 4070' (top of Mesozoic) to 10750' (T.D.). Geological Survey of Canada (Atlantic) internal report no. EPGS-PAL.21-81PA.

Ascoli, P. 1986. Supplementary report on the biostratigraphy (foraminifera and ostracoda) and depositional environments of the Elf *et al*. Emerillon C-56 well (SW Grand Banks), from 3710' to 4010' (T.D. 10750'). Geological Survey of Canada (Atlantic) internal report no. EPGS-PAL.1-86PA.

Ascoli, P. 1988. Mesozoic-Cenozoic foraminiferal, ostracod and calpionellid zonation of the north Atlantic margin of North America: Georges Bank–Scotian basins and northeastern Grand Banks (Jeanne d'Arc, Carson and Flemish Pass basins). Biostratigraphic correlation of 51 wells. Geological Survey of Canada Open File 1791, 41 p. https://doi.org/10.4095/130500

Ascoli, P. 1990. Foraminiferal, ostracode and calpionellid zonation and correlation of 42 selected wells from the North Atlantic margin of North America. Bulletin of Canadian Petroleum Geology, 38, pp. 485–492.

Balkwill, H.R. and Legall, F.D. 1989. Chapter 15: Whale Basin, offshore Newfoundland: extension and salt diapirism. *In* Extensional tectonics and stratigraphy of the North Atlantic margins. *Edited by* A. J. Tankard and H. R. Balkwill. American Association of Petroleum Geologists, Memoir 46, pp. 233–245. https://doi.org/10.1306/M46497C15

Barss, M.S., Bujak, J.P., and Williams, G.L. 1979. Palynological zonation and correlation of sixty-seven wells, eastern Canada. Geological Survey of Canada, Paper 78-24, 118 p. https://doi.org/10.4095/104894

Bartenstein, H. 1976. Benthonic index foraminifera in the Lower Cretaceous of the northern hemisphere between east Canada and north west Germany. Erdöl und Kohle, 29, pp. 254–256.

Bartenstein, H. 1979. Worldwide zonation of the Lower Cretaceous using benthonic foraminifera. Newsletters in Stratigraphy, 7, pp. 142–154. https://doi.org/10.1127/nos/7/1979/142

Blow, W.H. 1969. Late Middle Eocene to Recent planktonic foraminiferal biostratigraphy. Proceedings First International Conference on Planktonic Microfossils Geneva 1967, 1, pp. 199–422.

Bolli, H.M., Saunders, J.B., and Perch-Nielsen, K. 1985.

Copyright © Atlantic Geoscience, 2023

Plankton stratigraphy. Cambridge University Press. 2 vols, 1006 p.

Boomer, I., Ainsworth, N.R., and Exton, J. 1998. A re-examination of the Pliensbachian and Toarcian ostracoda of Zambujal, west-central Portugal. Journal of Micropalaeontology, 17, pp. 1–14. https://doi.org/10.1144/jm.17.1.1

Boudagher-Fadel, M.K., Banner, F.T., and Whittaker, J.E. 1997. The early evolutionary history of planktonic foraminifera. British Micropalaeontological Society Publication Series; Chapman and Hall, London, 269 p. https://doi.org/10.1007/978-94-011-5836-7

Boutakiout, M. 1990. Les foraminifères du Jurassique des Rides Sud-Rifaines et des regions voisines (Maroc). Documents des Laboratoires de Géologie, Lyon, 112, 247 p.

Bowman, S.J. 2010. Cretaceous tectonism and volcanism in the eastern Scotian Basin, offshore Nova Scotia. Unpublished M.Sc. thesis, Saint Mary's University, Halifax, Nova Scotia, 261 p.

Bowman, S.J., Pe-Piper, G., Piper, D.J.W., Fensome, R.A., and King, E.L. 2012. Early Cretaceous volcanism in the Scotian Basin. Canadian Journal of Earth Sciences, 49, pp. 1523–1539. https://doi.org/10.1139/e2012-063

Bown, P.R. (Editor). 1998. Calcareous nannofossil biostratigraphy. British Micropalaeontological Society Series, Chapman & Hall, London, 314 pp. https://doi.org/10.1007/978-94-011-4902-0

Bown, P.R. and Cooper, M.K.E. 1998. Jurassic. *In* Calcareous nannofossil biostratigraphy. *Edited by* P.R. Bown. British Micropalaeontological Society Publication Series, Chapman and Hall, London, pp. 34–85. https://doi.org/10.1007/978-94-011-4902-0_4

Bujak, J.P. and Williams, G.L. 1977. Jurassic palynostratigraphy of offshore eastern Canada. *In* Stratigraphic micropaleontology of Atlantic basin and borderlands. *Edited by* F.M. Swain. Developments in Palaeontology and Stratigraphy, 6, pp. 321–339. https://doi.org/10.1016/S0920-5446(08)70358-3

Cabral, M.C., Colin, J.-P., Azerêdo A.C, Silva, R.L., and Duarte, L.V. 2015. Brackish and marine ostracode assemblages from the Sinemurian of western Portugal, with descriptions of new species. Micropaleontology, 61, pp. 3–24. https://doi.org/10.47894/mpal.61.1.02

Cabral, M.C., Lord, A.R., Pinto, S., Duarte, L.V., and Azerêdo, A.C. 2020. Ostracods of the Toarcian (Jurassic) of Peniche, Portugal: taxonomy and evolution across and beyond the GSSP interval. Bulletin of Geosciences, 95, pp. 243–278. https://doi.org/10.3140/bull.geosci.1778

Cawood, A.J., Ferrill, D.A., Norris, D., Bowness, N.P., Glass, E.J., Smart, K.J., Morris, A.P., and Gillis, E. 2022. Crustal structure and tectonic evolution of the Newfoundland Ridge, Fogo Basin, and southern Newfoundland transform margin. Marine and Petroleum Geology, 143, 105764, 28 p. https://doi.org/10.1016/j.marpetgeo.2022.105764

Coleman, B. 1981. The Bajocian to Callovian. *In* Stratigraphical atlas of fossil foraminifera. *Edited by* D.G. Jenkins and J.W. Murray. Ellis Horwood Limited, Chichester, 310 pp.

ConocoPhillips. 2010. E. Wolverine G-37, Laurentian Basin, NL. Well history report. Exploration license 1087R, 10 June 2010. [Report cover cites "ConocoPhillips Canada Resources Corp." for authorship.]

Copestake, P. and Johnson, B. 2014. Lower Jurassic foraminifera from the Llanbedr (Mochras Farm) Borehole, north Wales, UK. Monographs of the Palaeontographical Society, 641, 403 p, 21 pls. https://doi.org/10.1080/02693445.2013.11963952

Davies, E.H. 1985. The miospore and dinoflagellate cyst Oppel-zonation of the Lias of Portugal. Palynology, 9, pp. 105–132; pl. 1–4. https://doi.org/10.1080/01916122.1985.9989291

Davies, T.D. and Huang, T.C. 2001. Bio- and sequence stratigraphy of the Bandol-1 Well, Laurentian Sub-basin, offshore eastern Canada. Exxon Mobil Exploration Company EMEC.28A.BIO.01, October 2001: 26 p. + App. A.e

de Kaenel, E., Bergan, J.A., and von Salis Perch-Nielsen K. 1996. Jurassic calcareous nannofossil biostratigraphy of western Europe. Compilation of recent studies and calibration of bioevents. Bulletin de la Societé Géologique de France, 167, pp. 15–28.

Deptuck, M.E. and Altheim, B.2018. Rift basins of the central LaHave Platform, offshore Nova Scotia. Canada–Nova Scotia Offshore Petroleum Board Geoscience Open File Report, 2018-001MF, 54 p.

Deptuck, M.E. and Campbell, D.C. 2012. Widespread erosion and mass failure from the ~51 Ma Montagnais marine bolide impact off southwestern Nova Scotia, Canada. Canadian Journal of Earth Sciences, 49, pp. 1567–1594. https://doi.org/10.1139/e2012-075

Deptuck, M.E., MacRae, R.A., Shimeld, J.W., Williams, G.L., and Fensome, R.A. 2003. Revised Upper Cretaceous and lower Paleogene lithostratigraphy and depositional history of the Jeanne d'Arc Basin, offshore Newfoundland, Canada. American Association of Petroleum Geology Bulletin, 87, pp. 1459–1483. https://doi.org/10.1306/050203200178

Doeven, P.H. 1983. Cretaceous nannofossil stratigraphy and paleoecology of the Canadian Atlantic Margin. Geological Survey of Canada, Bulletin 356, 70 p. https://doi.org/10.4095/109267

Elf Oil Exploration & Production Canada Limited. 1974. Well History Log of Elf *et al*. EMERILLON C-56.

Emery, D. and Myers, K.J. (Editors). 1996. Sequence stratigraphy. Blackwell Science Ltd., Malden, Massachusetts, 297 pp. https://doi.org/10.1002/9781444313710

Enachescu, M.E. 1988. Extended basement beneath the intracratonic rifted basins of the Grand Banks of Newfoundland. Canadian Journal of Exploration Geophysics, 24, pp. 48–65.

Fensome, R.A., Crux, J.A., Gard, I.G., MacRae, R.A., Williams, G.L., Thomas, F.C., Fiorini, F., and Wach, G. 2008. The last 100 million years on the Scotian Margin, offshore eastern Canada: an event-stratigraphic scheme emphasizing biostratigraphic data. Atlantic Geology, 44, pp. 93–126. https://doi.org/10.4138/6506

Fensome, R.A., Williams, G.L., and MacRae, R.A. 2009. Late

Copyright © Atlantic Geoscience, 2023

Cretaceous and Cenozoic fossil dinoflagellates and other palynomorphs from the Scotian Margin, offshore Eastern Canada. Journal of Systematic Palaeontology, 7, pp. 1–79. https://doi.org/10.1017/S1477201908002538

Fensome, R.A., Williams, G.L., and MacRae, R.A. 2019. The Lentin and Williams index of fossil dinoflagellates: 2019 edition. American Association of Stratigraphic Palynologists Contributions Series 50, 1173 p.

Fenton, J.P.G. 1984. Palynological investigation of the Triassic–Middle Jurassic sequences at Deep Sea Drilling Project Leg 79, Sites 545, 546, and hole 547B, off central Morocco. *In* Initial reports of the Deep Sea Drilling Project. *Edited by* K. Hinz, E.L. Winterer *et al.* U.S. Government Printing Office, Washington, 79, pp. 715–718. https://doi.org/10.2973/dsdp.proc.79.129.1984

Geological Survey of Canada, St. Pierre Survey. 1983. URL <https://basin.marine-geo.canada.ca/seismic/single_location_e.php?project=ST.%20PIERRE%20SURVEY> 6 September 2022.

Gradstein, F.M. 1977. Biostratigraphy (foraminifera) and depositional environment of Amoco Imp. Heron H-73, Grand Banks. Geological Survey of Canada (Atlantic) internal report no. EPGS-PAL. FMG22-77.

Gradstein, F.M. 1978. Jurassic Grand Banks foraminifera. Journal of Foraminiferal Research, 8, pp. 97–109. https://doi.org/10.2113/gsjfr.8.2.97

Gradstein, F.M. 1979. Jurassic micropalaeontology of the Grand Banks. Ciências da Terra (Universidade Nova de Lisboa), 5, pp. 85–96.

Gradstein, F.M., Ogg, J.G., and Smith, A.G. 2005 A geologic time scale 2004. Cambridge University Press, 589 p. https://doi.org/10.1017/CBO9780511536045

Gradstein, F.M., Gale, A., Kopaevich, L., Waskowska, A., Grigelis, A., and Glinskikh, L. 2017a. The planktonic foraminifera of the Jurassic. Part I: material and taxonomy. Swiss Journal of Palaeontology, 136, pp. 187–257. https://doi.org/10.1007/s13358-017-0131-z

Gradstein, F.M., Gale, A., Kopaevich, L., Waskowska, A., Grigelis, A., Glinskikh, L, L., and Görög, Á. 2017b. The planktonic foraminifera of the Jurassic. Part II: stratigraphy, palaeoecology and palaeobiogeography. Swiss Journal of Palaeontology, 136, pp. 259–271. https://doi.org/10.1007/s13358-017-0132-y

Gradstein, F.M., Ogg, J.G., Schmitz, M.D., and Ogg, G.M. 2020. Geologic time scale 2020. Elsevier, 2 vols., 1357 p.

Grant, A.C. and McAlpine, K.D. 1990. Chapter 6: The continental margin around Newfoundland. *In* Geology of the Continental Margin of Eastern Canada. *Edited by* M.J. Keen and G.L. Williams. Geological Survey of Canada, Geology of Canada Series 2, pp. 239–292. https://doi.org/10.1130/DNAG-GNA-I1.239

Grigelis, A. and Ascoli, P. 1995. Middle Jurassic–Early Cretaceous foraminiferal zonation and paleoecology of offshore eastern Canada and the East European Platform. Geological Survey of Canada Open File 3099, 26 p. https://doi.org/10.4095/203755

Haddoumi, H., Charrière, A., Andreu, B., and Mojon, P.-O. 2008. Les dépôts continentaux du Jurassique moyen au Crétacé inférieur dans le Haut Atlas oriental (Maroc): paléoenvironnements successifs et signification paléogéographique. Carnets de Géologie, Article 2008/06, pp. 1–29. https://doi.org/10.4267/2042/18122

Hanafi, B.R., Withjack, M.O., Durcanin, M.A. and Schlische, R.W. 2022. The development of the eastern Orpheus rift basin, offshore eastern Canada: A case study of the interplay between rift-related faulting and salt deposition and flow. Marine and Petroleum Geology, 139, pp. 1-18. https://doi.org/10.1016/j.marpetgeo.2022.105629

Haq, B.U. 2018. Jurassic sea-level variations: a reappraisal. GSA Today, 28, pp. 4–10. https://doi.org/10.1130/GSATG359A.1

Hardenbol, J., Thierry, J., Farley, M.B., Jacquin, T., de Graciansky, P.-C. and Vail, P. R. 1998. Mesozoic and Cenozoic sequence chronostratigraphic framework of the European basins. *In:* Mesozoic and Cenozoic sequence stratigraphy of European basins. *Edited by* P.-C. de Graciansky, J. Hardenbol, T. Jacquin, and P.R. Vail SEPM Special Publication, pp. 3-13. https://doi.org/10.2110/pec.98.02.0003

Hinz, K., Winterer, E.L., and 26 others. 1984. Initial reports of the Deep Sea Drilling Project, Leg 79. US Government Printing Office, Washington, 79, 934 p. https://doi.org/10.2973/dsdp.proc.79.1984

Hylton, M.D. 1999. Hettangian to Sinemurian (Lower Jurassic) sea-level change and palaeoenvironments: evidence from benthic foraminifera at East Quantoxhead, west Somerset, U.K. Geoscience in Southwest England, 9, pp. 285–288.

Jansa, L.F. and Wade, J.A. 1975. Geology of the continental margin off Nova Scotia and Newfoundland. *In* Offshore geology of eastern Canada, volume 2 — regional geology. *Edited by* W.J.M Van Der Linden and J.A. Wade. Geolog-ical Survey of Canada, Paper 74-30. pp. 51–105. https://doi.org/10.4095/123963

Jenkins, D.G. and Murray, J.W. (Editors) 1989. Stratigraphical atlas of fossil foraminifera: second edition. Ellis Horwood Limited, Chichester, 593 pp.

Kennett, J.P. and Srinavasan, M.S. 1983. Neogene planktonic foraminifera: a phylogenetic atlas. Hutchinson Ross Publishing Company, Stroudsburg, Pennsylvania, 263 p.

Koch, W. 1977. Biostratigraphie in der Oberkreide und Taxonomie von Foraminiferen. Geologisches Jahrbuch., Reihe A, 38, 128 p.

Labails, C., Olivet, J.-L., Aslanian, D., and Roest, W.R.2010. An alternative early opening scenario for the central Atlantic Ocean. Earth and Planetary Science Letters, 297, pp. 355–368. https://doi.org/10.1016/j.epsl.2010.06.024

MacLean, B.C. and Wade, J.A. 1992. Petroleum geology of the continental margin south of the islands of St. Pierre and Miquelon, offshore eastern Canada. Bulletin of Canadian Petroleum Geology, 40, pp. 222–253.

MacLean, B.C. and Wade, J.A. 1993. Seismic markers and stratigraphic picks in the Scotian Basin wells. East Coast

Copyright © Atlantic Geoscience, 2023

Basin Atlas Series, Energy, Mines and Resources, Canada, 276 p. https://doi.org/10.4095/221116

Martini, E. 1971. Standard Tertiary and Quaternary calcareous nannoplankton zonation. Proceedings of the Second International Conference on Planktonic Microfossils, Roma, 2, pp. 739–785.

Mattiole, E. and Erba. E. 1999. Synthesis of calcareous nannofossil events in Tethyan Lower and Middle Jurassic successions. Rivista Italiana di Paleontologia e Stratigrafia, 105, pp. 343–376.

McAlpine, K.D. 1990. Mesozoic stratigraphy, sedimentary evolution, and petroleum potential of the Jeanne d'Arc Basin, Grand Banks of Newfoundland. Geological Survey of Canada Paper 89-17, 50 p. https://doi.org/10.4095/130934

McAlpine, K.D., Deptuck, M.E., Wielens, J.B.W., Jauer, C.D., and Moir, P.N. 2004. Lithostratigraphy I, Jeanne d'Arc Basin cross sections A-A' and B-B'. *In* East Coast Basin Atlas Series: Grand Banks of Newfoundland—lithostratigraphy. *Edited by* P.N. Moir, K.D. McAlpine, A. Edwards, M.E. Deptuck, J.S. Bell, J.B.W. Wielens, J.A. Wade, and C.D. Jauer. Geological Survey of Canada, Open File 4640; 4 sheets.

McIver, N.L. 1972. Cenozoic and Mesozoic stratigraphy of the Nova Scotia shelf. Canadian Journal of Earth Sciences, 9, pp.54–70. https://doi.org/10.1139/e72-005

OERA 2011. Play Fairway Analysis Atlas. Principal investigator: Beicip-Franlab. URL <https://oera.ca/research/play-fairway-analysis-atlas> September 21 2022.

OERA 2014. Laurentian Sub-Basin Atlas (2014). Principal investigator: Beicip-Franlab. URL <https://oera.ca/research/laurentian-sub-basin-atlas-2014> 21 September 2022

OERA 2015. SW Nova Scotia Expansion Atlas (2015). Principal investigator: Beicip-Franlab. URL <https://oera.ca/research/sw-nova-scotia-expansion-atlas-2015> 21 September 2022

OERA 2016 Central Scotian Slope Atlas (2016). Principal investigator: Beicip-Franlab. URL <https://oera.ca/research/central-scotian-slope-atlas-2016> 21 September 2022.

OERA 2017. Sydney Basin Play Fairway Analysis Atlas (2017). Principal investigator: Beicip-Franlab. URL <https://oera.ca/research/sydney-basin-play-fairway-analysis-atlas-2017> 21 September 2022.

OERA 2019. Shelburne Sub-Basin Play Fairway Analysis Update. Principal investigators: Beicip-Franlab, APT (Canada) Ltd. and Weston Stratigraphic Ltd. URL <https://oera.ca/research/shelburne-sub-basin-play-fairway-analysis-update> 21 September 2022.

Oertli, H.J. (Editor) 1985. Atlas des ostracodes de France. Bulletin des Centres Recherches et Exploration–Production Elf–Aquitaine, Memoir 9, 396 pp.

Ogg, J.G., Ogg, G.M., and Gradstein, F.M. 2016. A concise geologic time scale—2016. Amsterdam, Elsevier, 234 p.

Ogg, J.G., Ogg, G., and Gradstein, F.M. 2008. The concise geologic time scale. Cambridge University Press, Cambridge, 177 p.

Ohm, U. 1967. Zur Kenntnis der Gattungen *Reinholdella, Garantella* und *Epistomina* (Foramin.). Palaeontographica Abteilung A, 127, pp. 103–188.

Olsson, R.K., Hemleben, C., Berggren, W.A., and Huber, B.T. 1999. Atlas of Paleocene planktonic foraminifera. Smithsonian Contributions to Paleobiology, 85, 252 p. https://doi.org/10.5479/si.00810266.85.1

Pascucci, V., Gibling, M.R., and Williamson, M.A. 1999. Seismic stratigraphic analysis of Carboniferous strata on the Burin Platform, offshore Eastern Canada. Bulletin of Canadian Petroleum Geology, 47, pp. 298-316.

Pearson, P.N., Olsson, R.K., Huber, B.T., Hemleben, C., and Berggren, W.A. 2006. Atlas of Eocene planktonic foraminifera. Cushman Foundation for Foraminiferal Research, Special Publication 41. 513 p.

Pe-Piper, G. and Jansa, L.F. 1987. Geochemistry of late Middle Jurassic–Early Cretaceous igneous rocks on the eastern North American margin. Geological Society of America Bulletin, 99, pp. 803–813. https://doi.org/10.1130/0016-7606(1987)99<803:GOLMJC>2.0.CO;2

Pe-Piper, G. and Piper, D.J.W. 2004. The effects of strike-slip motion along the Cobequid–Chedabucto–southwest Grand Banks fault system on the Cretaceous–Tertiary evolution of Atlantic Canada. Canadian Journal of Earth Sciences, 41, pp. 799–808. https://doi.org/10.1139/e04-022

Perch-Nielsen, K. 1985a. Mesozoic calcareous nannofossils. *In* Plankton stratigraphy. *Edited by* H.M. Bolli, J.B. Saunders, and K. Perch-Nielsen. Cambridge University Press, pp. 329–426.

Perch-Nielsen, K. 1985b. Cenozoic calcareous nannofossils. *In* Plankton stratigraphy. *Edited by* H.M. Bolli, J.B. Saunders, and K. Perch-Nielsen. Cambridge University Press, pp. 427–554.

Poulsen, N.E. and Riding, J.B. 2003. The Jurassic dinoflagellate cyst zonation of subboreal northwest Europe. Geological Survey of Denmark and Greenland. Bulletin 1, pp. 115–144. https://doi.org/10.34194/geusb.v1.4650

Powell, A.J. (Editor). 1992. A stratigraphic index of dinoflagellate cysts. British Micropalaeontological Society Publication Series, Chapman and Hall, London, 290 p. https://doi.org/10.1007/978-94-011-2386-0

Premoli Silva, I. and Verga, D. 2004. Practical manual of Cretaceous planktonic foraminifera. *In* International school on planktonic foraminifera, 3rd course, Milan Italy: Cretaceous. *Edited by* D. Verga and R. Rettori. Universities of Perugia and Milan, Tipografia Pontefelcino, Perugia, Italy, 283 pp.

Riding, J.B. 1984. Dinoflagellate cyst range-top biostratigraphy of the uppermost Triassic to lowermost Cretaceous of northwest Europe. Palynology, 8, pp. 195–210. https://doi.org/10.1080/01916122.1984.9989277

Riegraf, W. Luterbacher, H., and Leckie, R.M. 1984. Jurassic foraminifers from the Mazagan Plateau, Deep Sea Drilling Project Site 547, Leg 79, off Morocco. *In* Initial reports of the Deep Sea Drilling Project. *Edited by* K. Hinz, E.L. Winterer and *et al.* U.S. Government Printing Office,

Copyright © Atlantic Geoscience, 2023

Washington, 79, pp. 671–702. https://doi.org/10.2973/dsdp.proc.79.126.1984

Robaszynski, F., Caron, M., Gonzalez Donoso, J.M., and Wonders, A.A.H. (Editors). 1984. Atlas of Late Cretaceous globotruncanids. Revue de Micropaleontologie, 26, pp. 145–305.

Robinson, S.A., Ruhl, M., Astley, D.L., Naafs, B.D.A., Farnsworth, A.J., Bown, P.R., Jenkyns, H.C., Lunt, D.J., O'Brien, C., Pancost, R.D., and Markwick, P.J. 2017. Early Jurassic North Atlantic sea-surface temperatures from TEX_{86} palaeothermometry. Sedimentology, 64, pp. 215-230. https://doi.org/10.1111/sed.12321

Rullkötter, J. and Mukhopadhyay, P.K. 1986. Comparison of Mesozoic carbonaceous claystone in the western and eastern North Atlantic (DSDP Legs 76,79 and 93). *In* North Atlantic palaeoceanography. *Edited by* C.P. Summerhayes, and N.J. Shackleton. Geological Society Special Publication, 22, pp. 377–387. https://doi.org/10.1144/GSL.SP.1986.021.01.27

Rutledge, D.C. 2010. Well East Wolverine G-37, Laurentian Basin, offshore Newfoundland: biostratigraphy of the interval 2920 m to 6857 m TD. PetroStrat Report no. PS10-49, September 2010, 63 pp., 12 encls.

Sheppard, L.M. 1981. Middle Jurassic ostracods from southern England and northern France. Unpublished Ph.D Thesis, University College, University of London, London, UK, 214 p.

Sibuet, J.-C., Rouzo, S., and Srivastava, S. 2012. Plate tectonic reconstructions and paleogeographic maps of the central and North Atlantic oceans. Canadian Journal of Earth Sciences, 49, pp. 1395–1415. https://doi.org/10.1139/e2012-071

Simoneit, B.R.T., Vuchev, V.T., and Grimalt, J.O. 1984. Organic matter along the sedimentary sequences of the Moroccan Continental Margin, Leg 79, Sites 545 and 547. *In* Initial reports of the Deep Sea Drilling Project. *Edited by* K. Hinz, E.L. Winterer, and *et al*. U.S. Government Printing Office, Washington, 79, pp. 807–824. https://doi.org/10.2973/dsdp.proc.79.133.1984

Sinclair, I.K. 1988. Evolution of Mesozoic–Cenozoic sedimentary basins in the Grand Banks area of Newfoundland and comparison with Falvey's (1974) rift model. Bulletin of Canadian Petroleum Geology, 36, pp. 255–273.

Sinclair, I.K. 1995. Sequence stratigraphic response to Aptian–Albian rifting in conjugate margin basins: a comparison of the Jeanne d'Arc Basin, offshore Newfoundland, and the Porcupine Basin, offshore Ireland. *In* The tectonics, sedimentation and palaeoceanography of the North Atlantic region. *Edited by* R.A. Scrutton, R.A. Stoker, G.B. Shimmield, and A.W. Tudhope. Geological Society of London, Special Publication 90, pp. 29–49. https://doi.org/10.1144/GSL.SP.1995.090.01.02

Srivastava, S.P., Sibuet, J.C., Cande, S., Roest, W.R., and Reid, I.D. 2000. Magnetic evidence for slow seafloor spreading during formation of the Newfoundland and Iberian margins. Earth and Planetary Science Letters, 182, pp. 61–76. https://doi.org/10.1016/S0012-821X(00)00231-4

Stover, L.E., Brinkhuis, H., Damassa, S.P., de Verteuil, L., Helby, R.J., Monteil, E., Partridge, A.D., Powell, A.J., Riding, J.B., Smelror, M., and Williams, G.L.1996. Mesozoic–Tertiary dinoflagellates, acritarchs and prasinophytes. *In* Palynology principles and applications. *Edited by* J. Jansonius, and D.C. McGregor. American Association of Stratigraphic Palynologists Foundation, pp. 641–750.

Swift, J.H., Switzer, R.W., and Turnbull, W.F. 1975. The Cretaceous Petrel Limestone of the Grand Banks, Newfoundland. *In* Canada's continental margins and offshore petroleum exploration. *Edited by* C.J. Yorath, E.R. Parker, and D.J. Glass. Canadian Society of Petroleum Geologists, Memoir 4, pp. 181–194.

Thierstein, H.R. 1973. Lower Cretaceous calcareous nannoplankton biostratigraphy. Abhandlungen der Geologischen Bundesanstalt, 29, pp. 1–52.

Thusu, B. 1978. Distribution of biostratigraphically diagnostic dinoflagellate cysts and miospores from the northwest European continental shelf and adjacent areas. Continental Shelf Institute. Publication 100, 111 p.

Tucholke, B.E. and Sibuet, J.-C. 2007. Chapter 1: Leg 210 synthesis: tectonic, magmatic, and sedimentary evolution of the Newfoundland–Iberia rift. *In* Proceedings of the Ocean Drilling Program, Scientific Results, Volume 210. *Edited by* B.E. Tucholke, J.-C. Sibuet and A. Klaus, pp. 1–56. https://doi.org/10.2973/odp.proc.sr.210.101.2007

Tucholke, B.E., Sawyer, D.S., and Sibuet, J.C. 2007. Breakup of the Newfoundland–Iberia rift. *In* Imaging, mapping and modeling lithospheric extension. *Edited by* G.D. Kramer, G. Manatschel, and L. Pinheiro. Geological Society Special Publication 282, pp. 9–46. https://doi.org/10.1144/SP282.2

Viera, M., Jolley, D., and Shaw, D. 2021 A palaeoenvironmental study of uppermost Triassic to Lower Jurassic successions in high-pressure/high-temperature (HPHT) wells from the central North Sea, UK. Marine and Petroleum Geology, 132, pp. 1–10. https://doi.org/10.1016/j.marpetgeo.2021.105249

Wade, J.A. and MacLean, B.C. 1990. Chapter 5: The geology of the southeastern margin of Canada. *In* Geology of the continental margin of eastern Canada. *Edited by* M.J. Keen and G.L. Williams. Geology of Canada, no.2 (Geological Society of America, The Geology of North America, I-1), pp.167–238. https://doi.org/10.1130/DNAG-GNA-I1.167

Wade, B.S., Pearson, P.N., Berggren, W.A., and Pälike, H. 2011. Review and revision of Cenozoic tropical planktonic foraminiferal biostratigraphy and calibration to the geomagnetic polarity and astronomical time scale. Earth Science Reviews, 104, pp. 111–142. https://doi.org/10.1016/j.earscirev.2010.09.003

Wade, B.S., Olsson, R.K., Pearson, P.N., Huber, B.T., and Berggren, W.A. 2018. Atlas of Oligocene planktonic foraminifera. Cushman Foundation for Foraminiferal Research, Special Publication 46, 528 pp.

Warren, J.K. 1986. Perspectives: shallow-water evaporitic environments and their source rock potential. Journal of Sedimentary Petrology, 56, pp. 442–454. https://doi.

Copyright © Atlantic Geoscience, 2023

org/10.1306/212F8940-2B24-11D7-8648000102C1865D

Weston, J.F., MacRae, R.A., Ascoli, P., Cooper, M.K.E., Fensome, R.A., Shaw, D., and Williams, G.L. 2012. A revised biostratigraphic and well-log sequence stratigraphic framework for the Scotian Margin, offshore eastern Canada. Canadian Journal of Earth Sciences, 49, pp. 1417–1462. https://doi.org/10.1139/e2012-070

Whittaker, J.E. and Hart, M.B. (Editors) 2009. Ostracods in British stratigraphy. The Micropalaeontological Society, Special Publications; The Geological Society, London, 485 pp.

Williams, G.L. 1975. Dinoflagellate and spore stratigraphy of the Mesozoic–Cenozoic, offshore eastern Canada. *In* Offshore geology of eastern Canada. *Edited by* W.J.M. van der Linden and J.A. Wade. Geological Survey of Canada, Paper 74-30, pp. 107–161. https://doi.org/10.4095/102513

Williams, G.L. 1979. Palynological analysis of Elf *et al.* Emerillon C-56 and Elf Hermine E-94. Geological Survey of Canada (Atlantic) internal report no. EPGS-PAL.19-79GLW, 5 pp.

Williams, G.L. 2006. Palynological analysis of Amoco-Imperial-Skelly Osprey H-84, Carson Basin, Grand Banks of Newfoundland. Geological Survey of Canada, Open File 4974, 17 pp. https://doi.org/10.4095/221813

Williams, G.L., and Bujak, J.P. 1985. Mesozoic and Cenozoic dinoflagellates. *In* Plankton stratigraphy. *Edited by* H.M. Bolli, J.B. Saunders, and K. Perch-Nielsen. Cambridge University Press. pp. 847–964.

Williams, G.L., Ascoli, P., Barss, M.S., Bujak, J.P., Davies, E.H., Fensome, R.A., and Williamson, M.A. 1990. Biostratigraphy and related studies. *In* Geology of the continental margin of eastern Canada. *Edited by* M.J. Keen and G.L. Williams. Geology of Canada, no.2 (Geological Society of America, The Geology of North America, I-1), pp. 87–137. https://doi.org/10.1130/DNAG-GNA-I1.87

Williams, G.L., Bujak, J.P., Brinkhuis, H., Fensome, R.A., and Weegink, J.W. 1999. Mesozoic–Cenozoic dinoflagellate cyst course, Urbino, Italy, 17–22 May 1999, 98 p. (Unpublished short course manual).

Williams, G.L., Brinkhuis, H., Pearce, M.A., Fensome, R.A., and Weegink, J.W. 2004. Southern Ocean and global dinoflagellate cyst events compared: index events for the Late Cretaceous–Neogene. Proceedings of the Ocean Drilling Program, Scientific Results, 189, pp. 1–98. https://doi.org/10.2973/odp.proc.sr.189.107.2004

Williams, H. and Grant, A.C. 1998. Tectonic assemblage map, Atlantic region, Canada. Geological Survey of Canada Open File no. 3657, scale 1:3 000 000. https://doi.org/10.4095/209977

Woollam, R. and Riding, J.B. 1983. Dinoflagellate cyst zonation of the English Jurassic. Report of the Institute of Geological Sciences, 83/2, 41 pp.

Young, J.R., Bown, P.R., and Lees, J.A. 2017. Nannotax3 website. International Nannoplankton Association. URL<http://ina.tmsoc.org/Nannotax3/> 21 April 2017.

Editorial responsibility: Denise Brushett

Copyright © Atlantic Geoscience, 2023

Appendix A: List of taxa

Micropaleontological taxa mentioned in text

Acarinina bullbrooki (Bolli 1957) (foraminiferid)
Acarinina soldadoensis angulosa (Bolli 1957) (foraminiferid)
Acarinina soldadoensis soldadoensis (Brönnimann 1952) (foraminiferid)
Acarinina spinuloinflata (Bandy 1949) (foraminiferid)
Ammobaculites Cushman 1910 (foraminiferid)
Archaeoglobigerina bosquensis Pessagno 1967 (foraminiferid)
Berthelina berthelini (Keller 1935) (foraminiferid)
Berthelinella involuta (Terquem 1866) (foraminiferid)
Bolivinoides miliaris Hiltermann and Koch 1950 (foraminiferid)
Bulimina aff. *B. plena* Brotzen 1940 (foraminiferid)
Cenosphaera Ehrenberg 1854 (radiolarian)
Ciperoella ciperoensis (Bolli 1957) (foraminiferid)
Chiloguembelina ototara (Finlay 1940) (foraminiferid)
Clavihedbergella amabilis (Loeblich and Tappan 1961) (foraminiferid)
Conorboides hofkeri (Bartenstein and Brand 1951) (foraminifera)
Conorboides valendisensis (Bartenstein and Brand 1951) (foraminiferid)
Contusotruncana contusa (Cushman 1926) (foraminiferid)
Cyclammina cancellata Brady 1879 (foraminiferid)
Darwinula incurva Bate 1967 (ostracod)
Dicarinella asymetrica (Sigal 1952) (foraminiferid)
Dicarinella concavata (Brotzen 1934) (foraminiferid)
Dicarinella imbricata (Mornod 1950) (foraminiferid)
Dicarinella primitiva (Dalbiez 1955) (foraminiferid)
Dorothia aff. *filiformis* (Berthelin 1880) Ascoli 1976 (foraminiferid)
Dorothia gradata (Berthelin 1880) (foraminiferid)
Ektyphocythere Bate 1963 (ostracod)
Ektyphocythere lotharingiae (Donze 1967) (ostracod)
Epistomina caracolla (Roemer 1841) (foraminiferid)
Epistomina carpenteri (Reuss 1862) (foraminiferid)
Epistomina chapmani Ten Dam 1948 (foraminiferid)
Epistomina cretosa (Ten Dam 1947) (foraminiferid)
Epistomina hechti Bartenstein *et al.* 1957 (foraminiferid)
Epistomina cf. *nuda* (Terquem 1883) Coleman 1981 in Jenkins and Murray 1981 (foraminiferid)
Epistomina ornata (Roemer 1841) (foraminiferid)
Epistomina parastelligera (Hofker 1954) (foraminiferid)
Epistomina praecursor Ohm 1967 (foraminiferid)
Epistomina regularis Terquem 1883 (foraminiferid)
Epistomina soldanii Ohm 1967 (foraminiferid)
Epistomina spinulifera colomi Dubourdieu and Sigal 1949 (foraminiferid)
Epistomina spinulifera polypioides (Eichenberg 1933) (foraminiferid)
Epistomina tenuicostata Bartenstein and Brand 1951 (foraminiferid)
Fabanella bathonica (Oertli 1956) (ostracod)
Favusella washitensis (Carsey 1926) (foraminiferid)
Gansserina gansseri (Bolli 1951) (foraminiferid)
Garantella ornata (Hofker 1952) (foraminiferid)
Garantella semiornata (Schwager 1867) (foraminiferid)
Gavelinella barremiana Bettenstaedt 1952 (foraminiferid)
Gavelinella danica (Brotzen 1940) (foraminiferid)
Gavelinella intermedia (Berthelin 1880) (foraminiferid)
Gavelinella sigmoicostata (Ten Dam 1948) (foraminiferid)

Copyright © Atlantic Geoscience, 2023

Micropaleontological taxa mentioned in text: continued

Gavelinopsis tourainensis Butt 1966 (foraminiferid)
Globigerina apertura Cushman 1918 (foraminiferid)
Globigerinatheka subconglobata subconglobata Shutskaya 1958 (foraminiferid)
Globigerinelloides ferreolensis Moullade 1961 (foraminiferid)
Globoquadrina dehiscens (Chapman *et al.* 1934) (foraminiferid)
Globorotalia praemenardii Cushman and Stainforth 1945 (foraminiferid)
Globorotalia zealandica Hornibrook 1958 (foraminiferid)
Globotruncana ventricosa White 1928 (foraminiferid)
Globotruncanita conica (White 1928) (foraminiferid)
Globotruncanita elevata (Brotzen 1934) (foraminiferid)
Globuligerina balakhmatovae (Morozova 1961) (foraminiferid)
Globuligerina bathoniana (Pazdrowa 1969) (foraminiferid)
Globuligerina oxfordiana (Grigelis 1958) (foraminiferid)
Glomospira pattoni Tappan 1955 (foraminiferid)
Haplophragmoides Cushman 1910 (foraminiferid)
Hedbergella aptiana (Bartenstein 1965) (foraminiferid)
Helvetoglobotruncana helvetica (Bolli 1945) (foraminiferid)
Hutsonia sp. 3 Ascoli 1976 (ostracod)
Ichthyolaria terquemi (d'Orbigny 1849) plexus of Copestake and Johnson 2014 (forminiferid)
Involutina liassica (Jones 1853) (foraminiferid)
Klieana levis Oertli 1957 (ostracod)
Lenticulina argonauta Kopik 1969 (foraminiferid)
Lenticulina brueckmanni (Mjatliuk 1939) (foraminiferid)
Lenticulina busnardoi Moullade 1966 (foraminiferid)
Lenticulina dictyodes (Deecke 1884) (foraminiferid)
Lenticulina gaultina Berthelin 1880 (foraminiferid)
Lenticulina heiermanni Bettenstaedt 1952 (foraminiferid)
Lenticulina quenstedti (Guembel 1862) (foraminiferid)
Lenticulina saxonica Bartenstein and Brand 1951 (foraminiferid)
Lenticulina saxonica bifurcilla Bartenstein and Brand 1951 (foraminiferid)
Lenticulina varians (Bornemann 1854) (foraminiferid)
Lenticulina (*Planularia*) *tricarinella* (Reuss 1863) (foraminiferid)
Lingulina acuformis (Terquem 1866) (foraminiferid)
Lingulogavelinella ciryi ciryi Malapris-Bizouard 1967 (foraminiferid)
Marginotruncana Hofker 1956 (foraminiferid)
Marginotruncana coronata (Bolli 1945) (foraminiferid)
Marginotruncana marginata (Reuss 1845) (foraminiferid)
Marginotruncana pseudolinneiana Pessagno 1967 (foraminiferid)
Marginotruncana renzi (Gandolfi 1942) (foraminiferid)
Marginotruncana schneegansi (Sigal 1952) (foraminiferid)
Marginotruncana sigali (Reichel 1950) (foraminiferid)
Marginotruncana sinuosa Porthault 1970 (foraminiferid)
Marginulina prima (d'Orbigny 1849) plexus of Copestake and Johnson 2014 (forminiferid)
Marslatourella bullata Bate 1967 (ostracod)
Marssonella kummi Zedler 1961 (foraminiferid)
Massilina dorsetensis Cifelli 1959 (foraminiferid)
Micropneumatocythere brendae Sheppard 1978 (ostracod)
Micropneumatocythere falcata Sheppard 1978 (ostracod)
Micropneumatocythere quadrata Bate 1967 (ostracod)
Micropneumatocythere subconcentrica (Jones 1884) (ostracod)

Copyright © Atlantic Geoscience, 2023

Micropaleontological taxa mentioned in text: continued

Morozovella caucasica (Glaessner 1937) (foraminiferid)
Morozovella velascoensis (Cushman 1925) (foraminiferid)
Muricohedbergella delrioensis (Carsey 1926) (foraminiferid)
Muricohedbergella planispira (Tappan 1940) (foraminiferid)
Orbulina suturalis Brönnimann 1951 (foraminiferid)
Orbulina universa d'Orbigny 1839 (foraminiferid)
Neocythere vanveenae Mertens 1956 (ostracod)
Neoflabellina praerugosa Hiltermann 1952 (foraminiferid)
Neoflabellina suturalis (Cushman 1935) (foraminiferid)
Ogmoconcha Triebel 1941 (ostracod)
Ophthalmidium carinatum Kübler and Zwingli 1870 (foraminiferid)
Ophthalmidium strumosum (Guembel 1862) (foraminiferid)
Paalzowella feifeli (Paalzow 1932) (foraminiferid)
Paragloborotalia continuosa (Blow 1959) (foraminiferid)
Paragloborotalia opima opima (Bolli 1957) (foraminiferid)
Paralingulina tenera (Borneman 1854) plexus of Copestake and Johnson 2014 (foraminiferid)
Paralingulina tenera subprismatica (Franke 1936) (foraminiferid)
Pentacrinus Miller 1821 (crinoid)
Phacorhabdotus pokornyi Hazel andPaulson 1964 *forma A* of Ascoli 1976 (ostracod) *Pichottia magnamuris* Bate 1967 (ostracod)
Planularia crepidularis Roemer 1842 (foraminiferid)
Praeconocaryomma Pessagno 1976 (radiolarian)
Praeglobotruncana delrioensis (Plummer 1931) (foraminiferid)
Praeglobotruncana gibba Klaus 1960 (foraminiferid)
Praeglobotruncana stephani Gandolfi 1942 (foraminiferid)
Praeschuleridea arguta arguta Ainsworth 1986 (ostracod)
Praeschuleridea cf. *P. pseudokinkelinella* Bate and Coleman 1975 of Ainsworth 1986 (ostracod)
Praeschuleridea subtrigona (Jones and Sherborn 1888) (ostracod)
Prodentalina integra (Kübler and Zwingli 1870) (foraminiferid)
Prodentalina suboligostegia (Franke 1936) (foraminiferid)
Prodentalina teutoburgensis (Franke 1936) (foraminiferid)
Protocythere triplicata (Roemer 1841) (ostracod)
Pseudomacrocypris atypica Sheppard 1981 (ostracod)
Reinholdella crebra Pazdro 1969 (foraminiferid)
Reinholdella media (Kaptarenko 1959) (foraminiferid)
Rotalipora cushmani (Morrow 1934) (foraminiferid)
Rotalipora cushmani evoluta Sigal 1948 (foraminiferid)
Rotalipora deeckei (Franke 1925) (foraminiferid)
Rotalipora globotruncanoides Sigal 1948 (foraminiferid)
Rotalipora greenhornensis (Morrow 1934) (foraminiferid)
Rotalipora reicheli (Mornod 1950) (foraminiferid)
Rotalipora subticinensis (Gandolfi 1957) (foraminiferid)
Schuleridea jonesiana (Bosquet 1852) (ostracod)
Schuleridea (Eoschuleridea) batei Dépêche 1973 (ostracod)
Schuleridea (Eoschuleridea) bathonica Bate 1967 (ostracod)
Schuleridea (Eoschuleridea) trigonalis (Jones 1884) (ostracod)
Stensioina exsculpta exsculpta (Reuss 1860) (foraminiferid)
Stensioina exsculpta gracilis Brotzen 1945 (foraminiferid)
Stensioina granulata (Olbertz 1942) (foraminiferid)
Stensioina granulata humilis Koch 1977 (foraminiferid)

Copyright © Atlantic Geoscience, 2023

Micropaleontological taxa mentioned in text: continued

Stensioina granulata incondita Koch 1977 (foraminiferid)
Stensioina granulata perfecta Koch 1977 (foraminiferid)
Stensioina granulata polonica Witwicka 1958 (foraminiferid)
Subbotina ex gr. *linaperta* (Finlay 1939) (foraminiferid)
Subbotina triloculinoides (Plummer 1926) (foraminiferid)
Ticinella praeticinensis Sigal 1966 (foraminiferid)
Ticinella primula Luterbacher 1963 (foraminiferid)
Ticinella raynaudi Sigal 1966 (foraminiferid)
Ticinella roberti (Gandolfi 1942) (foraminiferid)
Trochammina Parker and Jones 1859 (foraminiferid)
Turborotalia ampliapertura (Bolli 1957) (foraminiferid)
Turborotalia cerroazulensis frontosa (Subbotina 1953) (foraminiferid)
Turborotalia increbescens (Bandy 1949) (foraminiferid)
Veenia spoori (Israelsky 1929) Ascoli 1976 (ostracod)
Whiteinella baltica Douglas and Rankin 1969 (foraminiferid)
Whiteinella brittonensis (Loeblich and Tappan 1961) (foraminiferid)

Nannofossil taxa mentioned in text

Ansulasphaera helvetica Grün and Zweili 1980
Arkhangelskiella cymbiformis Vekshina 1959
Biscutum dorsetensis (Varol and Girgis 1994) Bown in Bown and Cooper 1998
Biscutum intermedium Bown 1987
Biscutum novum (Goy in Goy *et al*. 1979) Bown 1987
Broinsonia enormis (Shumenko 1968) Manivit 1971
Broinsonia parca subsp. *constricta* Hattner *et al*. 1980
Calcicalathina oblongata (Worsley 1971) Thierstein 1971
Carinolithus , (Deflandre 1954) Prins *in* Grün *et al.* 1974
Chiasmolithus altus Bukry and Percival 1971
Chiasmolithus bidens (Bramlette and Sullivan 1961) Hay and Mohler 1967
Coccolithus formosus (Kamptner 1963) Wise 1973
Coccolithus pelagicus (Wallich 1877) Schiller 1930
Corannulus germanicus Stradner 1962
Corollithion achylosum (Stover 1966) Thierstein 1971
Corollithion kennedyi Crux 1981
Crepidolithus Noël 1965
Crepidolithus crassus (Deflandre in Deflandre and Fert 1954) Noël 1965
Crepidolithus granulatus Bown 1987
Crepidolithus pliensbachensis Crux 1985
Cruciellipsis cuvillieri (Worsley 1971) Thierstein 1971
Crucirhabdus primulus Prins 1969 ex Rood *et al.* 1971, as emended by Bown 1987
Cyclagelosphaera deflandrei (Manivit 1966) Roth 1973
Cyclagelosphaera margerelii Noël 1965
Cyclagelosphaera tubulata (Grun and Zweili 1980) Cooper 1987
Cyclicargolithus abisectus (Muller 1970) Wise 1973
Cyclicargolithus floridanus (Roth and Hay in Hay *et al.* 1967) Bukry 1971
Discoaster diastypus Bramlette and Sullivan 1961
Discoaster druggii Bramlette and Wilcoxon 1967
Discoaster exilis Martini and Bramlette 1963
Discoaster kuepperi Stradner 1959
Discoaster multiradiatus Bramlette and Riedel 1954

Copyright © Atlantic Geoscience, 2023

Nannofossil taxa mentioned in text: continued

Discoaster petaliformis Moshkovitz and Ehrlich 1980
Discorhabdus striatus Moshkovitz and Ehrlich 1976 (= *Biscutum striatum* in de Kaenel *et al.* 1996)
Eiffellithus eximius (Stover 1966) Perch-Neilsen 1968
Eiffellithus windii Applegate and Bergen 1988
Ellipsolithus distichus (Bramlette and Sullivan 1961) Sullivan 1964
Eprolithus floralis (Stradner 1962) Stover 1966
Fasciculithus Bramlette and Sullivan 1961
Fasciculithus alanii Perch-Neilsen 1971
Fasciculithus clinatus Bukry 1971
Fasciculithus tympaniformis Hay and Mohler in Hay *et al.* 1967
Gartnerago nanum Thierstein 1974
Helicosphaera ampliaperta Bramlette and Wilcoxon 1967
Helicosphaera compacta Bramlette and Wilcoxon 1967
Heliolithus riedelii Bramlette and Sullivan 1961
Hemipodorhabdus gorkae (Reinhardt 1969) Grün in Grün and Allemann 1975
Hexalithus gardetiae Bukry 1969
Hexalithus strictus Bergen 1994
Isthmolithus recurvus Deflandre in Deflandre and Fert 1954
Kokia curvata Perch-Neilsen 1988
Lithastrinus grillii Stradner 1962
Lithraphidites bollii (Thierstein 1971) Thierstein 1973
Lotharingius Noël 1973
Lotharingius crucicentralis (Medd 1971) Grün and Zweili 1980
Lotharingius hauffii Grün andZweili in Grün *et al.* 1974
Markalius inversus (Deflandre *in* Deflandre and Fert 1954) Bramlette and Martini 1964
Micrantholithus hoschulzii (Reinhardt 1966) Thierstein 1971
Microstaurus chiastius Black 1971
Micula staurophora (Gardet 1955) Stradner 1963
Mitrolithus elegans Deflandre in Deflandre and Fert 1954
Mitrolithus jansae (Wiegand 1984) Bown in Young *et al.* 1986
Nannoconus Kamptner 1931
Nannoconus bonetii Trejo 1959
Nannoconus bucheri Brönnimann 1955
Nannoconus fragilis Deres and Achéritéguy 1980
Nannoconus quadriangulus Deflandre and Deflandre-Rigaud 1962
Nannoconus steinmannii Kamptner 1931
Neochiastozygus modestus Perch-Neilsen 1971
Neochiastozygus perfectus Perch-Neilsen 1971
Neococcolithes dubius (Deflandre in Deflandre and Fert 1954) Black 1967
Orthogonoides hamiltoniae Wiegand 1984
Parhabdolithus liasicus Deflandre in Grassé 1952
Parhabdolithus marthae Deflandre in Deflandre and Fert 1954
Placozygus sigmoides (Bramlette and Sullivan 1961) Romein 1979
Podorhabdus grassei Noël 1965
Polycostella beckmannii Thierstein 1971
Prinsius martinii (Perch-Neilsen 1969) Haq1971
Pseudoconus enigma Bown and Cooper 1989
Quadrum gothicum Deflandre 1959
Quadrum intermedium Varol 1992
Quadrum trifidium (Stradner *in* Stradner and Papp 1961) Prins and Perch-Neilsen in Manivit *et al.* 1977

Copyright © Atlantic Geoscience, 2023

Nannofossil taxa mentioned in text: continued

Reinhardtites levis Prins and Sissingh in Sissingh 1977
Reticulofenestra reticulata (Gartner and Smith 1967) Roth and Thierstein 1972 [= *Cyclicargolithus reticulatus* in Rutledge (2010)]
Rhabdosphaera inflata Bramlette and Sullivan 1961
Rhagodiscus achlyostaurion (Hill 1976) Doeven 1983
Rhagodiscus angustus (Stradner 1963) Reinhardt 1971
Rhagodiscus asper (Stradner 1963) Reinhardt 1971
Rucinolithus irregularis Thierstein in Roth and Thierstein 1972
Schizosphaerella Deflandre and Dangeard 1938
Schizosphaerella punctulata Deflandre and Dangeard 1938
Similiscutum cruciulus de Kaenel and Bergen 1993
Sphenolithus belemnos Bramlette and Wilcoxon 1967
Sphenolithus disbelemnos Fornaciari and Rio 1996
Sphenolithus distentus (Martini 1965) Bramlette and Wilcoxon 1967
Sphenolithus furcatolithoides Locker 1967
Sphenolithus heteromorphus Deflandre 1953
Sphenolithus obtusus Bukry 1971
Sphenolithus predistentus Bramlette and Wilcoxon 1967
Sphenolithus primus Perch-Neilsen 1971
Sphenolithus spiniger Bukry 1971
Staurolithites aenigma Burnett 1997
Staurolithites canthus Jeremiah 1996
Stephanolithus bigotii subsp. *bigotii* Deflandre 1939
Stephanolithus speciosum subsp. *speciosum* Deflandre in Deflandre and Fert 1954
Tegumentum stradneri Thierstein in Roth and Thierstein 1972
Tetrapodorhabdus shawensis Medd 1979
Toweius Hay and Mohler 1967
Triquetrorhabdulus carinatus Martini 1965
Watznaueria Reinhardt 1964
Watznaueria barnesae (Black in Black and Barnes 1959) Perch-Neilsen 1968
Watznaueria britannica (Stradner 1963) Reinhardt 1964 (= *Ellipsagelosphaera britannica* in Rutledge 2010)
Watznaueria fossacincta (Black 1971) Bown and Cooper 1989 (= *Ellipsagelosphaera fossacincta* in Rutledge 2010)
Zebrashapka vanhintei Covington and Wise 1987
Zeugrhabdotus streetiae Bown *in* Kennedy *et al.* 2000
Zeugrhabdotus trivectis Bergen 1994

Palynomorph taxa mentioned in text

Achomosphaera andalousiensis Jan du Chêne 1977 (dinocyst)
Adnatosphaeridium caulleryi (Deflandre 1939) Williams and Downie 1969 (dinocyst)
Afropollis zonatus Doyle *et al.* 1982 (miospore)
Aldorfia aldorfensis (Gocht 1970) Stover and Evitt 1978 (dinocyst)
Appendicisporites problematicus (Burger 1966) Singh 1971 (miospore)
Aptea polymorpha Eisenack 1958 (dinocyst)
Aptea securigera Davey and Verdier 1974 (= *Pseudoceratium securigerum* Bint 1986) (dinocyst)
Areoligera circumsenonensis Fensome *et al.* 2009 (dinocyst)
Axiodinium Williams, Damassa, Fensome and Guerstein in Fensome *et al.* 2009 (dinocyst)
Axiodinium prearticulatum Williams, Damassa, Fensome and Guerstein in Fensome *et al.* 2009 (dinocyst) *Cadargasporites verrucosus* Reiser and Williams 1969 (miospore)
Callialasporites Dev 1961 (miospore)
Cannosphaeropsis passio de Verteuil and Norris 1996a (dinocyst)
Cerbia tabulata (Davey and Verdier 1974) Below 1981 (dinocyst)

Copyright © Atlantic Geoscience, 2023

Palynomorph taxa mentioned in text: continued

Chatangiella Vozzhennikova 1967 (dinocyst)
Chichaouadinium vestitum (Brideaux 1971) Bujak and Davies 1983 (dinocyst)
Chiropteridium dispersum Gocht 1960 (listed as synonym of *Chiropteridium galea* in Fensome *et al.* 2019) (dinocyst)
Chiropteridium galea (Maier 1959) Sarjeant 1983 (dinocyst)
Chiropteridium lobospinosum Gocht 1960 (dinocyst)
Chiropteridium mespilanum (Maier 1959) Lentin and Williams 1973 (listed as a synonym of *Chiropteridium galea* in Fensome *et al.* 2019) (dinocyst)
Chlamydophorella nyei Cookson andEisenack 1958 (dinocyst)
Classopollis spp. Pflug 1953 (miospore)
Classopollis torosus (Reissinger 1950) Balme 1957 (miospore) (= *Corollina torosa*)
Cleistosphaeridium ancyreum (Cookson andEisenack 1965) Eaton *et al.* 2001 (= *Systematophora ancyrea*) (dinocyst)
Cordosphaeridium cantharellus (Brosius 1963) Gocht 1969 (dinocyst)
Cordosphaeridium delimurum Fensome *et al.* 2009 (dinocyst)
Cordosphaeridium funiculatum Morgenroth 1966 (dinocyst)
Cribroperidinium Neale and Sarjeant 1962 (dinocyst)
Cribroperidinium crispum (Wetzel 1967) Fenton 1981 (=*Acanthaulax crispa*) (dinocyst)
Ctenidodinium combazii Dupin 1968 (dinocyst)
Ctenidodinium continuum Gocht 1970 (dinocyst)
Ctenidodinium elegantulum Millioud 1969 (dinocyst)
Ctenidodinium ornatum (Eisenack 1935) Deflandre 1939 (dinocyst)
Cycadopites subgranulosus (Couper 1958) Clarke 1965 (miospore)
Cyclonephelium Deflandre and Cookson 1955 (dinocyst)
Cymososphaeridium validum Davey 1982 (dinocyst)
Diacanthum filapicatum Gocht 1970b (=*Durotrigia filapicata*) (dinocyst)
Dichadogonyaulax sellwoodii Sarjeant 1975 (dinocyst)
Dingodinium albertii Sarjeant 1966 (dinocyst)
Dingodinium cerviculum Cookson and Eisenack 1958 (dinocyst)
Dinogymnium Evitt *et al* . 1967 (dinocyst)
Dinopterygium alatum Cookson and Eisenack 1962 (= *Xiphophoridium alatum*)
Diphyes colligerum (Deflandre and Cookson 1955) Cookson 1965 (dinocyst)
Diphyes ficusoides Islam 1983 (dinocyst)
Durotrigia filapicata (Gocht 1970) Riding and Bailey 1991 (= *Diacanthum filapicatum* and *Dichadogonyaulax filapicatum*) (dinocyst)
Echinitosporites sp. A of Bujak and Williams 1977 (miospore)
Echinitosporites cf. *iliacoides* Schulz and Krutzsch 1961 of Bujak and Williams 1977 (miospore)
Enneadocysta arcuata (Eaton 1971) Stover and Williams 1995 (dinocyst)
Escharisphaeridia pocockii (Sarjeant 1968) Erkmen and Sarjeant1980 (dinocyst)
Eucommiidites Erdtman 1948 (miospore)
Glaphyrocysta divarica (Williams and Downie 1966) Stover and Evitt 1978 (dinocyst)
Glaphyrocysta extensa Fensome *et al* . 2009 (dinocyst)
Gongylodinium erymnoteichon Fenton *et al* . 1980 (dinocyst)
Gonyaulacysta jurassica (Deflandre 1939) Norris and Sarjeant 1965 (dinocyst)
Gonyaulacysta pectinigera (Gocht 1970) Fensome 1979 (=*Leptodinium subtile pectinigerum*) (dinocyst)
Homotryblium floripes (Deflandre and Cookson) Stover 1975 (dinocyst)
Kleithriasphaeridium eoinodes (Eisenack 1958) Davey 1974 (dinocyst)
Kleithriasphaeridium simplicispinum (Davey and Williams 1966) Davey 1974 (generally now considered a junior synonym of *Kleithriasphaeridium eoinodes*) (dinocyst)
Korystocysta pachyderma (Deflandre 1939) Woollam 1983 (dinocyst)
Lentinia serrata Bujak in Bujak *et al* . 1980 (dinocyst)
Lithodinia Eisenack 1935 (dinocyst)
Litosphaeridium arundum (Eisenack and Cookson 1960) Davey 1979 (dinocyst)

Copyright © Atlantic Geoscience, 2023

Palynomorph taxa mentioned in text: continued

Litosphaeridium conispinum Davey and Verdier 1973 (dinocyst)
Litosphaeridium siphoniphorum (Cookson and Eisenack 1958) Davey and Williams 1966 (dinocyst)
Luehndea spinosa Morgenroth 1970 (dinocyst)
Mancodinium semitabulatum Morgenroth 1970 (dinocyst)
Meiourogonyaulax caytonensis (Sarjeant 1959) Sarjeant 1969 (= *Lithodinia caytonensis*) (dinocyst)
Moesiodinium raileanui Antonesçu 1974 (dinocyst)
Muderongia microperforata (Davey 1982) Monteil 1991 (*Muderongia perforata* in text) (dinocyst)
Muderongia perforata Alberti 1961 (dinocyst)
Muderongia simplex Alberti 1961 (= *Muderongia endovata*) (dinocyst)
Nannoceratopsis gracilis Alberti 1961 (dinocyst)
Odontochitina porifera Cookson 1956 (dinocyst)
Palaeocystodinium spp. Alberti 1961 (dinocyst)
Palaeohystrichophora infusorioides Deflandre 1935 (dinocyst)
Palaeoperidinium cretaceum (Pocock 1962ex Davey 1970) Lentin and Williams 1976 (dinocyst)
Palaeoperidinium pyrophorum (Ehrenberg 1837 ex Wetzel 1933) Sarjeant 1967b (dinocyst)
Pareodinia Deflandre 1947 (dinocyst)
Pentadinium laticinctum subspecies *granulatum* Gocht 1969 (dinocyst)
Pentadinium laticinctum subspecies *laticinctum* Gerlach 1961 (dinocyst)
Perisseiasphaeridium Davey and Williams 1966 (dinocyst)
Phoberocysta neocomica (Gocht 1957) Millioud 1969 (dinocyst)
Pseudoceratium pelliferum Gocht 1957 (dinocyst)
Reticulatosphaera actinocoronata (Benedek 1972) Bujak and Matsuoka 1986 (dinocyst)
Scriniocassis weberii Gocht 1964 (dinocyst)
Scriniodinium campanula Gocht 1959 (dinocyst)
Senoniasphaera protrusa Clarke and Verdier 1967 (dinocyst)
Sentusidinium Sarjeant and Stover 1978 (dinocyst)
Spheripollenites psilatus Couper 1958 (miospore)
Spiniferites pseudofurcatus (Klumpp 1953) Sarjeant 1970 (dinocyst)
Subtilisphaera Jain and Millepied 1973 (dinocyst)
Surculosphaeridium longifurcatum (Firtion 1952) Davey *et al* . 1966 (dinocyst)
Tanyosphaeridium xanthiopyxides (Wetzel 1933 ex Deflandre 1937) Stover and Evitt 1978 (dinocyst)
Trithyrodinium spp. Drugg 1967 (dinocyst)
Trithyrodinium evittii Drugg 1967 (dinocyst)
Tubotuberella dangeardii (Sarjeant 1968) Stover and Evitt 1978 (dinocyst)
Unipontidinium aquaeductus (Piasecki 1980) Lentin and Williams 1985 (dinocyst)
Wetzeliella Eisenack 1938 (dinocyst)
Xenascus ceratioides (Deflandre 1937) Lentin and Williams 1973 (dinocyst)

Copyright © Atlantic Geoscience, 2023

APPENDIX

Supplementary data files 1, 2, 3, 4, and 5 are also in open access here: https://doi.org/10.25545/QWOZWH